Australian Government
Forest and Wood Products Research and Development Corporation

MARKET KNOWLEDGE & DEVELOPMENT

PROJECT NUMBER: PN04.2005

Maximising impact sound resistance of timber framed floor/ceiling systems

Volume 2

FEBRUARY 2006

FWPRDC
PO Box 69, World Trade Centre
Melbourne 8005, Victoria
T: +61 3 9614 7544 F: +61 3 9614 6822

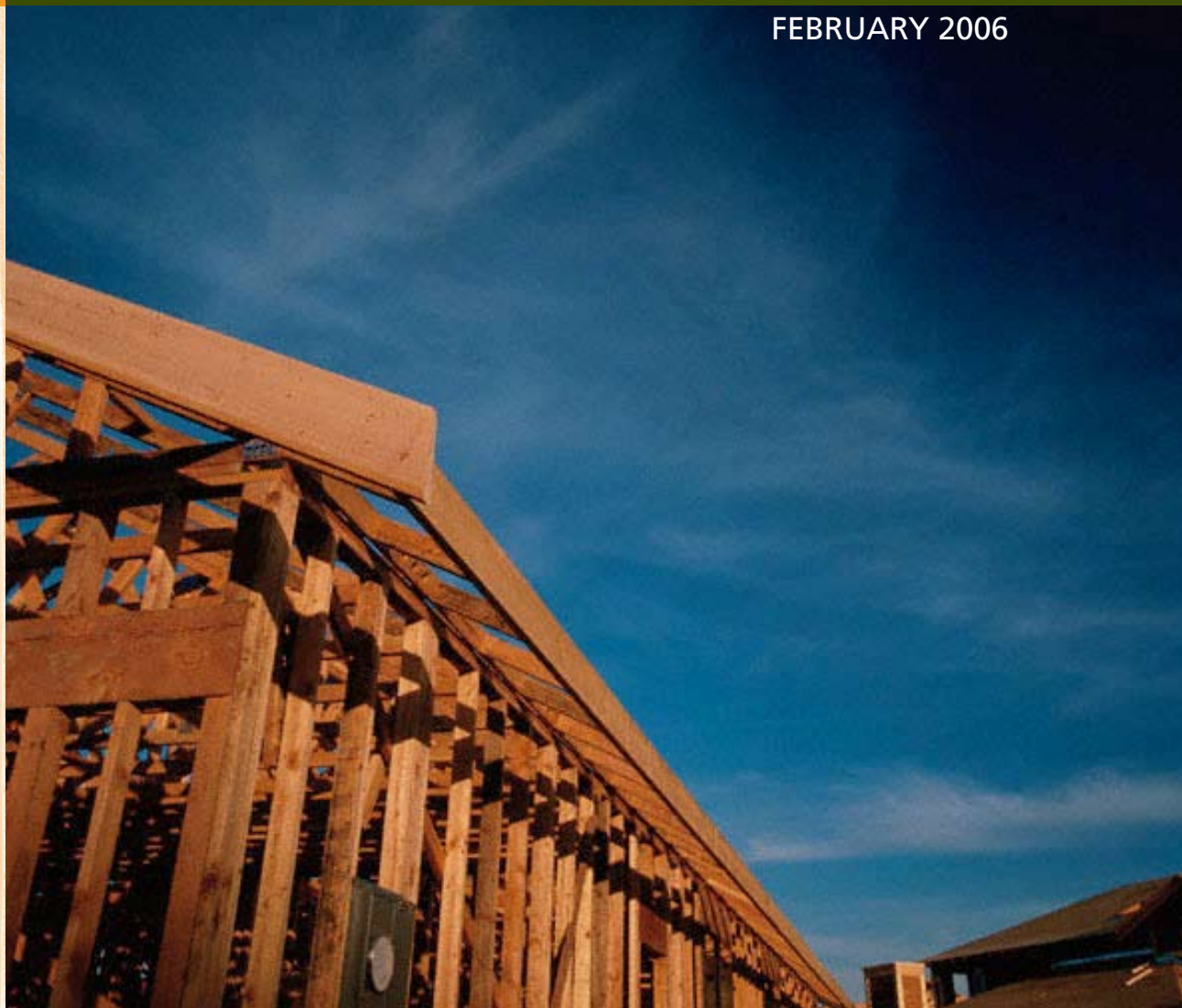

Maximising impact sound resistance of timber framed floor/ceiling systems Volume 2

Prepared for the

Forest and Wood Products Research and Development Corporation

by

H. Chung, G. Dodd, G. Emms, K. McGunnigle and G. Schmid

The FWPRDC is jointly funded by the Australian forest and wood products industry and the Australian Government.

Table of Contents

VOLUME 1

Executive Summary i

Preface iii

1. Project overview 1
   1.1 Introduction 1
   1.2 Overview of the issues 1
   1.3 Overview of existing knowledge 3
   1.4 The structure of the research report 5
   1.5 Conclusions of the analyses 6
   1.6 Successful floor designs 10
   1.7 Suggestions for further work 14
   1.8 Technology transfer of outputs 14
   1.9 References 15

2. Overview of existing floor system designs and recent research results 16
   2.1 Introduction 16
   2.2 Existing low-frequency performance understanding 16
   2.3 Existing high-frequency performance understanding 17
   2.4 Existing lightweight floor components in use around the world 18
   2.5 References 24

3. Theoretical modelling of a joist floor 26
   3.1 Introduction 26
   3.2 Part I: Review of existing models 27
   3.3 Part II: Our modelling for LTF floor systems 37
   3.4 Modelling fibrous infill 46
   3.5 Further comparison of the floor model with experimental results 48
   3.6 Part III: Modelling the receiving room 58
   3.7 References 60

VOLUME 2

4. Floor model analysis 63
   4.1 Introduction 63
   4.2 Single figure ratings 63
   4.3 150mm concrete reference floor 67
   4.4 Floor joist properties 69

4.5 Floor upper layer properties 77
4.6 Cavity and ceiling connection properties..... 85
4.7 Ceiling properties 95
4.8 Effects of floor span and room size 103
4.9 Conclusions of the trend analysis..... 109
4.10 References 110

5. Analysis of experimental results 111
5.1 Introduction 111
5.2 Examination of the low-frequency results 111
5.3 Examination of the high-frequency results 130
5.4 Brief examination of the vibration waveforms observed 131
5.5 References 144

6. Subjective listening tests and assessments 145
6.1 Introduction 145
6.2 Subjective versus objective testing 146
6.3 Previous research on subjective acceptability 146
6.4 IEC listening room 148
6.5 Objective evaluation of performance 149
6.6 Experimental setup 150
6.7 The subjects and their task 152
6.8 Results and discussion 153
6.9 References 158
6.10 Questionnaires used in the subjective testing 160

VOLUME 3

7. Low-frequency measurement results 169
7.1 Introduction 169
7.2 Experimental setup 169
7.3 Experimental technique 173
7.4 Experimental results overview 173
7.5 3-dimensional vibration plots 174
7.6 Average surface velocity plots 174
7.7 References 215

8. High-frequency measurement results 216
8.1 Summary of the measurement of impact sound insulation of floors 216
8.2 The results for each measured floor 217

9. Floor cost comparison 236

10. Properties of materials used 238
10.1 Panel products 238
10.2 Poured-on toppings/screenings 238
10.3 Joists 238
10.4 Infill materials 239
10.5 Ceiling fixtures 239

11. Floor diagrams and photographs 240
11.1 The test chamber 240
11.2 Reference concrete floor (Floor O) 242
11.3 Floor 2 243
11.4 Floor 3 249
11.5 Floor 4 251
11.6 Floor 5 252
11.7 Floor 6 254
11.8 Floor 7 255
11.9 Floor 8 258
11.10 Floor 9 261
11.11 Floor 10 262
11.12 Floor 11 264
11.13 Floor 12 266
11.14 Floor 13 270
11.15 Floor 14 272
11.16 Floor 15 273
11.17 Floor 16 278
11.18 Floor 17 279
11.19 Floor 18 281
11.20 Floor 19 283
11.21 Floor 20 284
11.22 Floor 21 293
11.23 Floor 22 294
11.24 Floor 23 296
11.25 Floor 24 297
11.26 Floor 25 300
11.27 Floor 26 301

4. FLOOR MODEL ANALYSIS

4.1 INTRODUCTION

In this chapter we consider results obtained from the theoretical floor (and room) model. One of the problems we face in doing this is that there are many variables which can be altered to produce a multidimensional space within which we search for some solution. The solution we are looking for being the matching of the low-frequency performance of a joist floor to that of a 150mm thick concrete floor.

Since the possibilities are almost endless and the variables aren't independent, we will attempt to examine the effect of changing various variables by starting with a model of a timber floor which, by today's standards (in Australasia, that is), performs reasonably well in the area of low-frequency impact insulation. This floor is the floor designated 'Floor 3', with the exception being that it has a span of 5.5m. It consists of 38mm of Gypsum Fibreboard screwed onto a plywood subfloor with 300mm deep LVL joists and a plasterboard ceiling consisting of 2 layers of 13mm dense plasterboard connected to the ceiling via rubber resilient clips; the ceiling cavity is filled with sound control fibreglass. This floor spans 5.5m and is 3.2m wide, and is on a rectangular room 2.4m deep with an average surface sound absorption coefficient of 0.15.

With the model of 'Floor 3' with all its parameters as the starting point, we then vary certain parameters of the floor while holding the rest constant. This enables us to observe the effects of changing these parameters in a theoretical way to produce indications of trends.

There are many parameters to consider, so in order to package the results up into more digestible packages, we divide the floor up into four different sections:-

- The joists.
- The upper surface or floor upper, consisting of everything that exists on top of the joists.
- The cavity, consisting of everything that acoustically connects the floor upper to the ceiling (this includes ceiling clips and battens).
- The ceiling.

We also consider one further aspect of the floor: the span of the floor and other dimensions associated with the floor and the room beneath.

In each section, we consider a number of apparently important parameters by varying each parameter in turn. For each parameter we produce low-frequency spectra of the predicted average vibration levels on the ceiling and the predicted average sound pressure levels in the receiving room. These spectra are for a force of 1N averaged over 10 forcing positions distributed over the floor.

4.2 SINGLE FIGURE RATINGS

Producing vibration and sound pressure spectra as the floor properties are varied is useful to see what aspects of the spectra are changing, but it is also useful to obtain single figure ratings for each floor. To do this, we go to the knowledge gained in the subjective analysis we've done in this project which gave us a subjective correlation between loudness of impact sounds and subjective desirability for the floor. We will, therefore, consider the Loudness produced by two different low-frequency dominated impacts:-

1) Idealised footstep
2) Japanese standard ball drop.

To produce these numbers, we get the spectra of sound pressures in the receiving room we calculate for each floor, and multiply them by the force spectra of the two impacts. We are limited to frequencies below 200Hz for the modelling; hence the loudness ratings are restricted to frequencies below 200Hz with higher frequencies assumed to have no contribution.

These low-frequency single figure ratings enable us to produce simple plots of floor performance against the parameter we are changing.

One purpose of these low-frequency single figure ratings is to enable comparison with the performance of a 150mm deep concrete floor. To achieve this, such a concrete floor was modelled and the corresponding frequency spectra and single figure ratings produced. These ratings are also shown on the plots.

As with all single figure ratings, care has to be exercised: much information can be lost when generating a single figure rating. So while one can obtain a general feel for trends, it is always wise to look at the full spectrum plots to observe in more detail what is happening.

The force produced by the Japanese Impact Ball

The force produced by the Japanese Ball (Rion Impact Ball YI-01) was measured using an impact plate mounted on a force transducer which was mounted on another plate sitting on a concrete floor. The manufacturers of the ball provide a calibration sheet with a recording of the impact signal produced by the ball without absolute determination of the forces produced. This experimental set-up was used to calibrate the amplitude and duration of the pulse. From experimental recordings the impact pulse duration was 20msec (± 0.5msec), the peak amplitude 1400 N (± 50N), and peak location at 8.5msec from the start of the pulse. Figure 4-1 shows the resulting time domain pulse and spectrum.

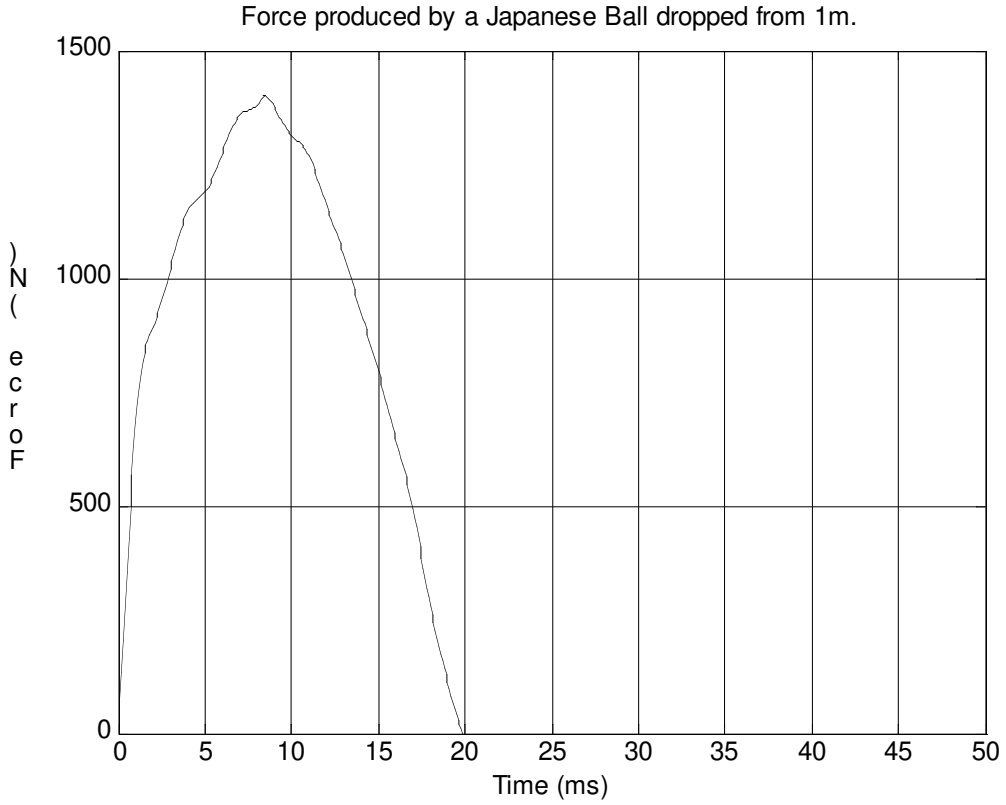

(a)

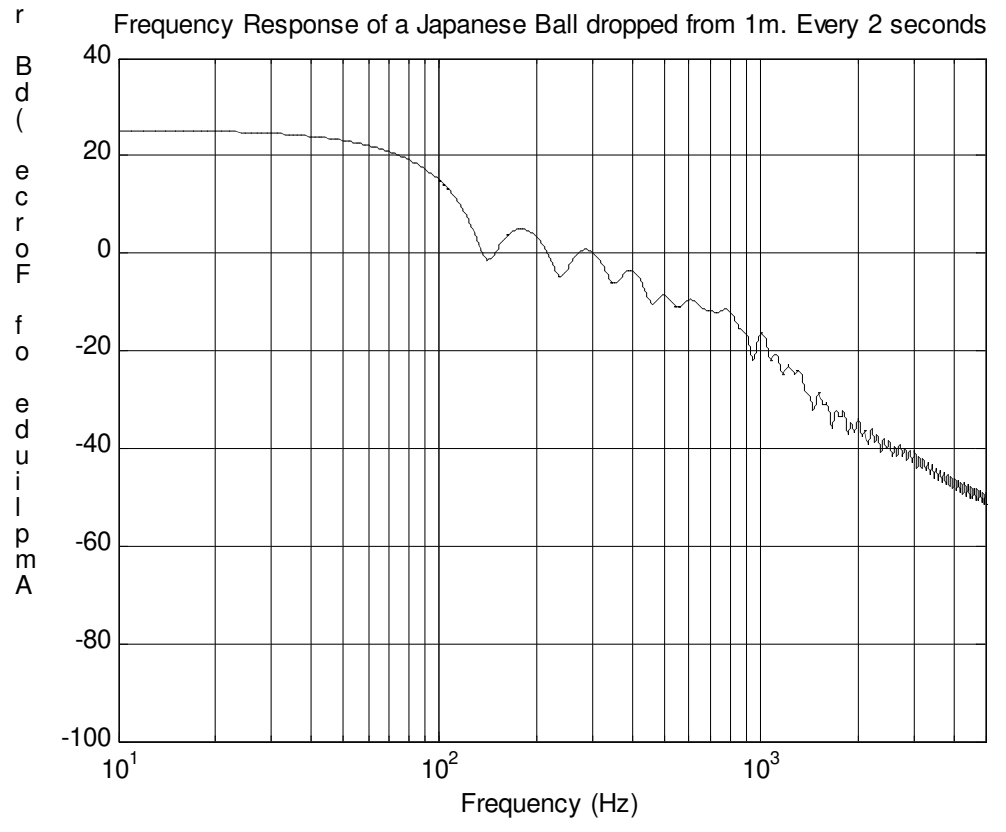

(b)

Figure 4-1. Plots of the time response and frequency response of an impact produced by a Japanese Ball (Rion Impact Ball) dropped from 1m above the floor. The frequency response assumes the ball drop is repeated every 2 seconds.

The force produced by footsteps

We assume from measurements made by Shi et al.(1997) that the forces produced by a footstep of a 80kg person in soft shoes are given by Figure 4-2. This is an averaging of the results presented by Shi et al. the first peak is assumed to be the heel strike and the second is the toe push off. The corresponding spectrum is shown in Figure 4-3.

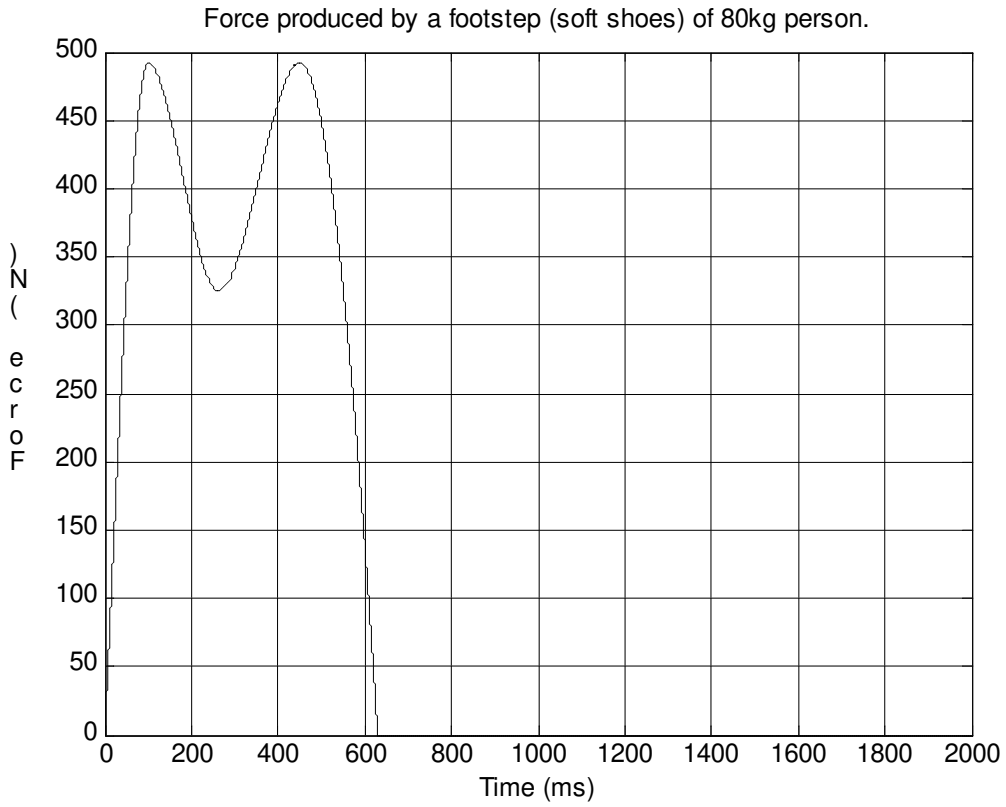

Figure 4-2. The force produced by a footstep as a function of time.

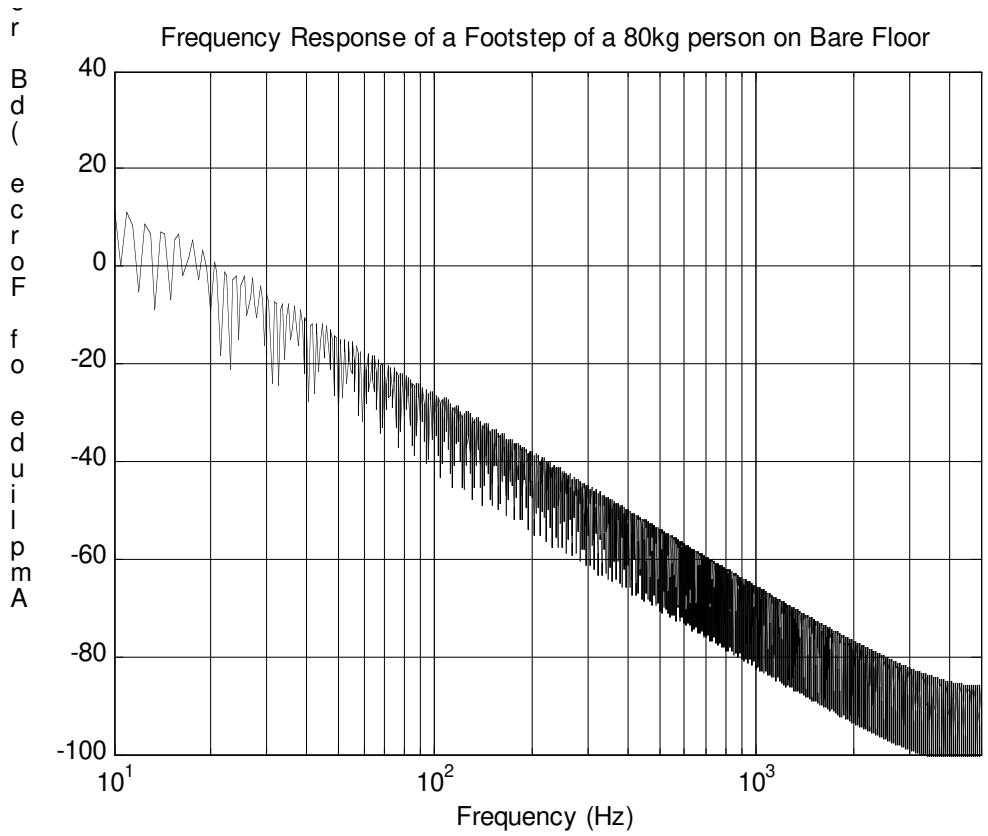

Figure 4-3. The force spectrum produced by a footstep.

In Shi et al. we find that tests were done on people of different weights, resulting in a correlation between the size of the peaks and the mass of the person. (viz. $f_{\max} = 5.35(mass) + 64.09$).

It is assumed that the speed of walking is 1.5 steps per second, so that by also assuming coherent addition of footstep forces (amplitude addition) we get a gain of 3.5dB on the previous spectra (Figure 4-3). It is worth noting that Blazier and duPree (1994) have some limited results about the influence of the speed of walking on results. Faster walking produces greater increases in sound level because of both the increase in step frequency and because of the greater peak forces produced by such impacts – the tendency is towards greater higher frequency levels because of the shorter duration of the impacts, as is also shown in results by Shi et al. (1997).

4.3 150MM CONCRETE REFERENCE FLOOR

For reference purposes, it useful to have the low-frequency impact insulation results for a 150mm concrete slab. Modelling such a slab at low-frequencies is relatively easy, since it is essentially a homogeneous plate. We assume that the concrete is dense concrete with a density of 2300 kg/m^3 and a Young's modulus of 27 GPa. Although concrete in itself has very low internal damping (loss factors of around 0.006), the slab is assumed to be part of a building and hence can lose its energy to the rest of the building. Work by Koizumi et al. (2002) suggests that such a slab should have a loss factor of 0.06, when considering the energy lost to the rest of the structure.

The slab is assumed to have the same size as the joist floors we are comparing it against (mostly 3.2 x 5.5m), and sits on the same room with the same height and acoustic properties (often 2.4m high with an absorption coefficient of 0.15). For example, the results of a

concrete slab 3.2 x 5.5m on a room 2.4m high with an absorption coefficient of 0.15 are shown in Figure 4-2 and Figure 4-3. Using an absorption coefficient of 0.15 assumes that the room has plasterboard walls. A bare room with masonry walls will have an absorption coefficient which is much lower (around 0.02).

It is thus to be realised that by taking the loss factor of the slab to be 0.06 and the absorption coefficient of the room under the floor to be 0.15 we are assuming a best possible situation for the concrete floor – the impact insulation performance will be worse for a concrete floor in isolation with masonry walls below.

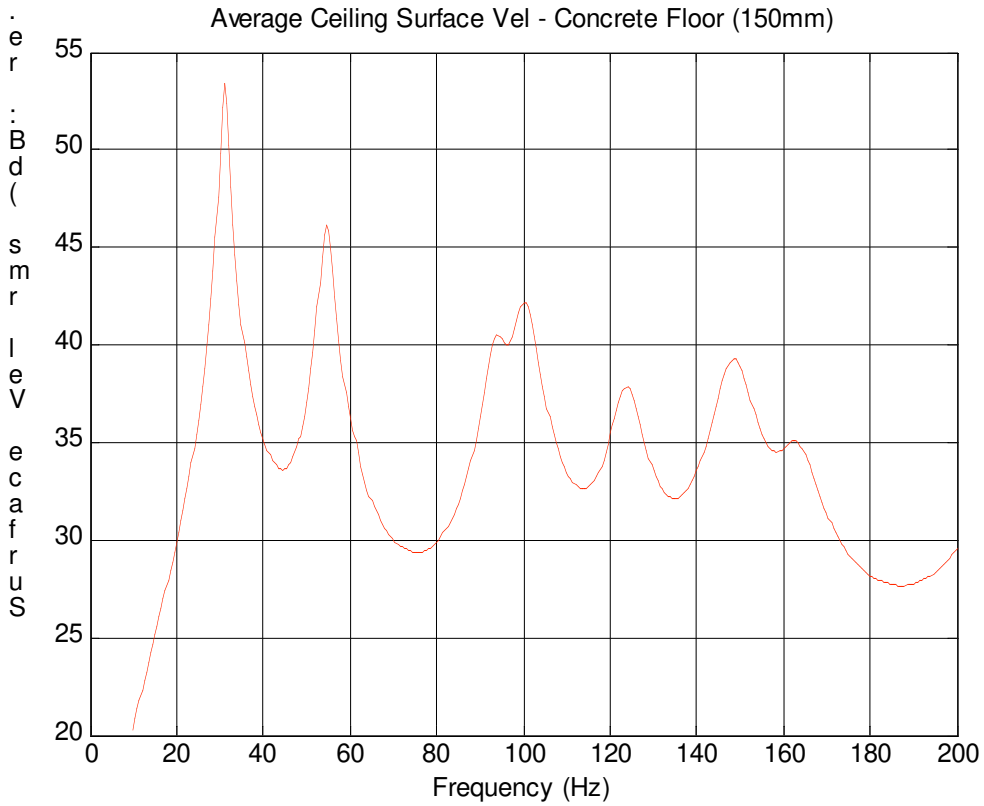

Figure 4-4. The predicted average ceiling surface velocity normalised against the force of the impact on the floor.

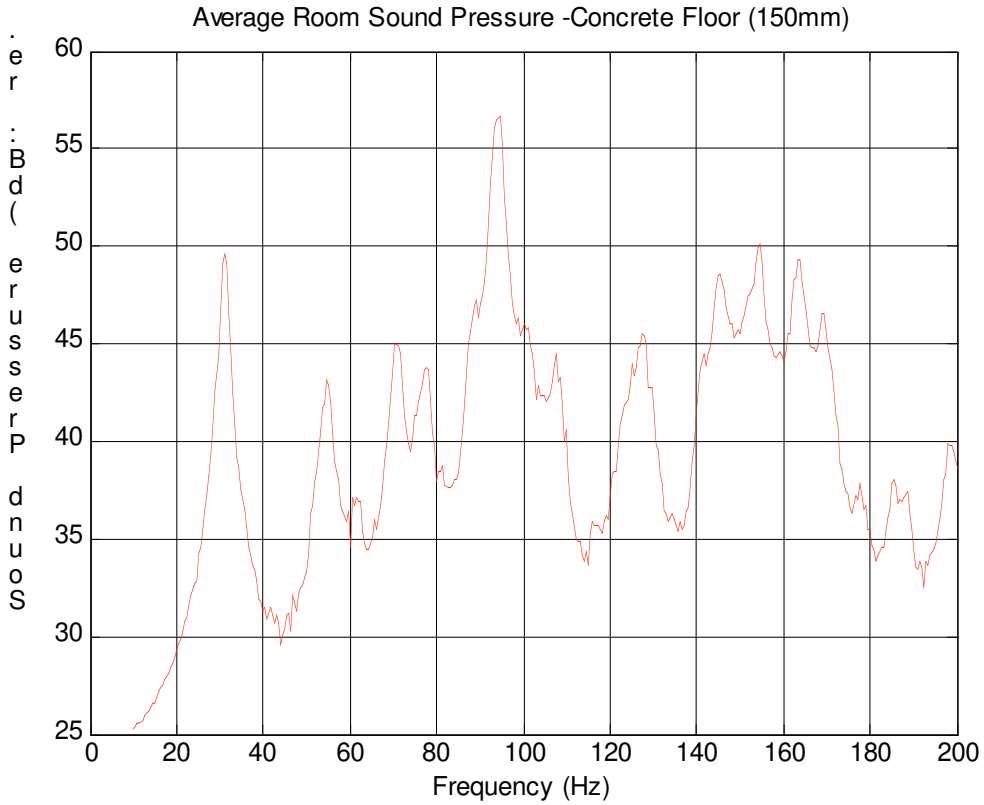

Figure 4-5. The predicted average room sound pressure generated in the receiving room normalised against the force of the impact on the floor.

4.4 FLOOR JOIST PROPERTIES

In this section we consider the influences of the parameters of the floor joists on the floor performance.

Changing the bending stiffness of the joists

In this section we look at what happens when the joist bending stiffness is changed. For reference, a 300 by 45mm 14.5GPa joist has a bending stiffness of 1468100 Nm^2.

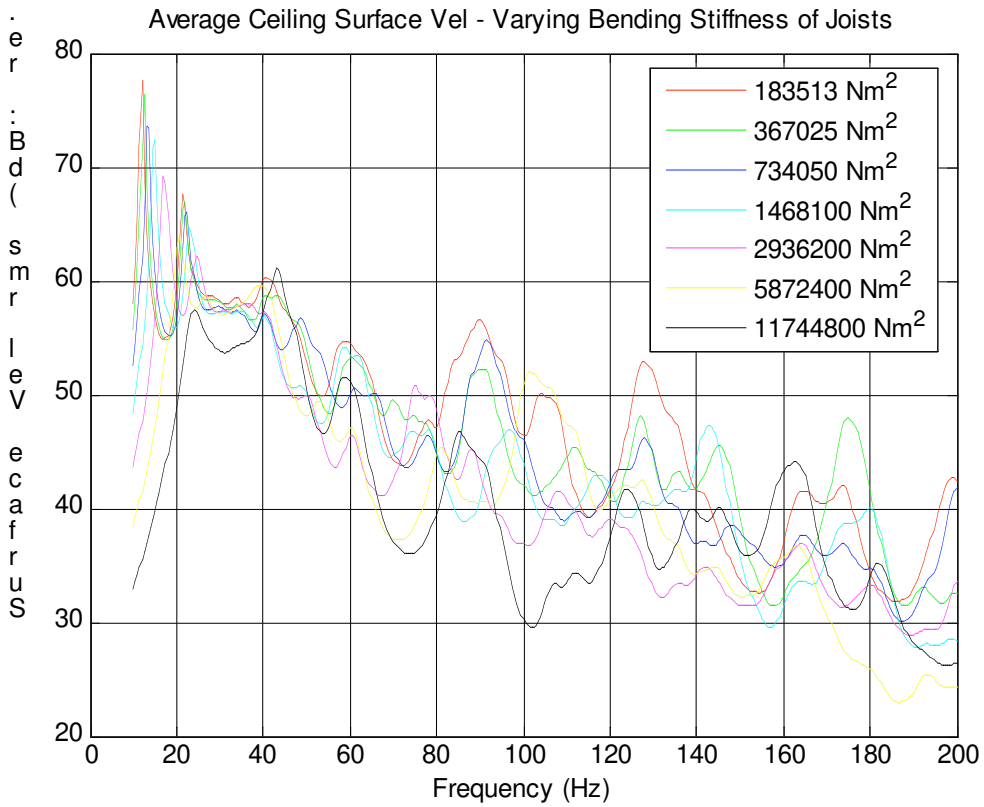

Figure 4-6. The predicted average ceiling surface velocity normalised against the force of the impact on the floor.

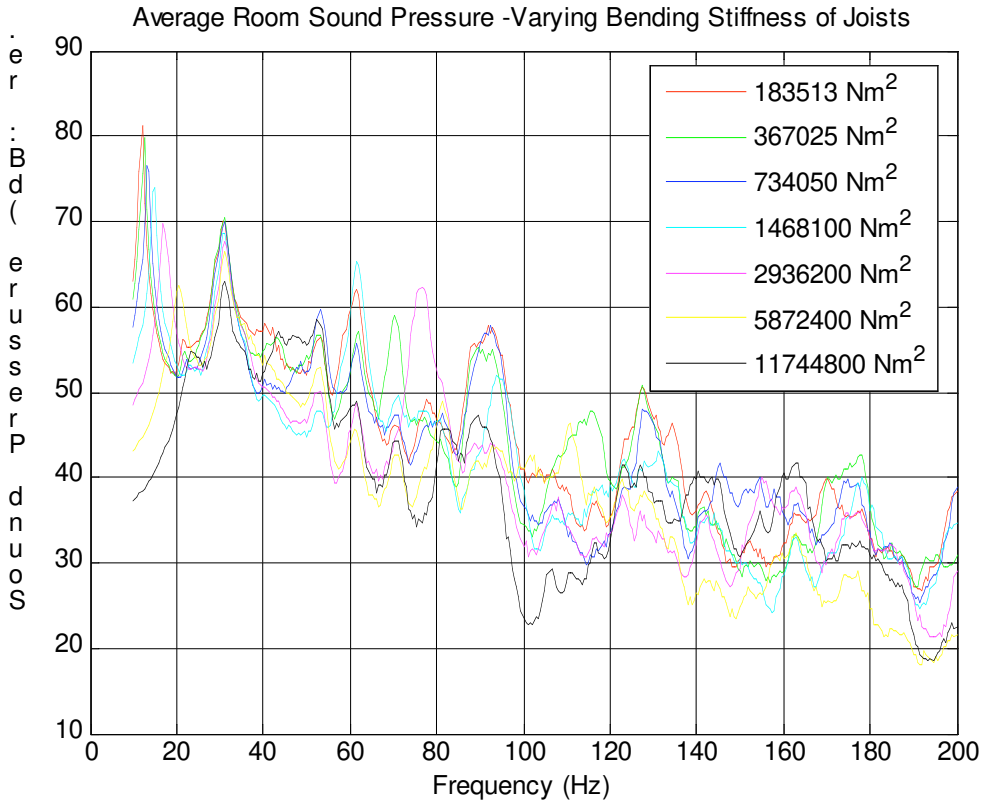

Figure 4-7. The predicted average room sound pressure generated in the receiving room normalised against the force of the impact on the floor.

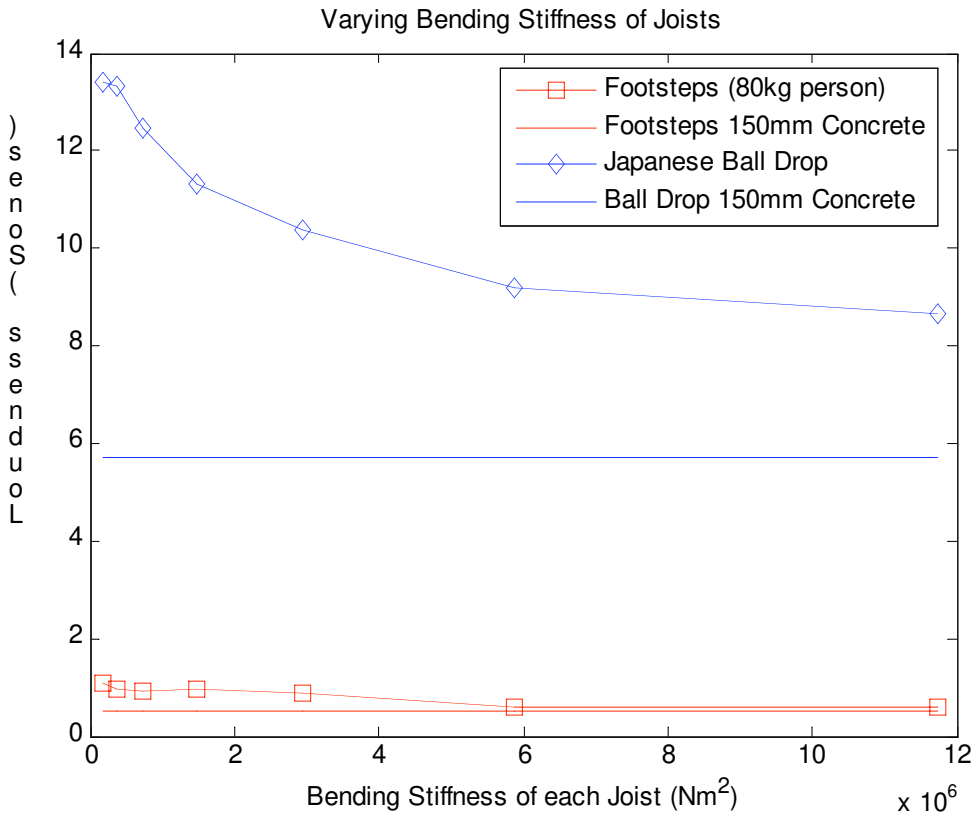

Figure 4-8. The average overall Loudness in Sones produced by a model footstep and a Japanese impact ball in the receiving room below the floor.

Changing the vibrational damping of the joists

In this section we examine the effect of changing the vibrational damping of the joists. Timber normally has a damping loss factor of 0.03.

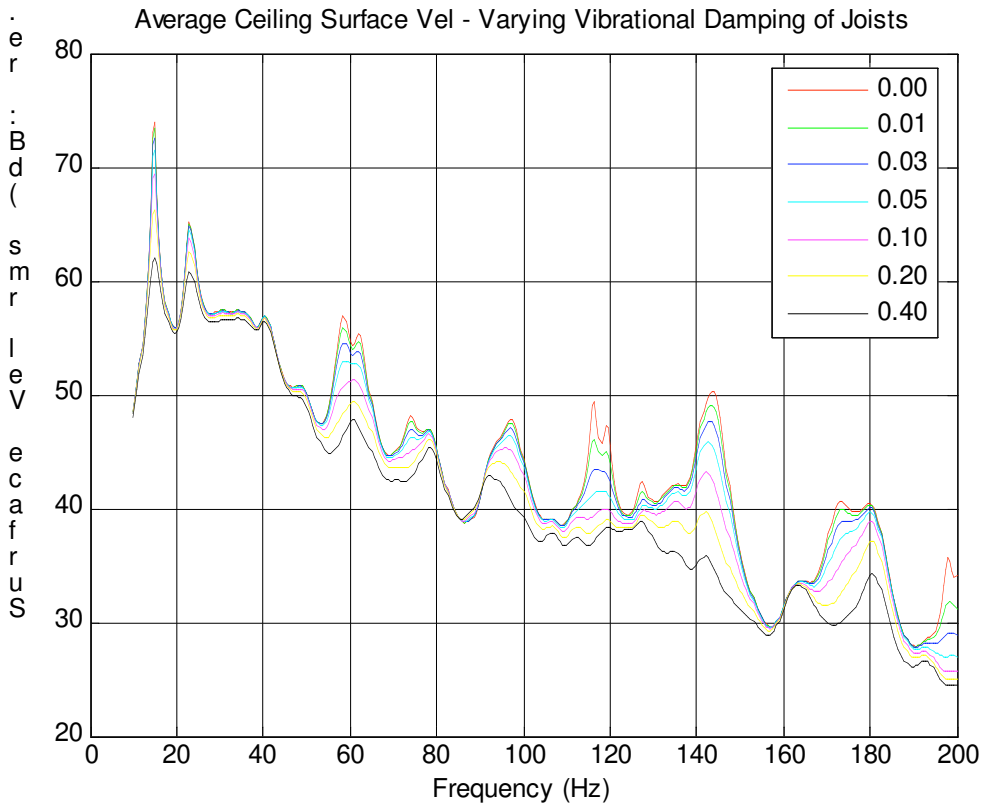

Figure 4-9. The predicted average ceiling surface velocity normalised against the force of the impact on the floor.

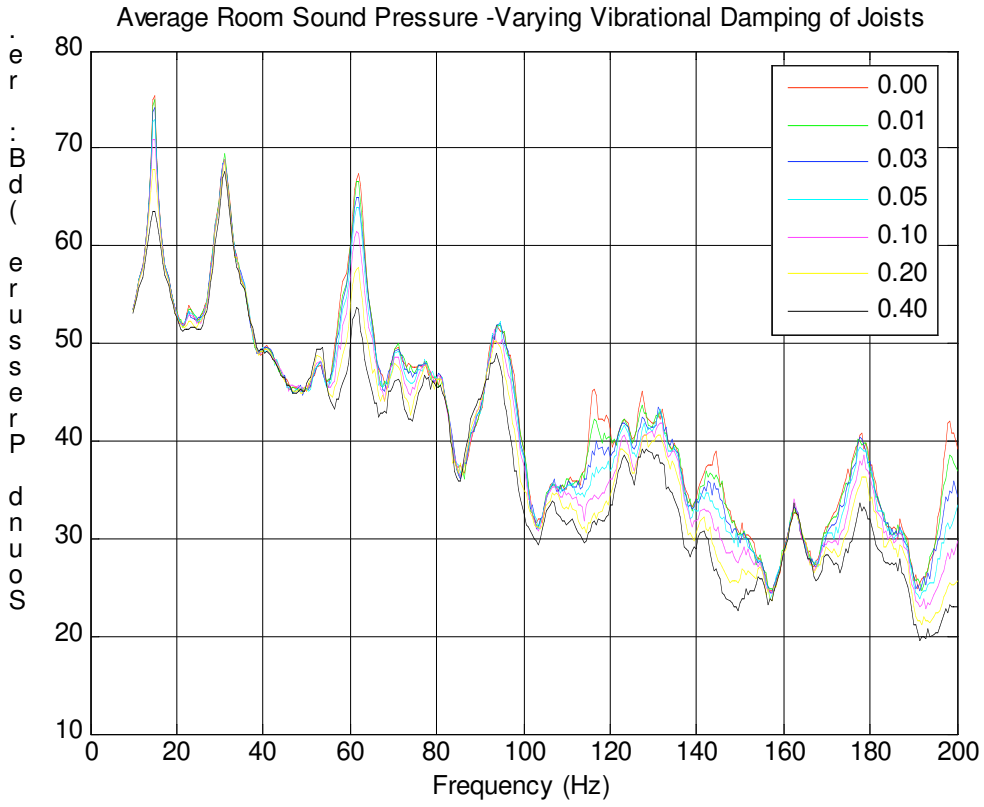

Figure 4-10. The predicted average room sound pressure generated in the receiving room normalised against the force of the impact on the floor.

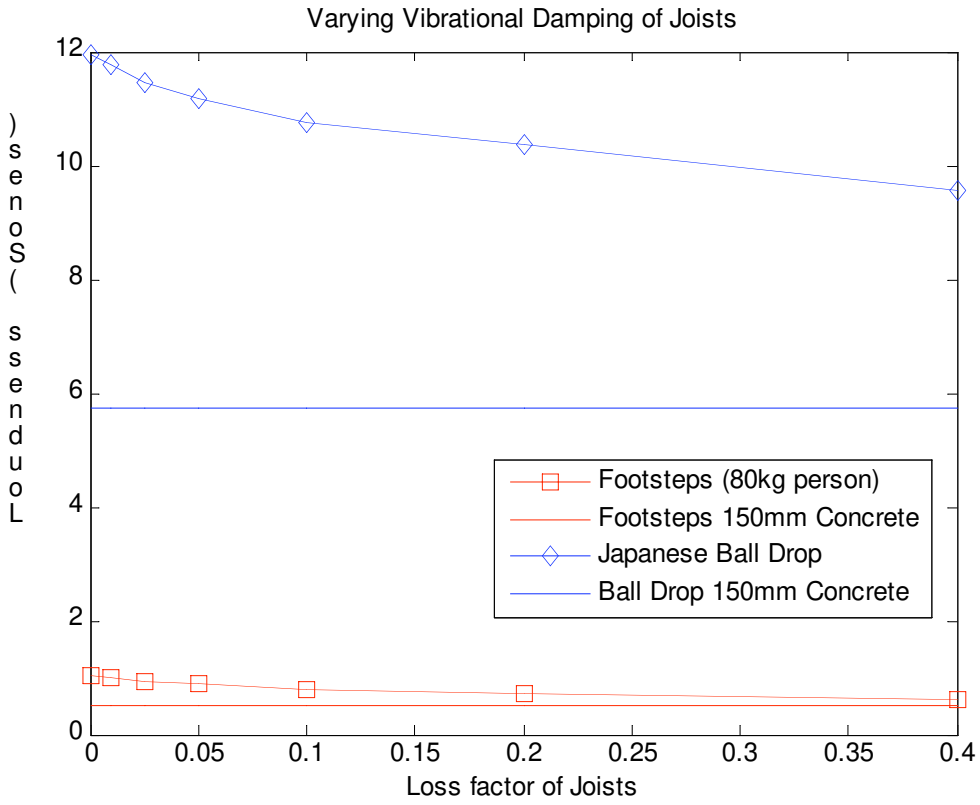

Figure 4-11. The average overall Loudness in Sones produced by a model footstep and a Japanese impact ball in the receiving room below the floor.

Inclusion of transverse stiffening across joists

One way to stiffen up a floor is to add transverse stiffening by way of blocking between joists, which has been clamped together with tie rods – such a series of blocking clamped with a tie rod is termed a 'transverse stiffener'. In this section we look at the effect of an even spacing of transverse stiffeners along the floor; we vary the total number of transverse stiffeners along the 5.5m length of the floor.

It was presumed that the effectiveness of transverse stiffening relies upon the transverse stiffening reducing the density of modes at higher frequencies, thus reducing the overall vibration levels. We expect that the effectiveness of reduction of modal density to be more challenging at greater floor widths.

To test this idea of transverse stiffening we consider two cases:-

1) A floor 3.2m wide (Figure 4-12 to Figure 4-14)
2) An extremely wide floor 10m wide (Figure 4-15 to Figure 4-17).

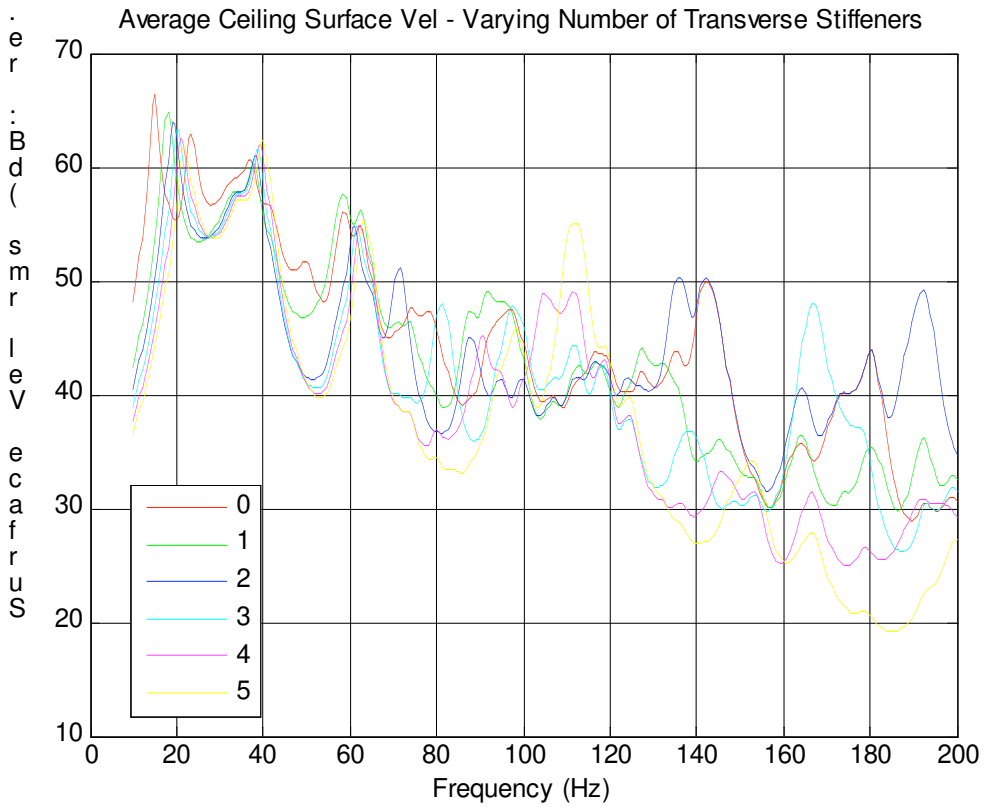

Figure 4-12. The predicted average ceiling surface velocity normalised against the force of the impact on the floor.

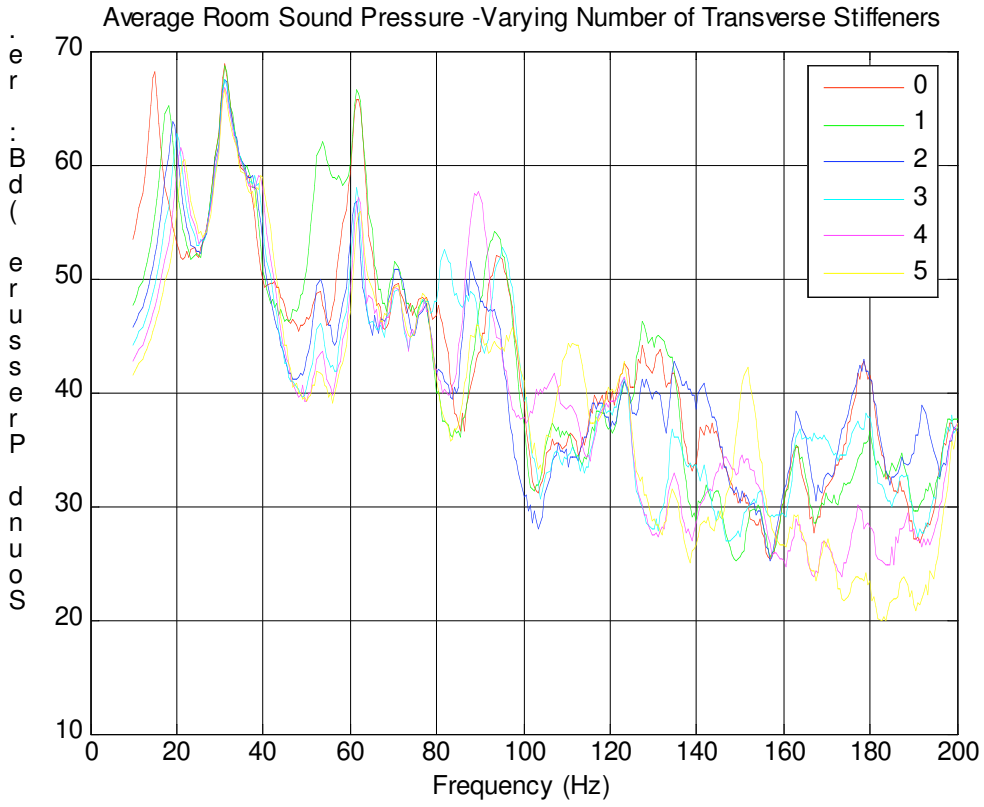

Figure 4-13. The predicted average room sound pressure generated in the receiving room normalised against the force of the impact on the floor.

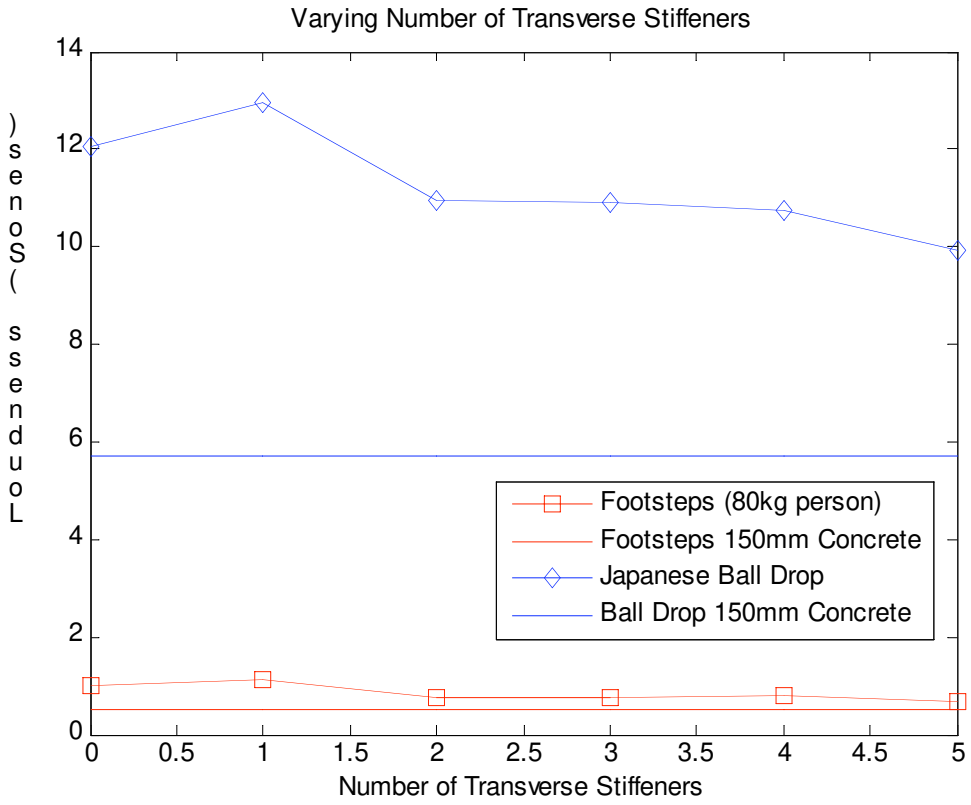

Figure 4-14. The average overall Loudness in Sones produced by a model footstep and a Japanese impact ball in the receiving room below the floor.

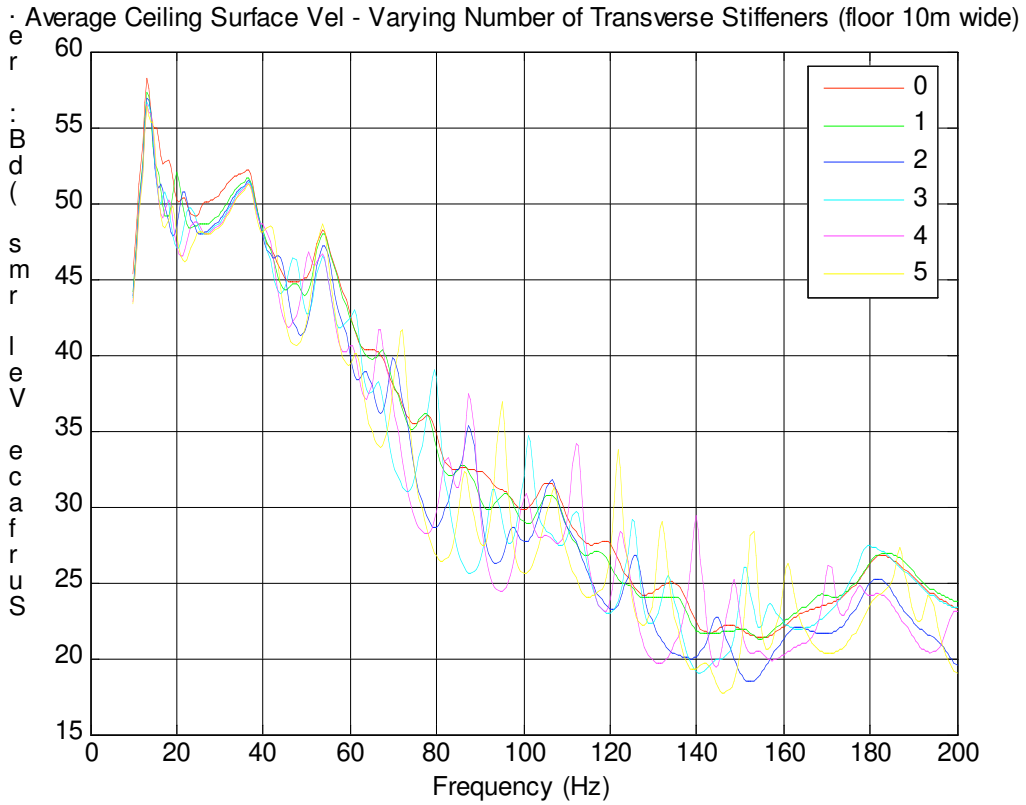

Figure 4-15. The predicted average ceiling surface velocity normalised against the force of the impact on the floor.

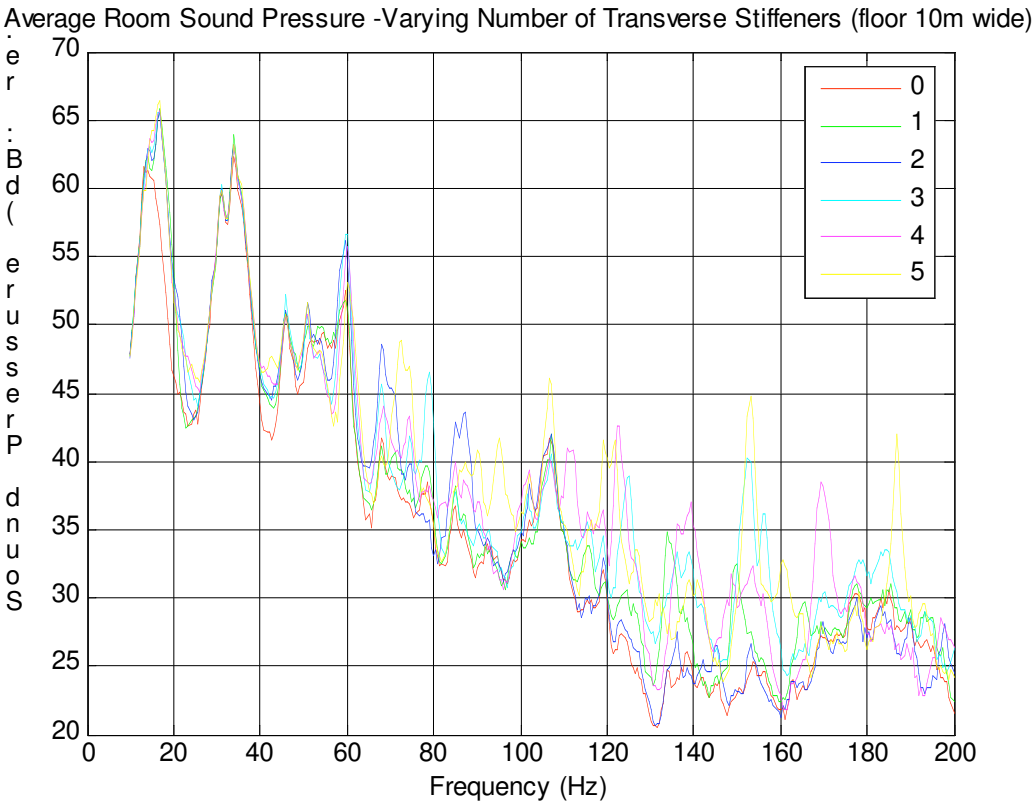

Figure 4-16. The predicted average room sound pressure generated in the receiving room normalised against the force of the impact on the floor.

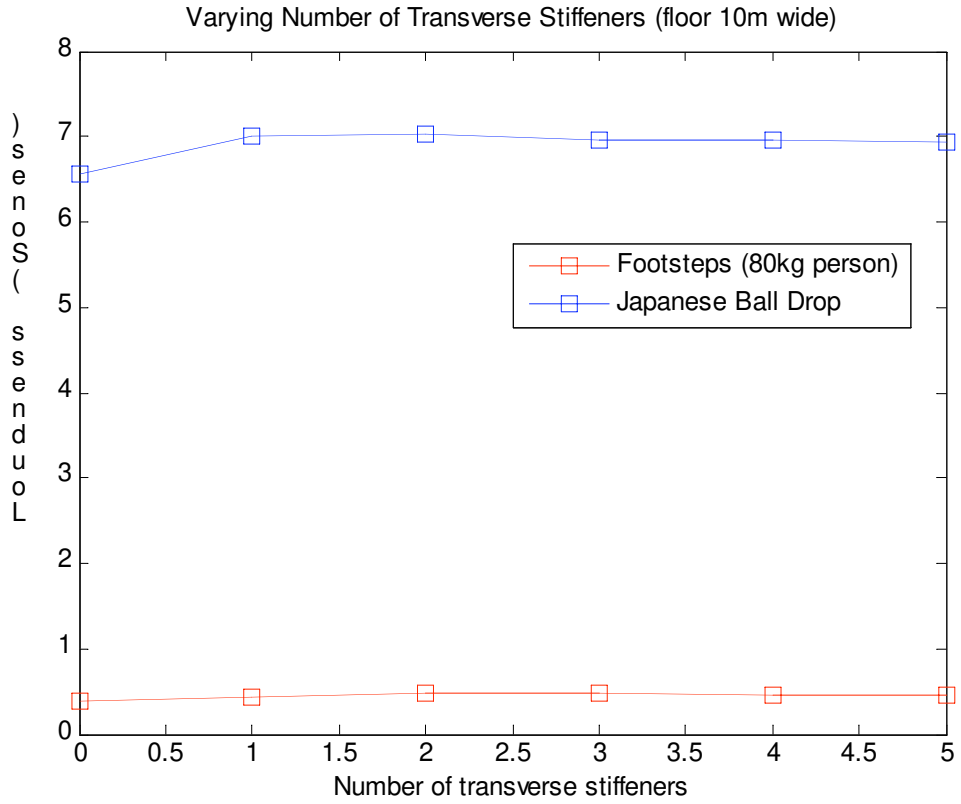

Figure 4-17. The average overall Loudness in Sones produced by a model footstep and a Japanese impact ball in the receiving room below the floor.

4.5 FLOOR UPPER LAYER PROPERTIES

In this section we consider the effects of the parameters of the floor upper – this is the part of the floor which lies on the joists, and stops people form falling through to the room below.

Changing the surface density of upper surface of the floor

In this section the effect of changing the surface density of the floor upper is observed. Only the surface density is changed; we keep the bending stiffness of the floor upper equal to that of 3 layers of GFB on plywood found on Floor 3. For reference, the surface density of the floor upper of Floor 3 is 48 kg/m^2, and 150mm of dense concrete is about 350 kg/m^2.

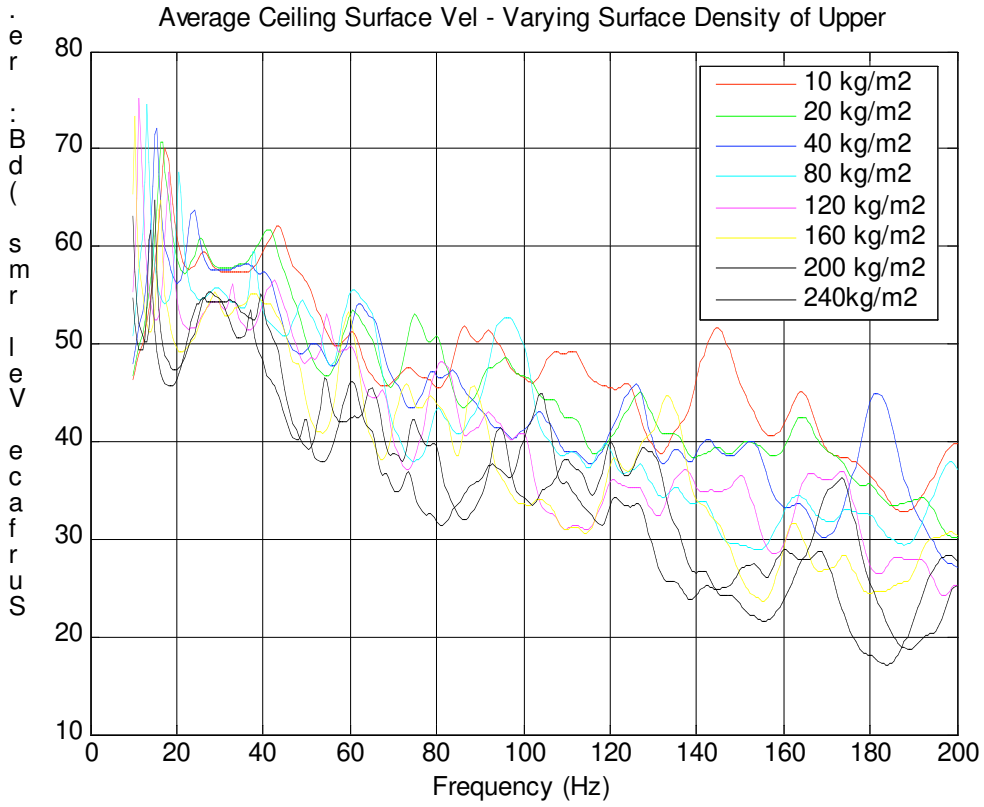

Figure 4-18. The predicted average ceiling surface velocity normalised against the force of the impact on the floor.

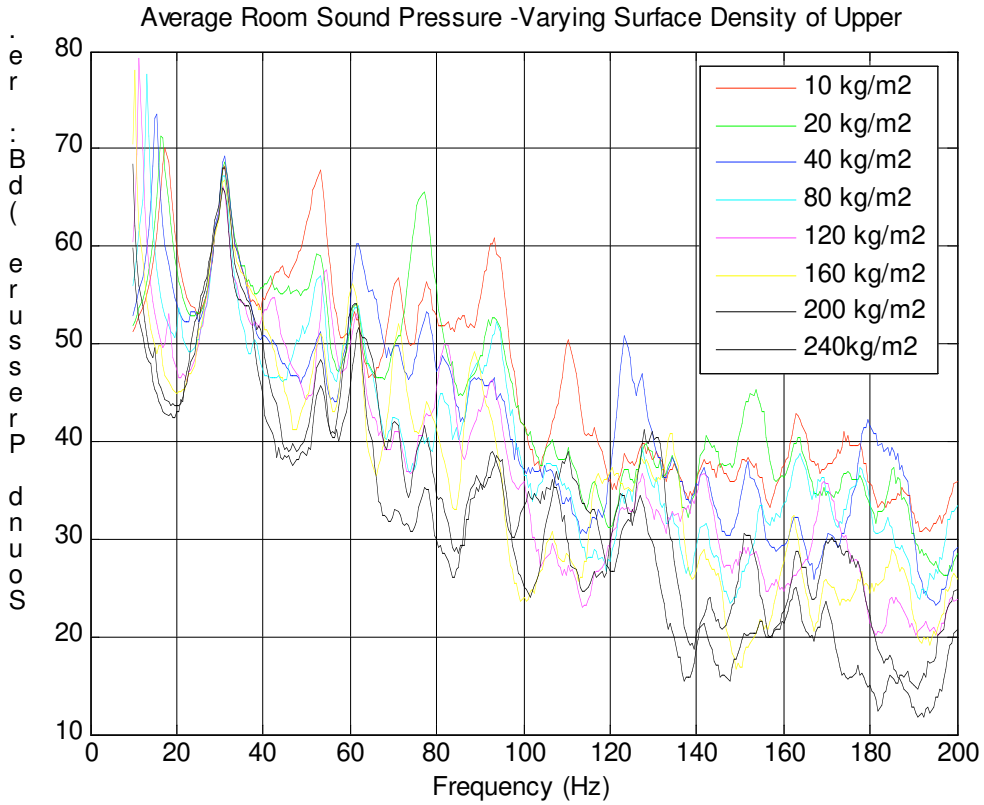

Figure 4-19. The predicted average room sound pressure generated in the receiving room normalised against the force of the impact on the floor.

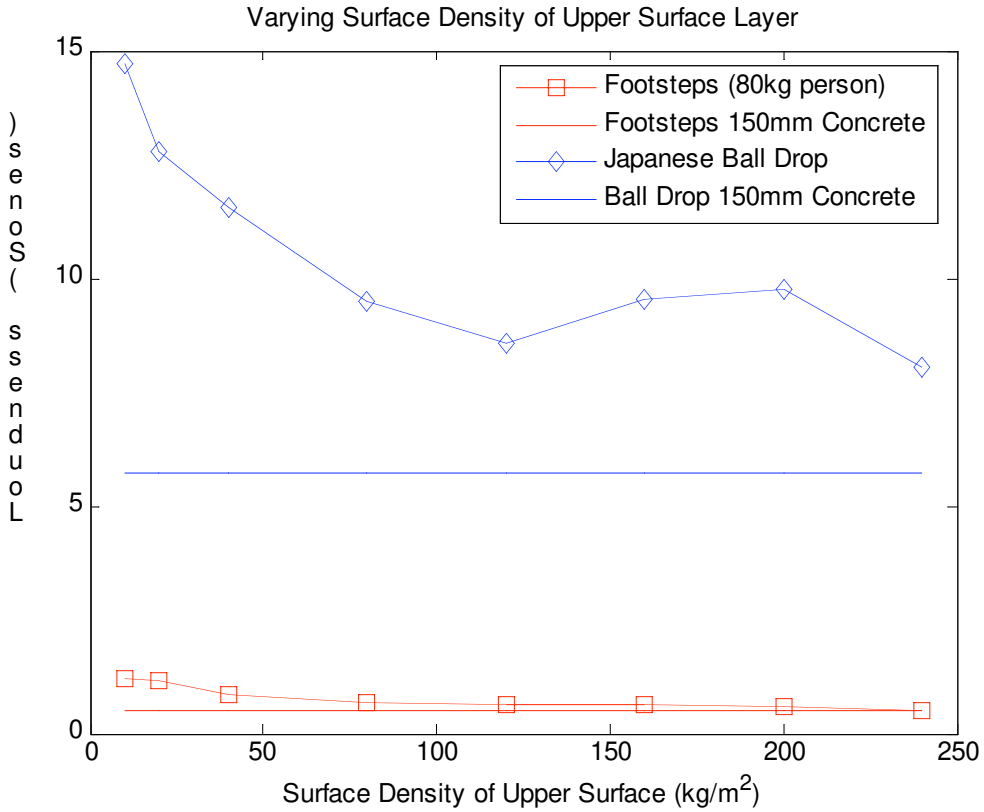

Figure 4-20. The average overall Loudness in Sones produced by a model footstep and a Japanese impact ball in the receiving room below the floor.

Changing bending stiffness of the upper surface of floor

In this section the effect of changing the bending stiffness of the floor upper is observed. Only the bending stiffness is changed; we keep the surface density of the floor upper equal to that of 3 layers of GFB on plywood found on Floor 3. For reference, the bending stiffness of 20mm particleboard is about equal to 2000 Nm, and 150mm of dense concrete is about $11x10^6$ Nm.

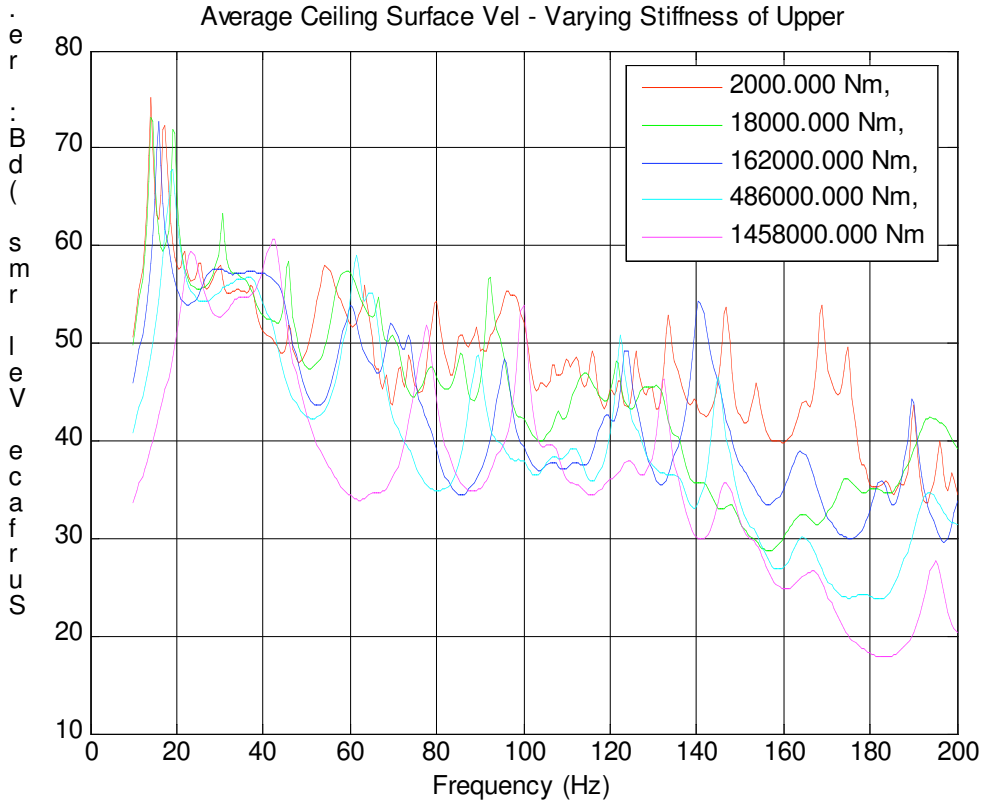

Figure 4-21. The predicted average ceiling surface velocity normalised against the force of the impact on the floor.

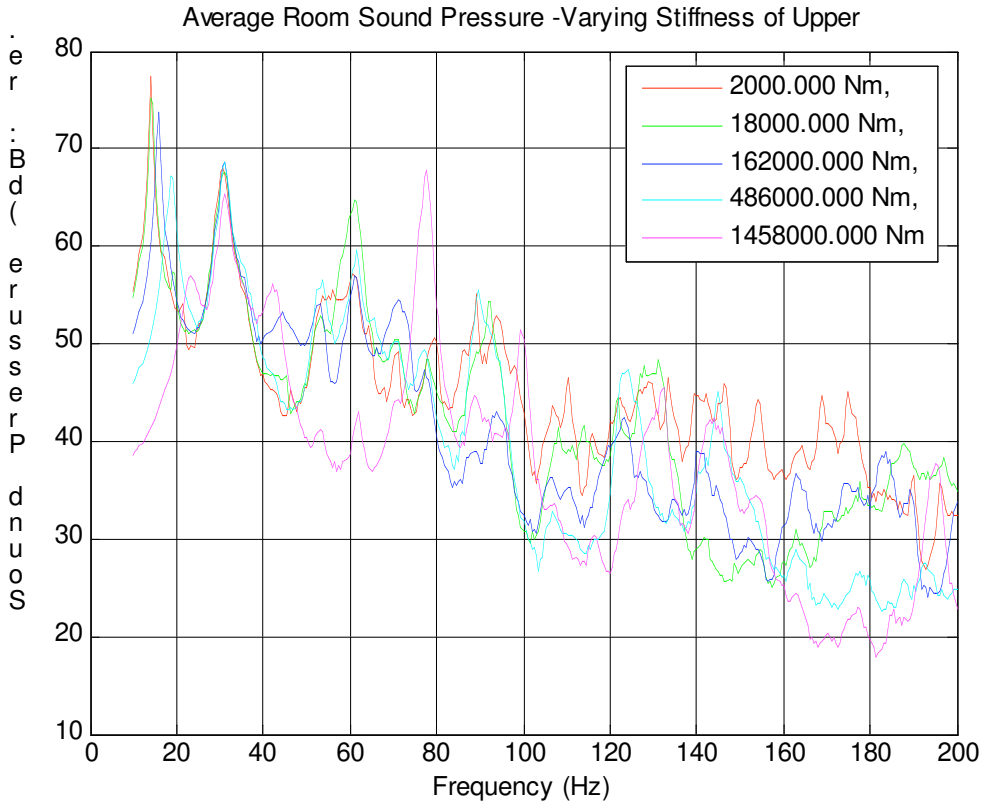

Figure 4-22. The predicted average room sound pressure generated in the receiving room normalised against the force of the impact on the floor.

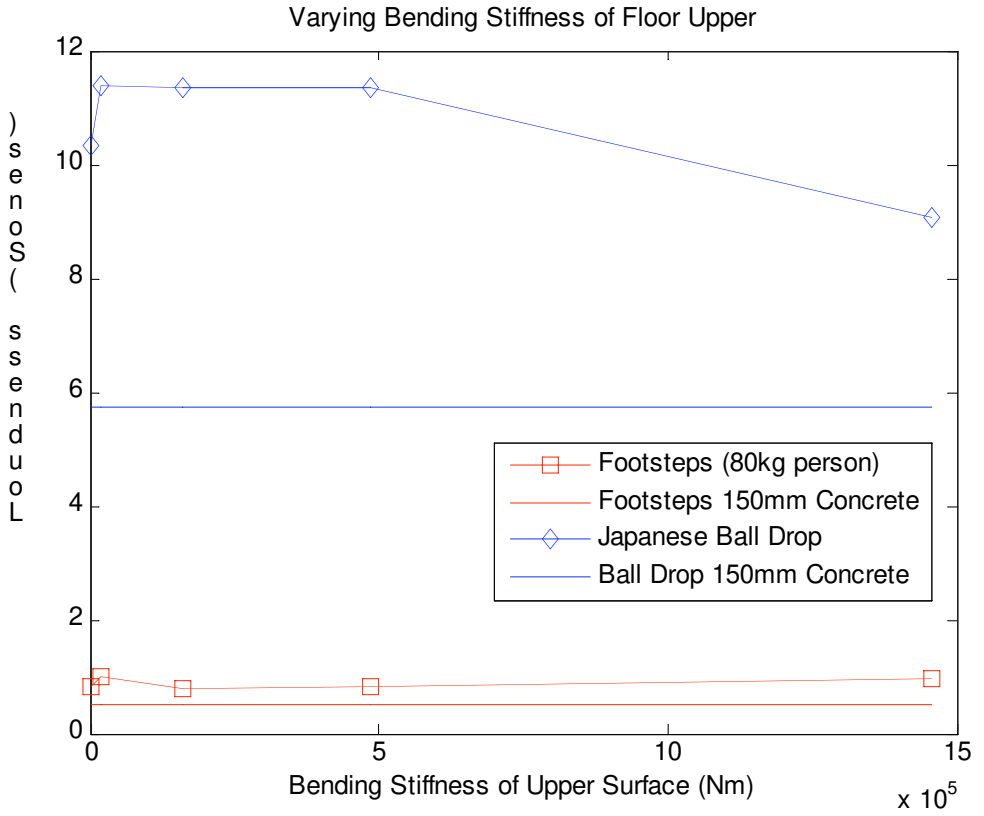

Figure 4-23. The average overall Loudness in Sones produced by a model footstep and a Japanese impact ball in the receiving room below the floor.

Changing the vibration damping of the upper surface of floor

In this section the effect of changing the vibrational damping of the floor upper is observed. For reference, we expect the damping loss factor of the upper of Floor 3 to be about 0.04.

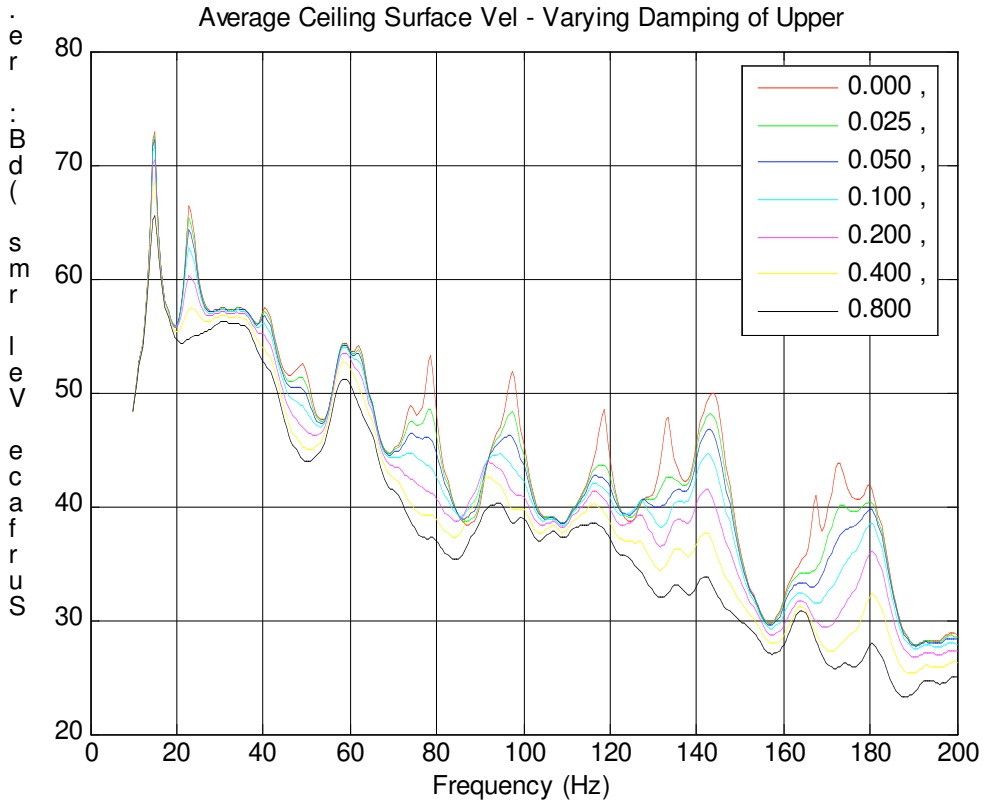

Figure 4-24. The predicted average ceiling surface velocity normalised against the force of the impact on the floor.

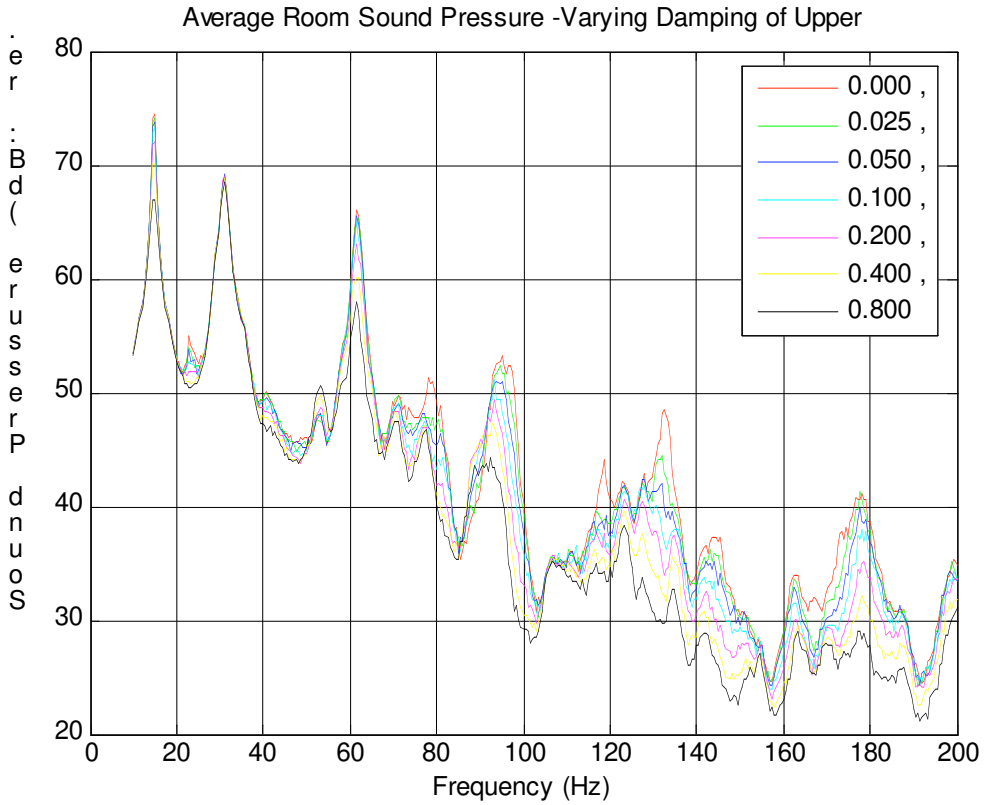

Figure 4-25. The predicted average room sound pressure generated in the receiving room normalised against the force of the impact on the floor.

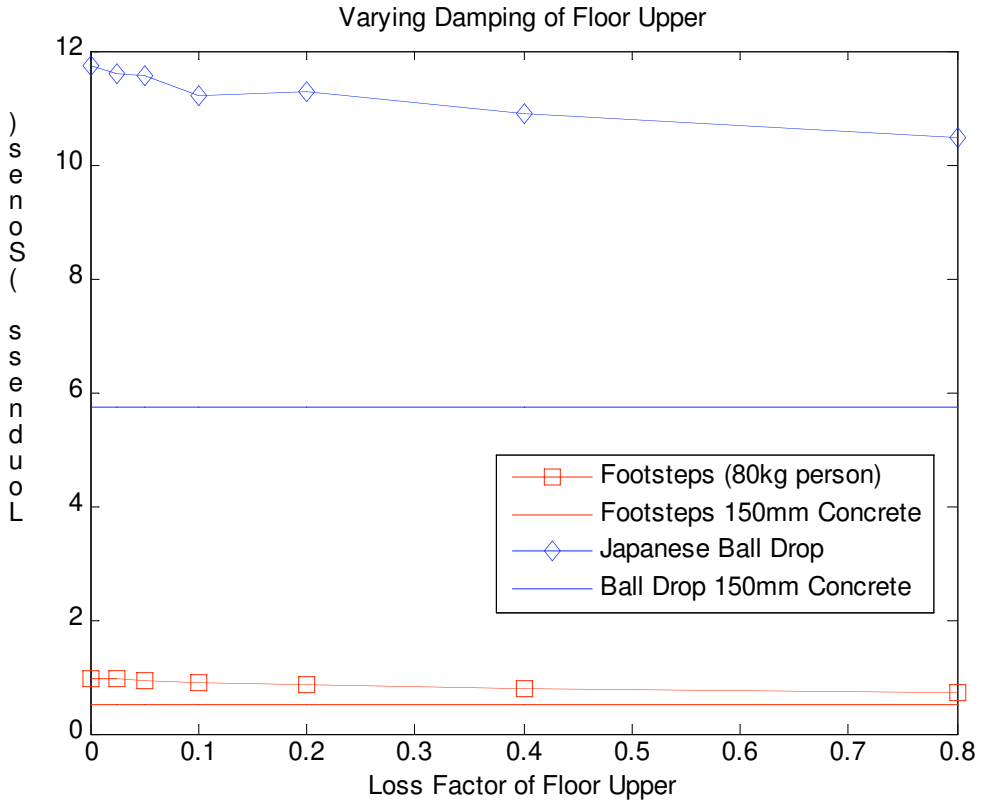

Figure 4-26. The average overall Loudness in Sones produced by a model footstep and a Japanese impact ball in the receiving room below the floor.

Changing the number of layers of gypsum fibreboard on the floor upper

In the previous sections where we looked at the floor upper we changed one parameter and somewhat artificially held other parameters constant. In this section we look at what happens when we increase the depth of the gypsum fibreboard on the plywood – we are changing both the surface density and bending stiffness of the floor upper. The gypsum fibreboard has a Young's modulus of 4.5GPa and a density of 1040 kg/m^2. Each board is 12.7mm thick, and it is assumed that they are screwed down so that the layers do not slip when bent.

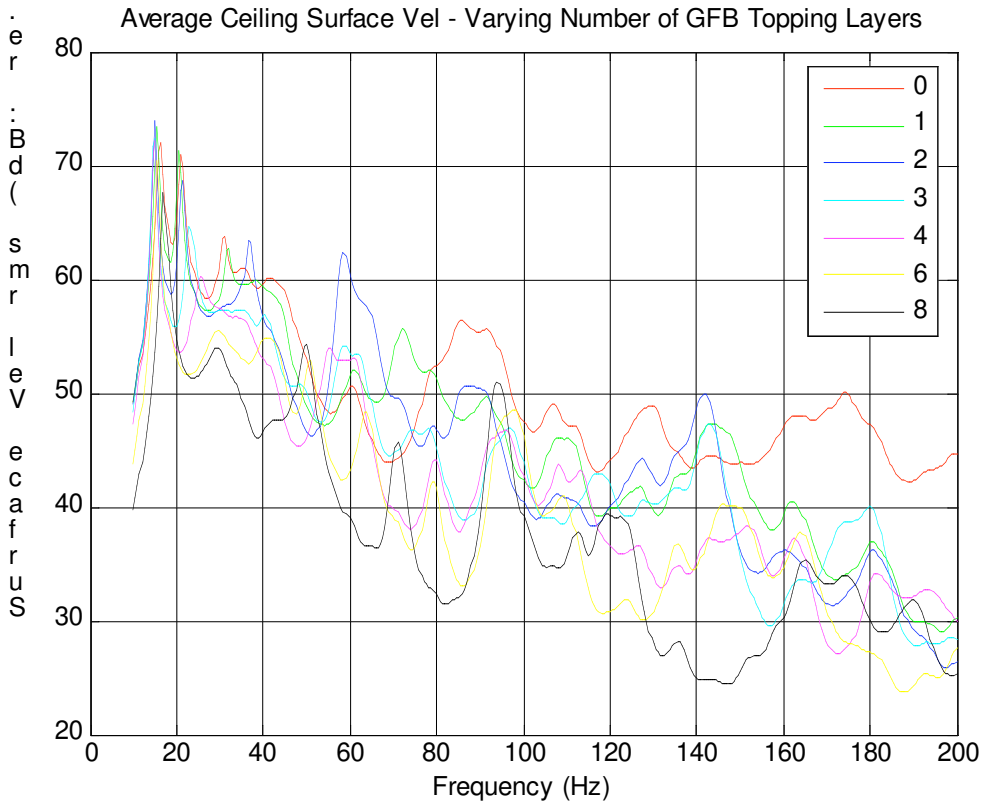

Figure 4-27. The predicted average ceiling surface velocity normalised against the force of the impact on the floor.

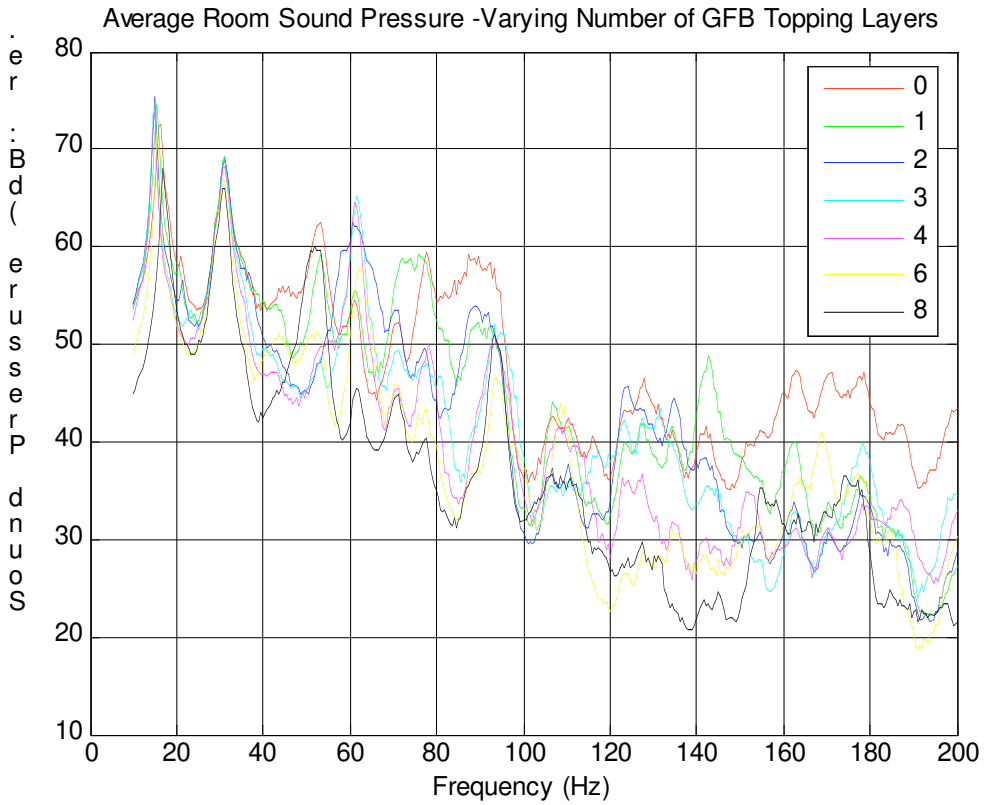

Figure 4-28. The predicted average room sound pressure generated in the receiving room normalised against the force of the impact on the floor.

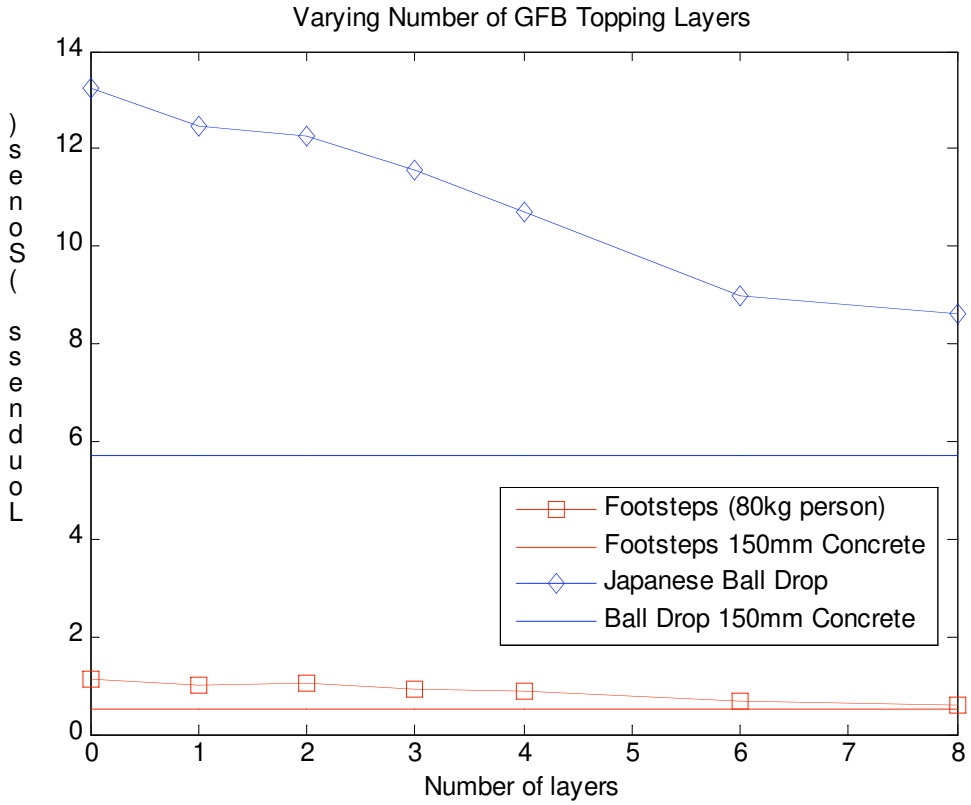

Figure 4-29. The average overall Loudness in Sones produced by a model footstep and a Japanese impact ball in the receiving room below the floor.

4.6 CAVITY AND CEILING CONNECTION PROPERTIES

In this section we consider the effects of the parameters of the region which acoustically joins the floor upper and the ceiling. This covers the cavity, its infill, and the properties of the ceiling clips and ceiling battens.

Changing cavity depth

In this section we look at the effect varying the cavity depth has on the floor's performance. Normal cavity depths might range from 200mm to 400mm.

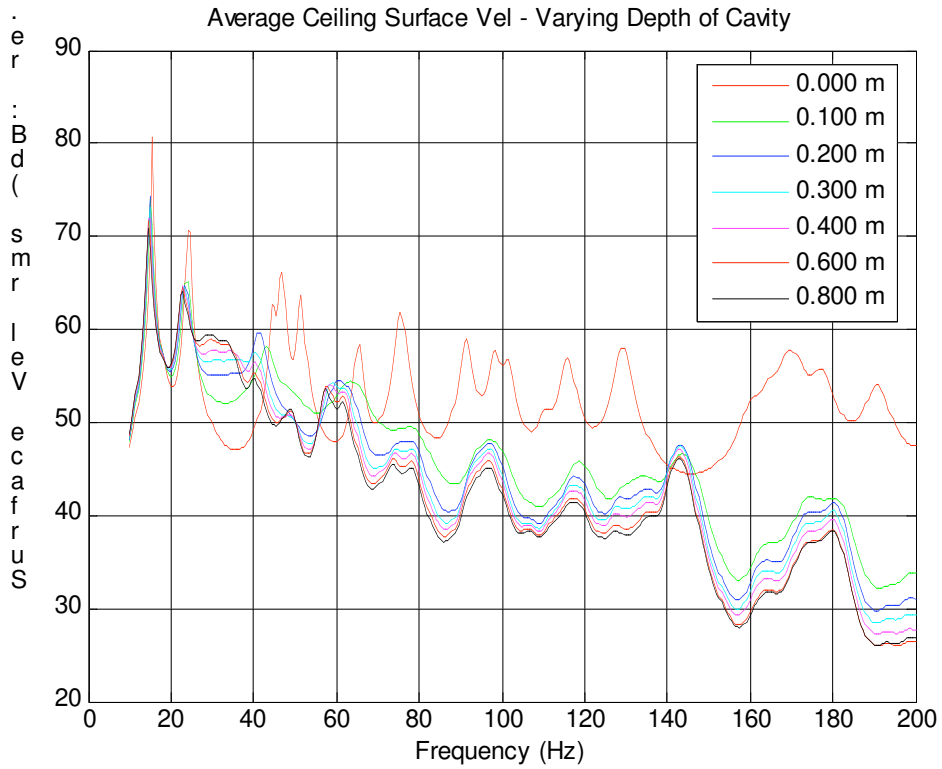

Figure 4-30. The predicted average ceiling surface velocity normalised against the force of the impact on the floor.

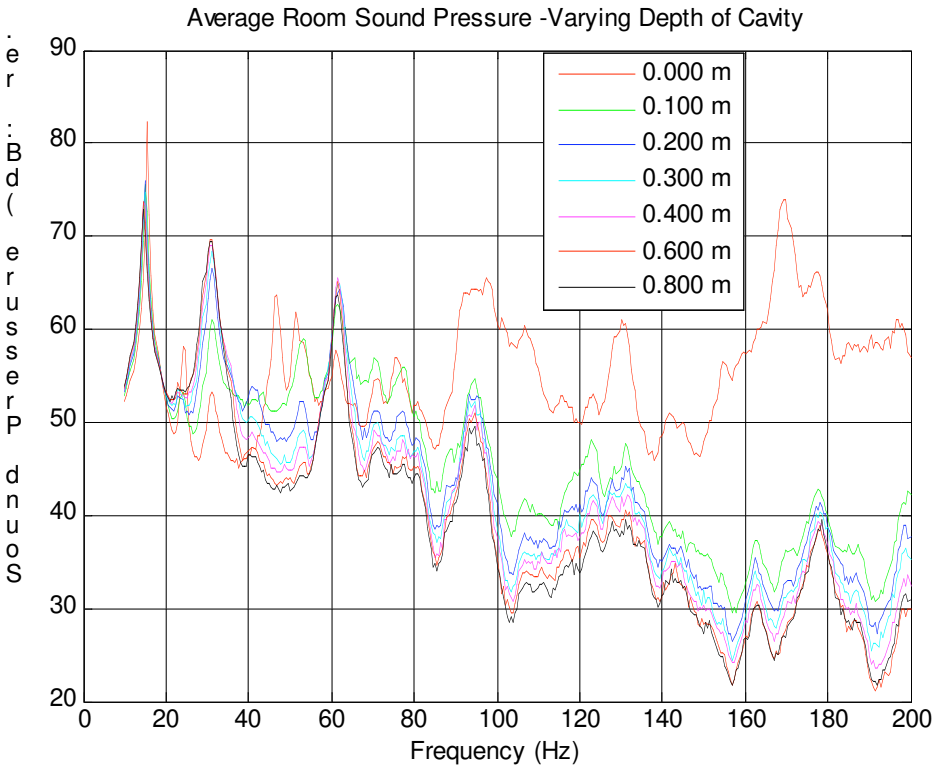

Figure 4-31. The predicted average room sound pressure generated in the receiving room normalised against the force of the impact on the floor.

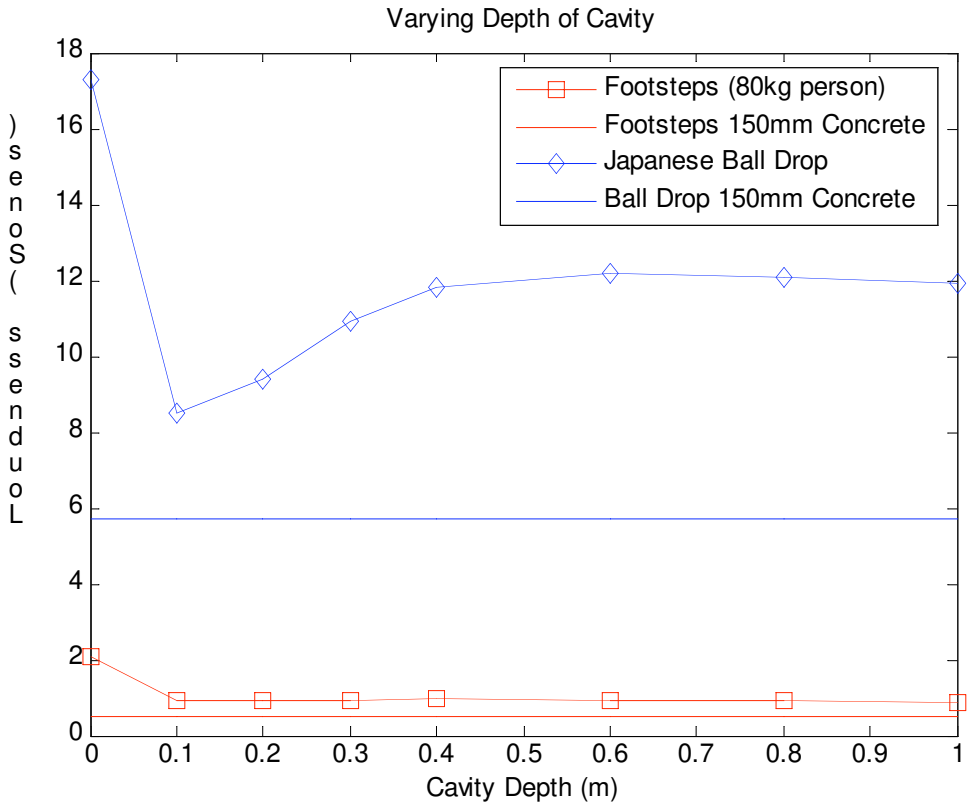

Figure 4-32. The average overall Loudness in Sones produced by a model footstep and a Japanese impact ball in the receiving room below the floor.

Changing absorption of cavity infill

In this section we look at the effect of varying the acoustic absorption of the cavity infill. We assume that the cavity is completely full of infill, and we change the flow resistivity of the infill. For reference, normal fibreglass used for thermal insulation (e.g. Pink Batts) has a flow resistivity of about 1600 Rayls/m, whereas sound control fibreglass infill can have a flow resistivity of about 7000 Rayls/m.

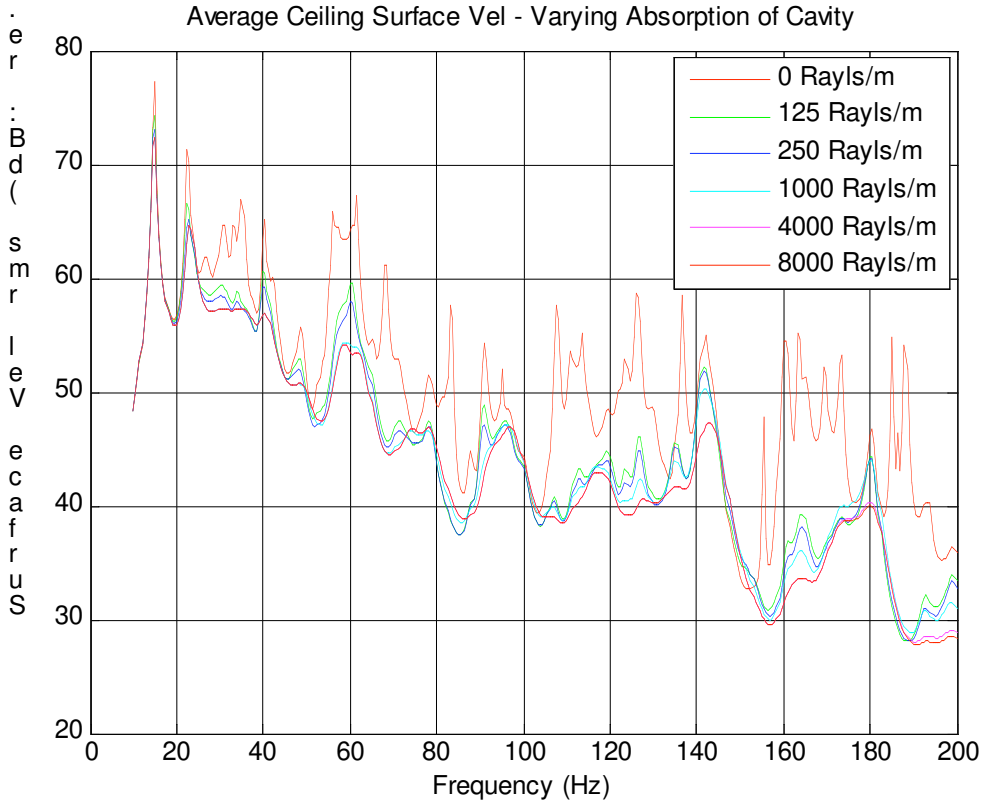

Figure 4-33. The predicted average ceiling surface velocity normalised against the force of the impact on the floor.

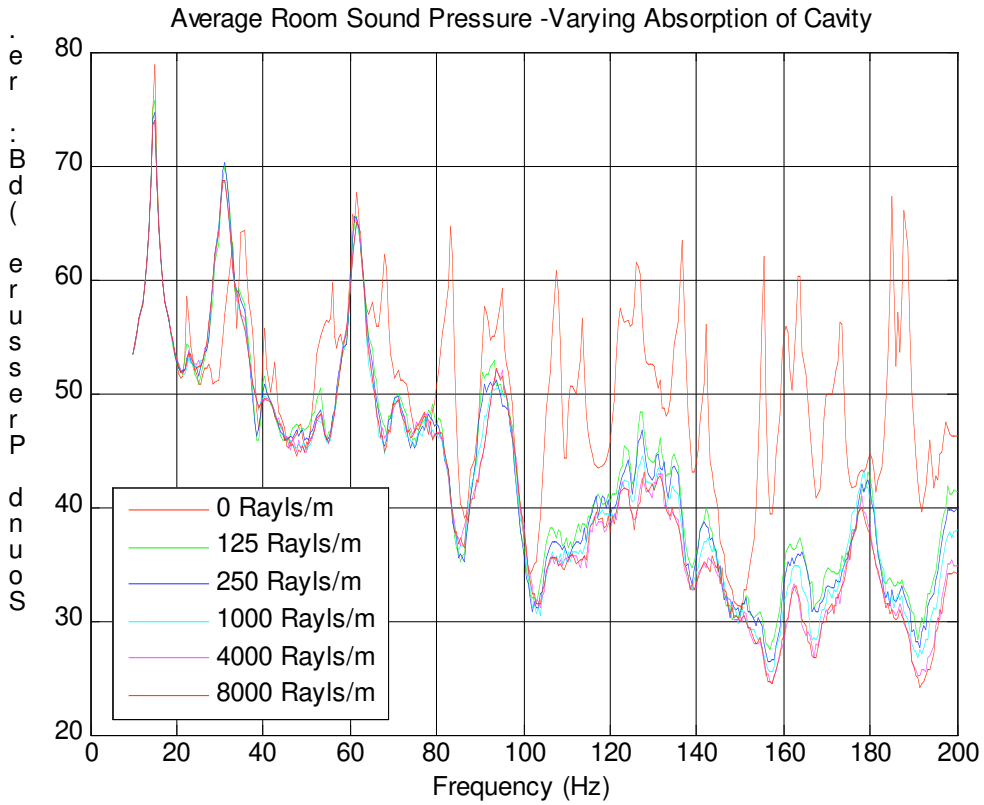

Figure 4-34. The predicted average room sound pressure generated in the receiving room normalised against the force of the impact on the floor.

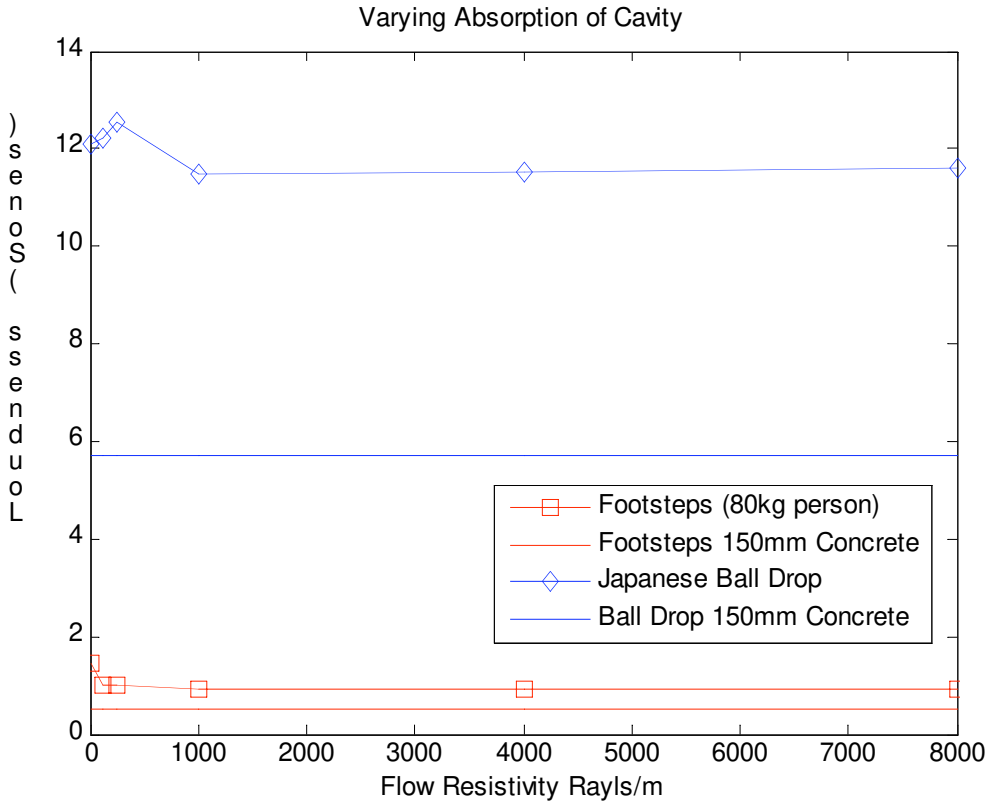

Figure 4-35. The average overall Loudness in Sones produced by a model footstep and a Japanese impact ball in the receiving room below the floor.

Changing ceiling clip stiffness

In this section we examine the effect of changing the stiffness of the ceiling clips. It is assumed that there is a ceiling clip under every joist for every batten (rather than every other batten, as is normal – a constraint of the floor model), so for this floor we have ceiling clips at 400mm centres along the ceiling batten. For reference, a RSIC-1 clip has a stiffness of 220000 N/m, which for the model is reduced to about half that value since they are attached at 800mm centres (every other joist).

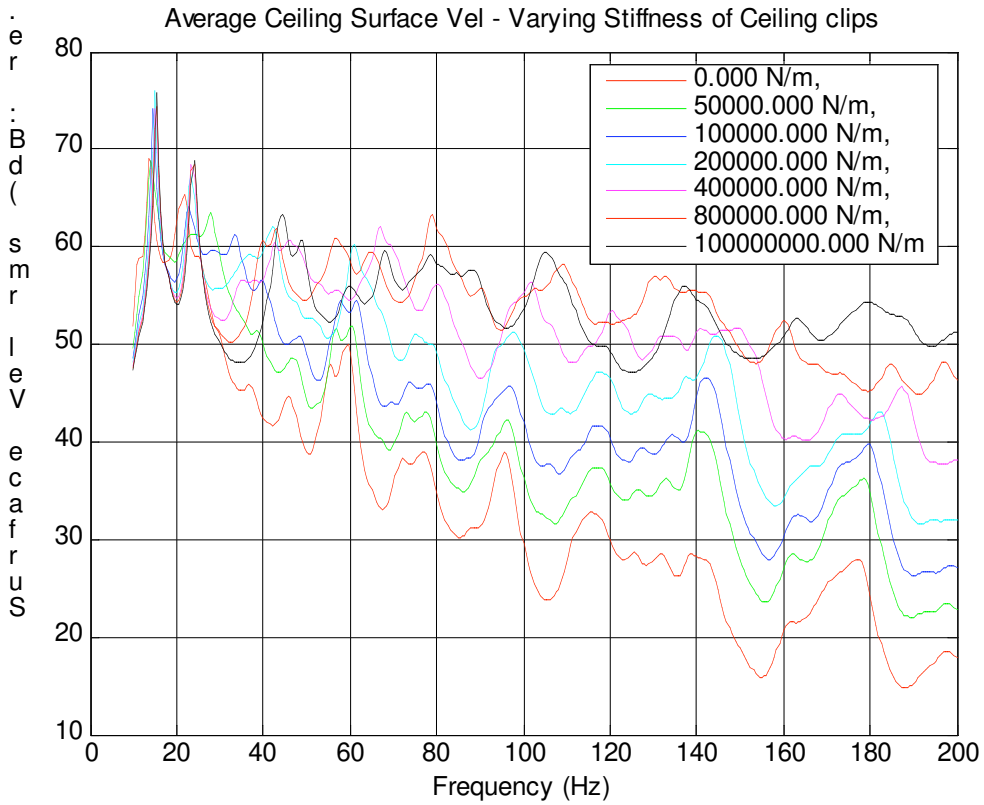

Figure 4-36. The predicted average ceiling surface velocity normalised against the force of the impact on the floor.

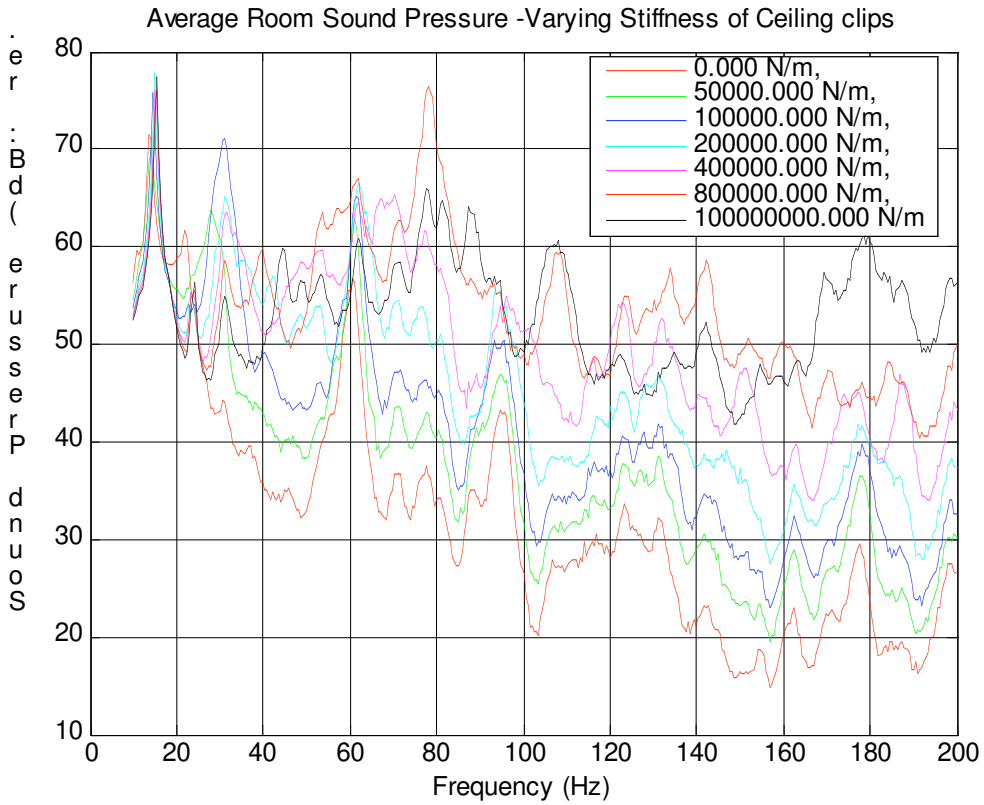

Figure 4-37. The predicted average room sound pressure generated in the receiving room normalised against the force of the impact on the floor.

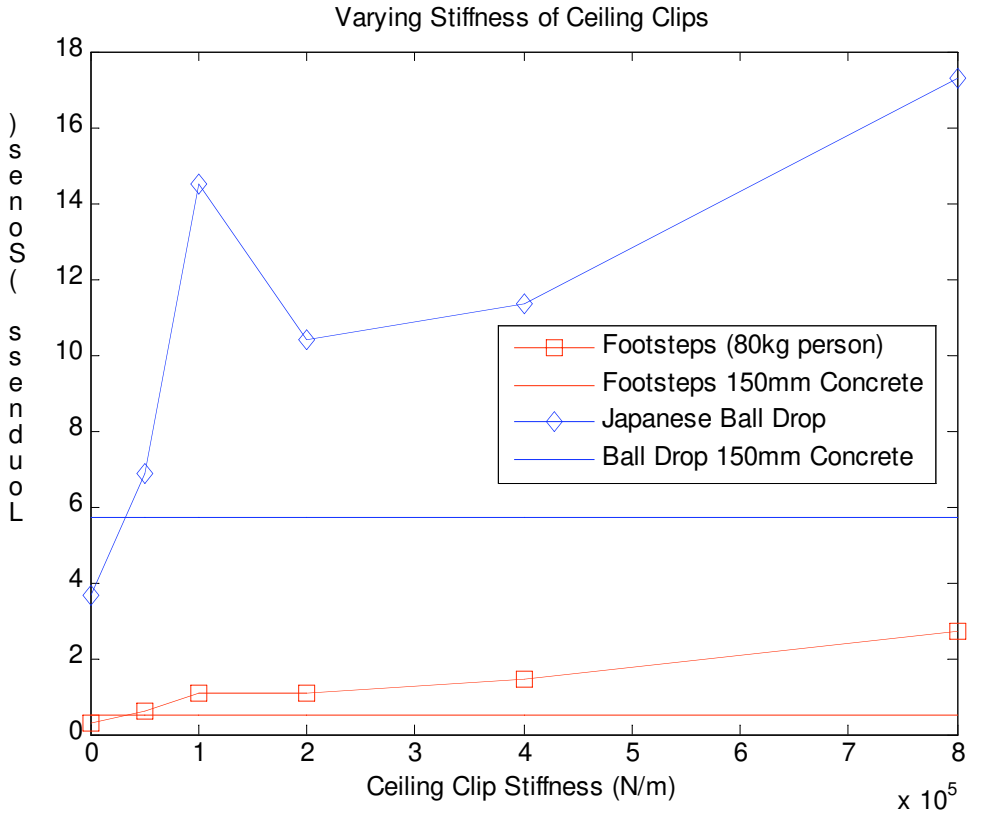

Figure 4-38. The average overall Loudness in Sones produced by a model footstep and a Japanese impact ball in the receiving room below the floor.

Changing the vibrational damping of the ceiling clips

In this section we examine the effect of changing the vibrational damping of the ceiling clips. For reference, the RSIC-1 clips, which are rubber, have a damping coefficient of about 0.1.

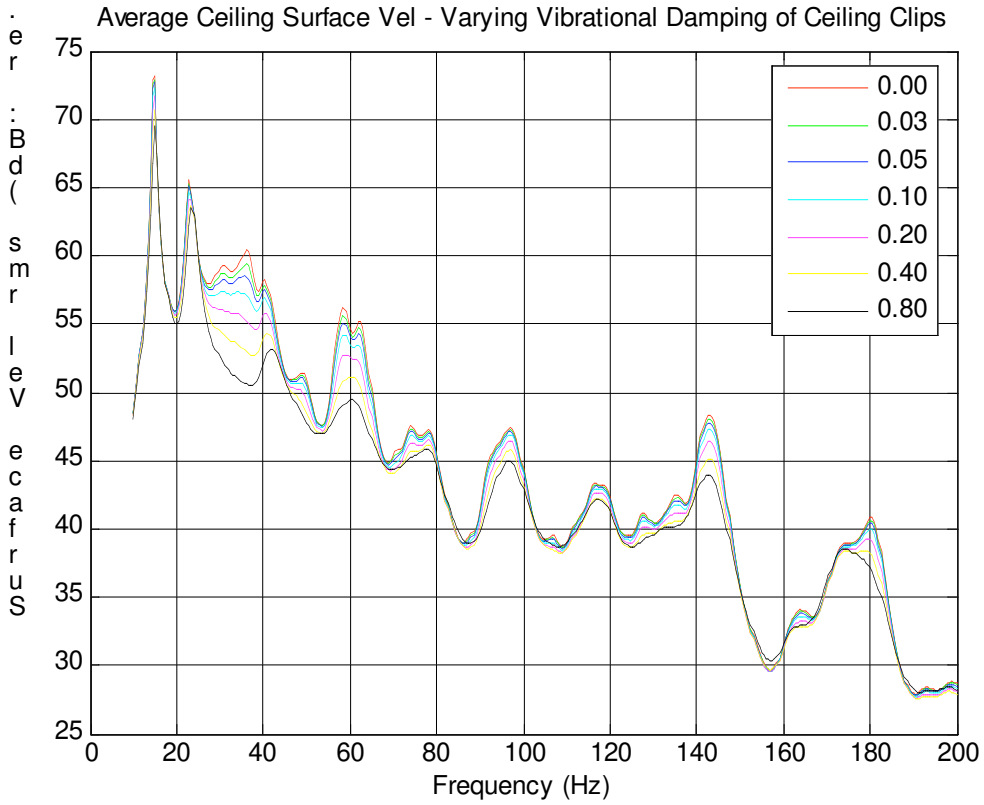

Figure 4-39. The predicted average ceiling surface velocity normalised against the force of the impact on the floor.

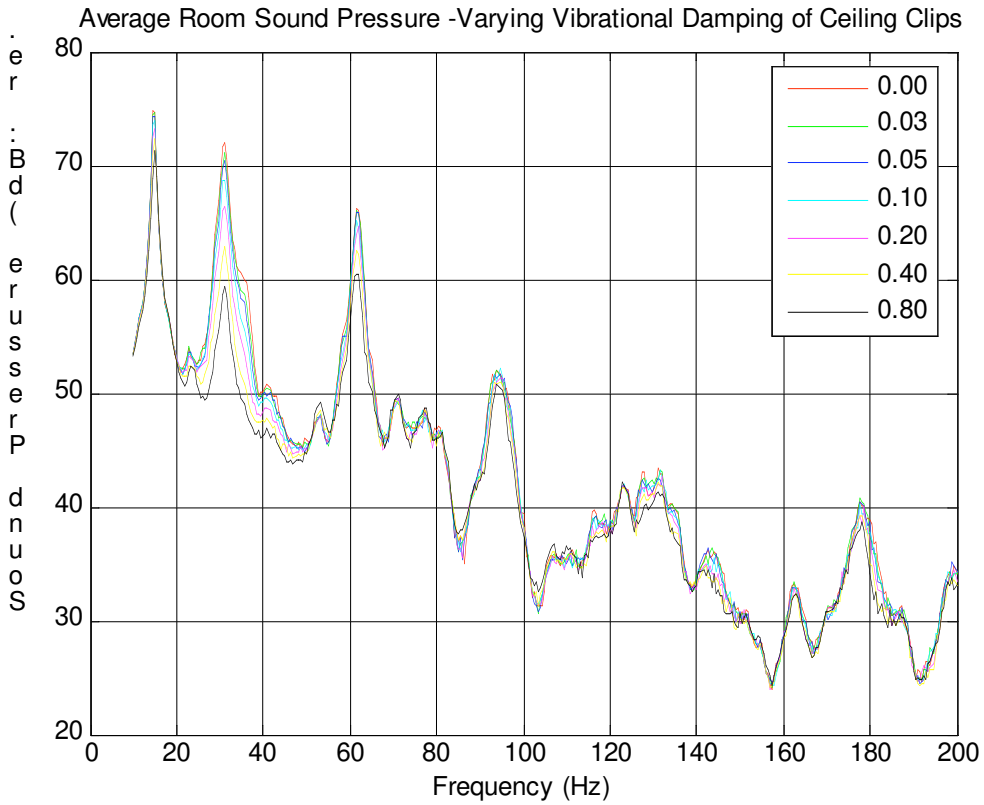

Figure 4-40. The predicted average room sound pressure generated in the receiving room normalised against the force of the impact on the floor.

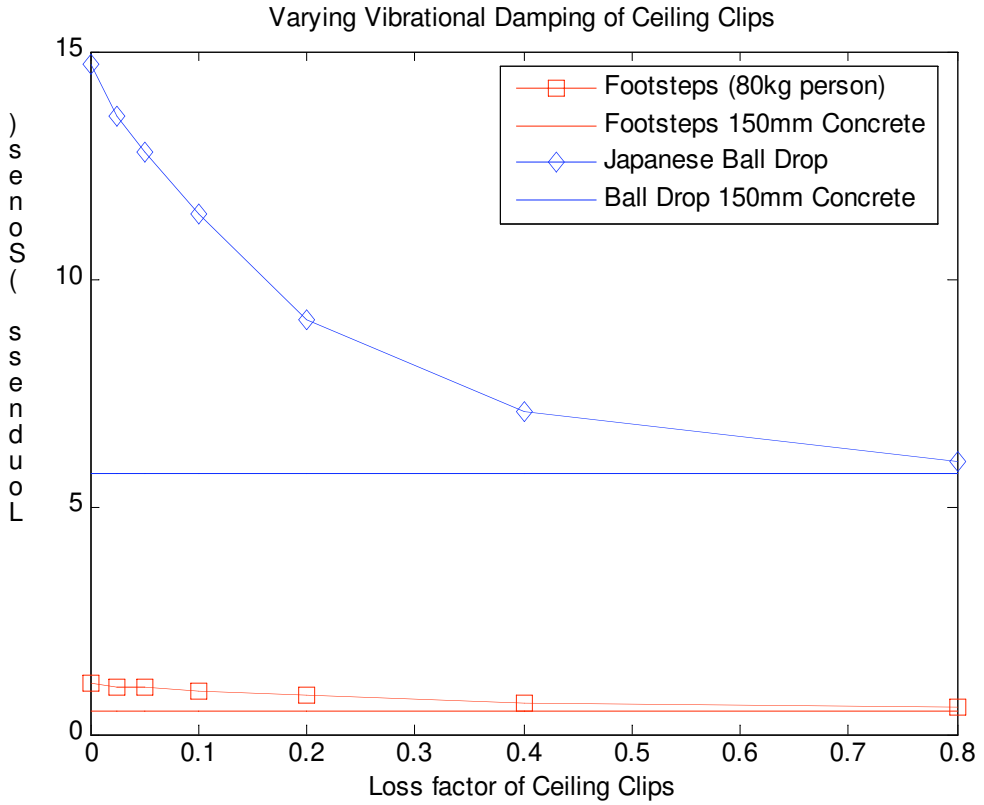

Figure 4-41. The average overall Loudness in Sones produced by a model footstep and a Japanese impact ball in the receiving room below the floor.

Changing the bending stiffness of the ceiling battens

In this section we see the effect of changing the bending stiffness of the ceiling battens. For reference, the pressed steel battens of Floor 3 had a bending stiffness of about 11000 Nm^2.

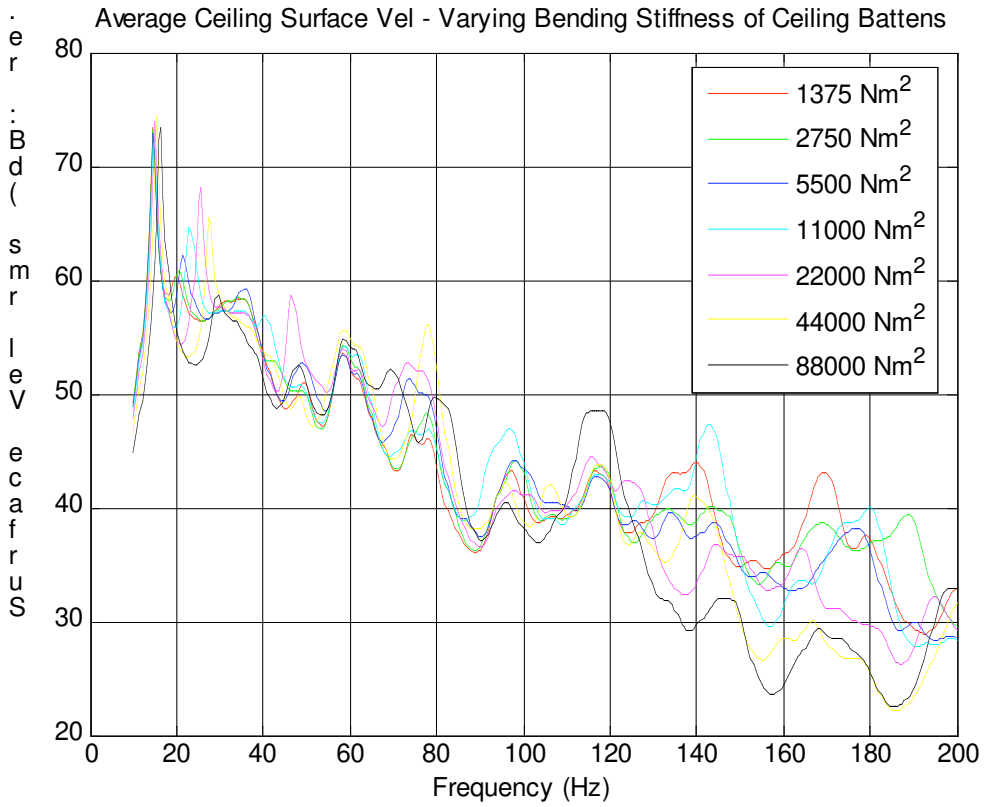

Figure 4-42. The predicted average ceiling surface velocity normalised against the force of the impact on the floor.

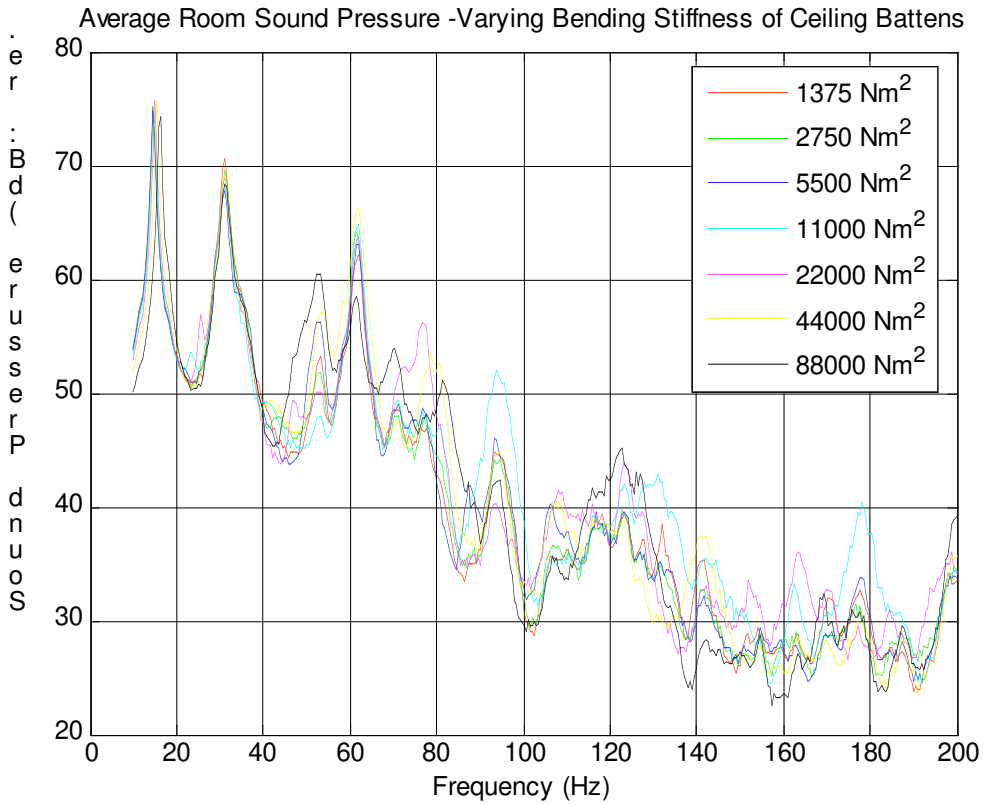

Figure 4-43. The predicted average room sound pressure generated in the receiving room normalised against the force of the impact on the floor.

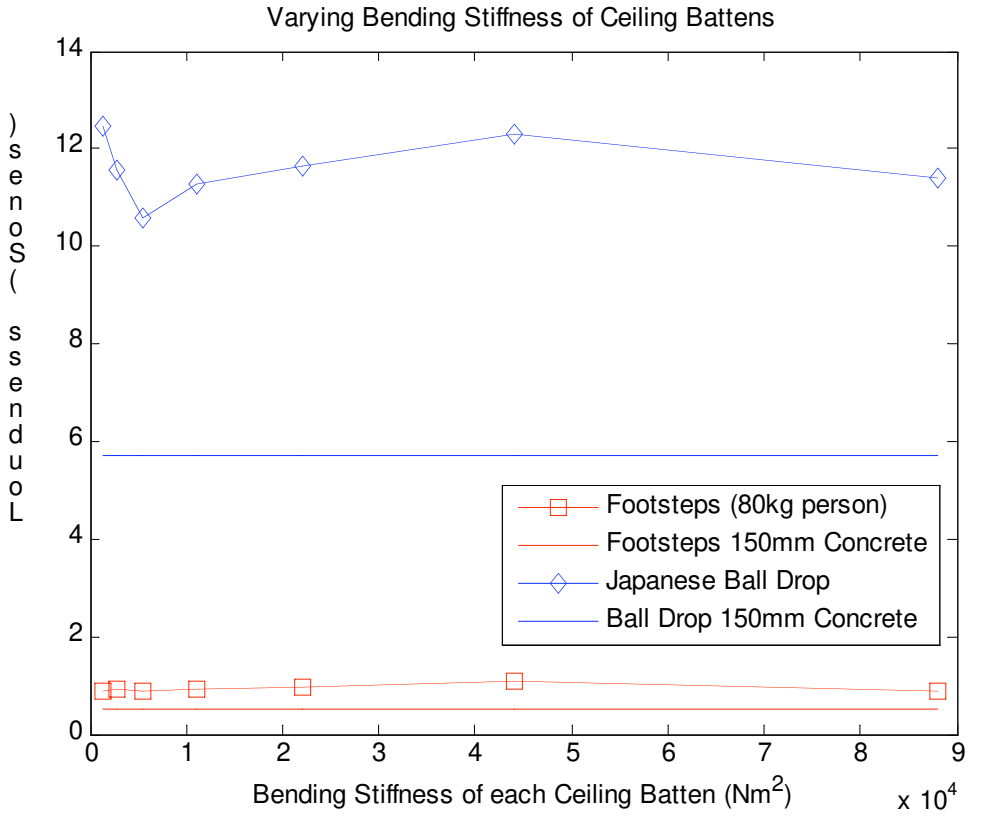

Figure 4-44. The average overall Loudness in Sones produced by a model footstep and a Japanese impact ball in the receiving room below the floor.

4.7 CEILING PROPERTIES

Changing the surface density of the ceiling

In this section the effect of changing the surface density of the ceiling is observed. Only the surface density is changed; we keep the bending stiffness of the ceiling equal to that of 2 layers of 13mm noise control plasterboard. For reference, the surface density of the ceiling of Floor 3 is 25 kg/m^2.

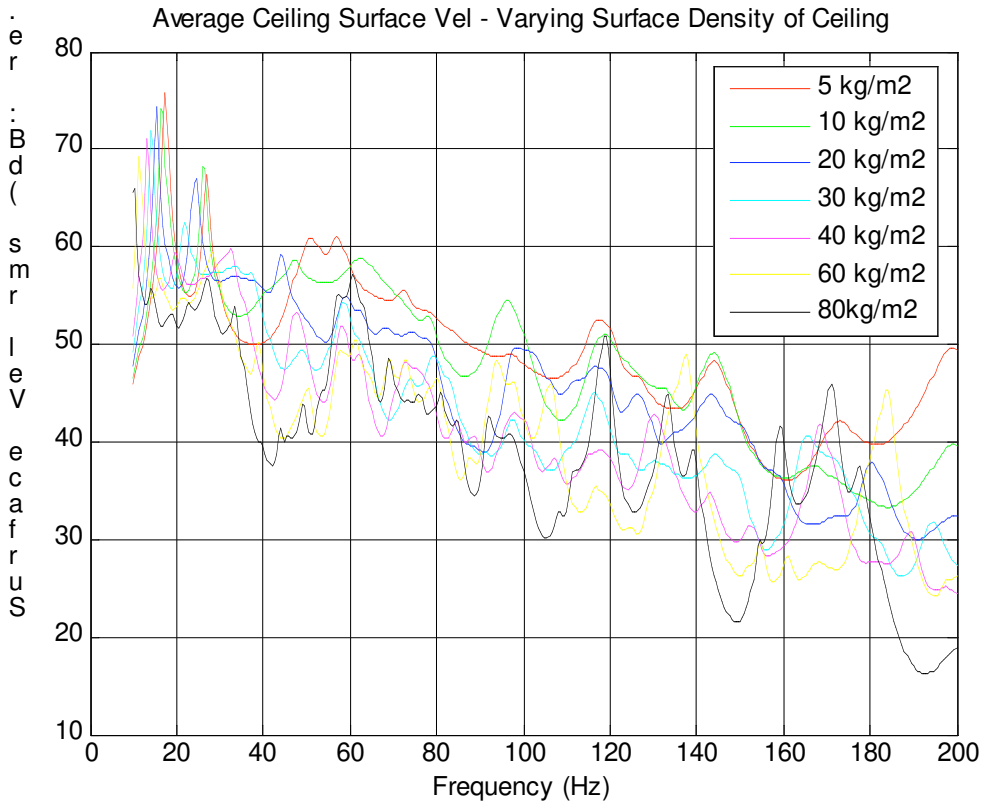

Figure 4-45. The predicted average ceiling surface velocity normalised against the force of the impact on the floor.

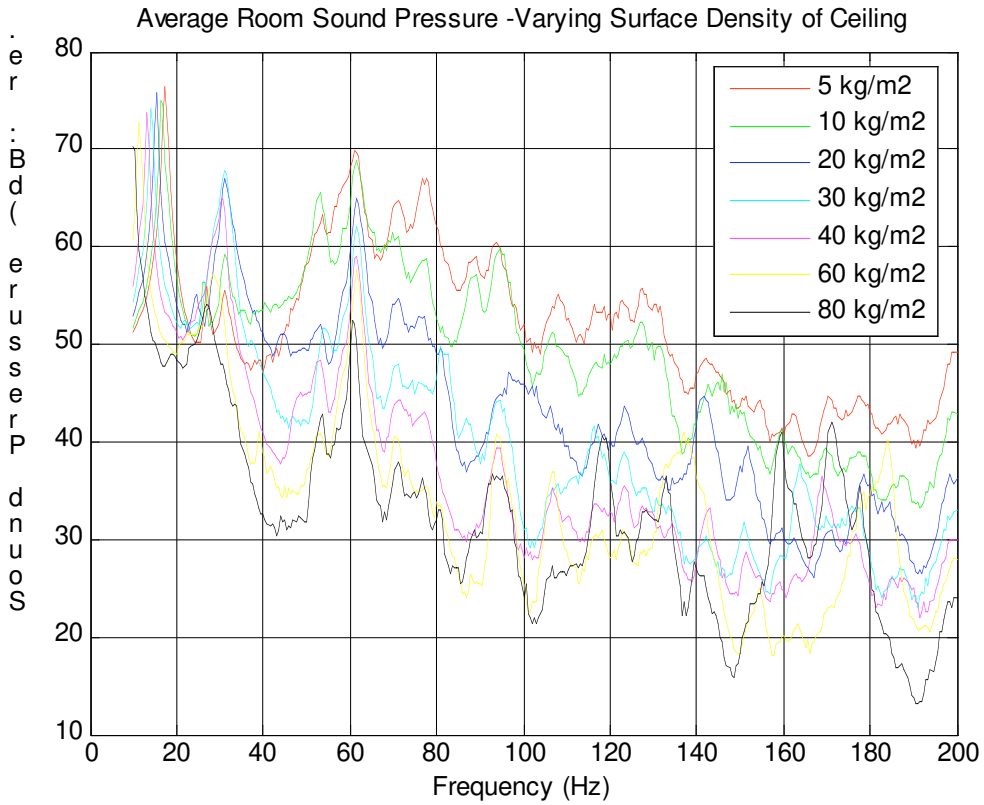

Figure 4-46. The predicted average room sound pressure generated in the receiving room normalised against the force of the impact on the floor.

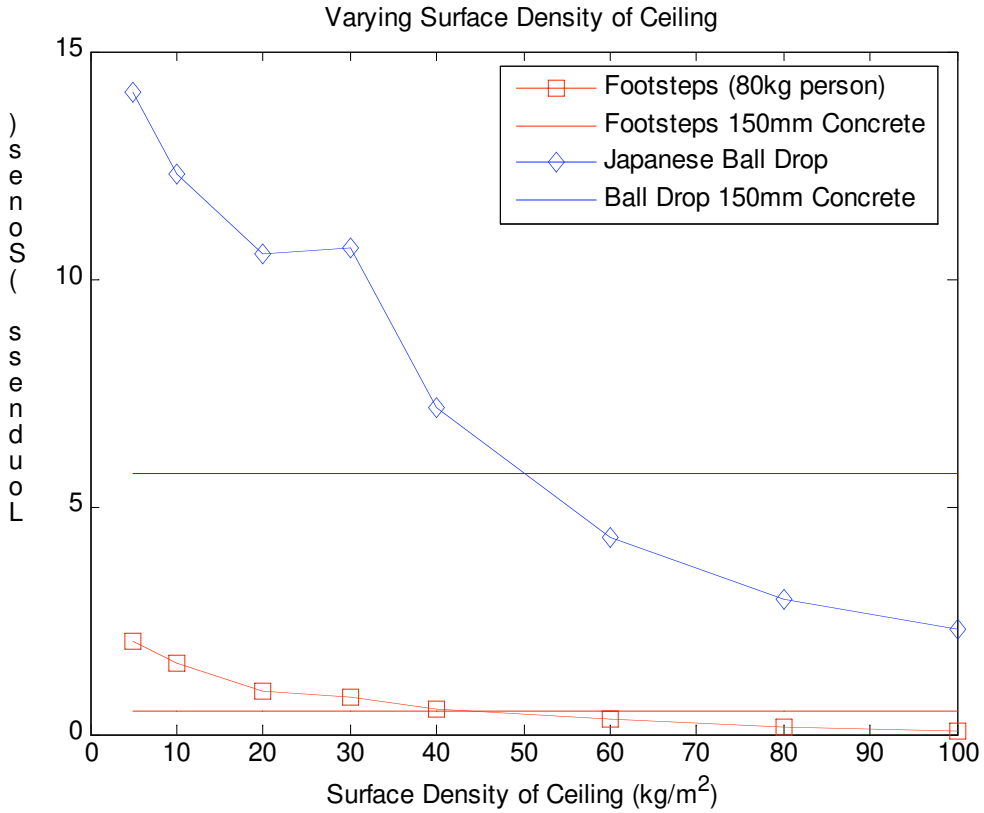

Figure 4-47. The average overall Loudness in Sones produced by a model footstep and a Japanese impact ball in the receiving room below the floor.

Changing the bending stiffness of the ceiling

In this section the effect of changing the bending stiffness of the ceiling is observed. Only the bending stiffness is changed; we keep the surface density of the ceiling equal to that of 2 layers of 13mm noise control plasterboard. For reference, the bending stiffness of the ceiling of Floor 3 is 1500 Nm.

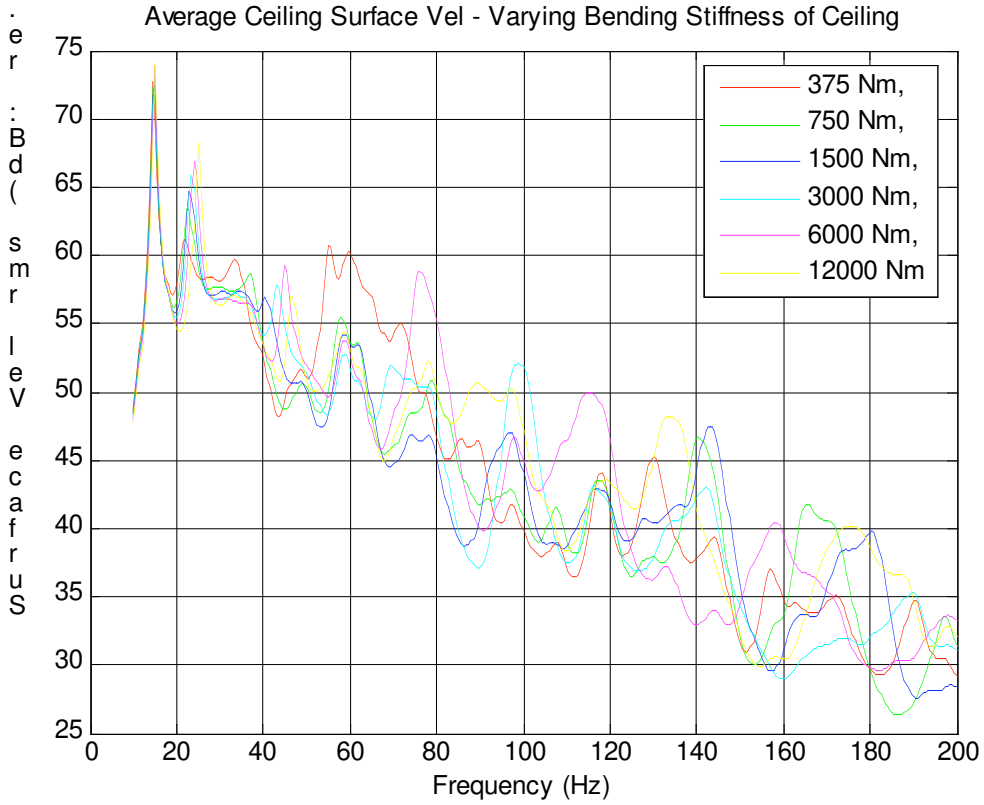

Figure 4-48. The predicted average ceiling surface velocity normalised against the force of the impact on the floor.

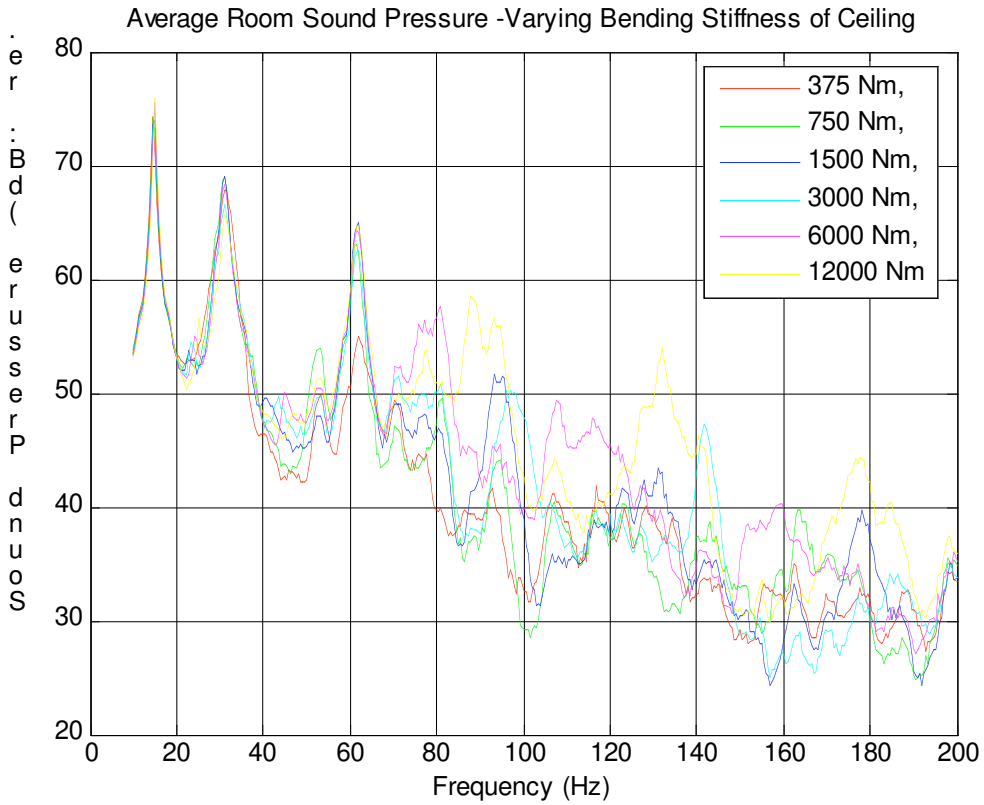

Figure 4-49. The predicted average room sound pressure generated in the receiving room normalised against the force of the impact on the floor.

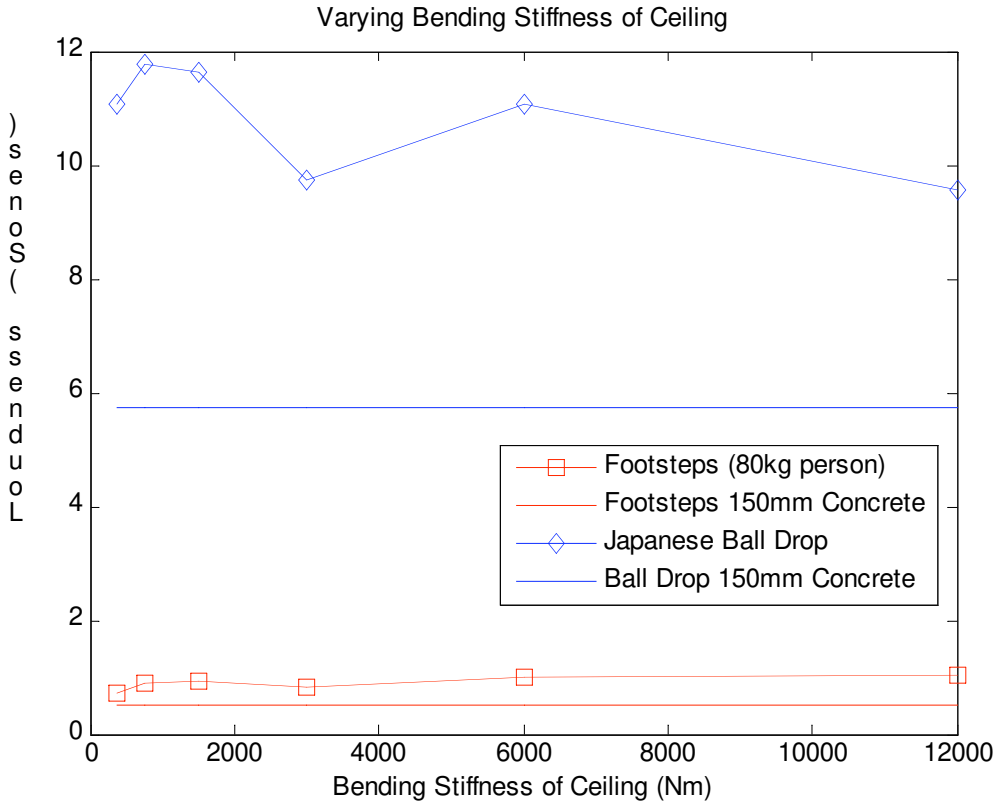

Figure 4-50. The average overall Loudness in Sones produced by a model footstep and a Japanese impact ball in the receiving room below the floor.

Changing the vibration damping of the ceiling

In this section the effect of changing the vibration damping of the ceiling is observed. For reference, we expect the damping loss factor of the ceiling of Floor 3 to be about 0.02.

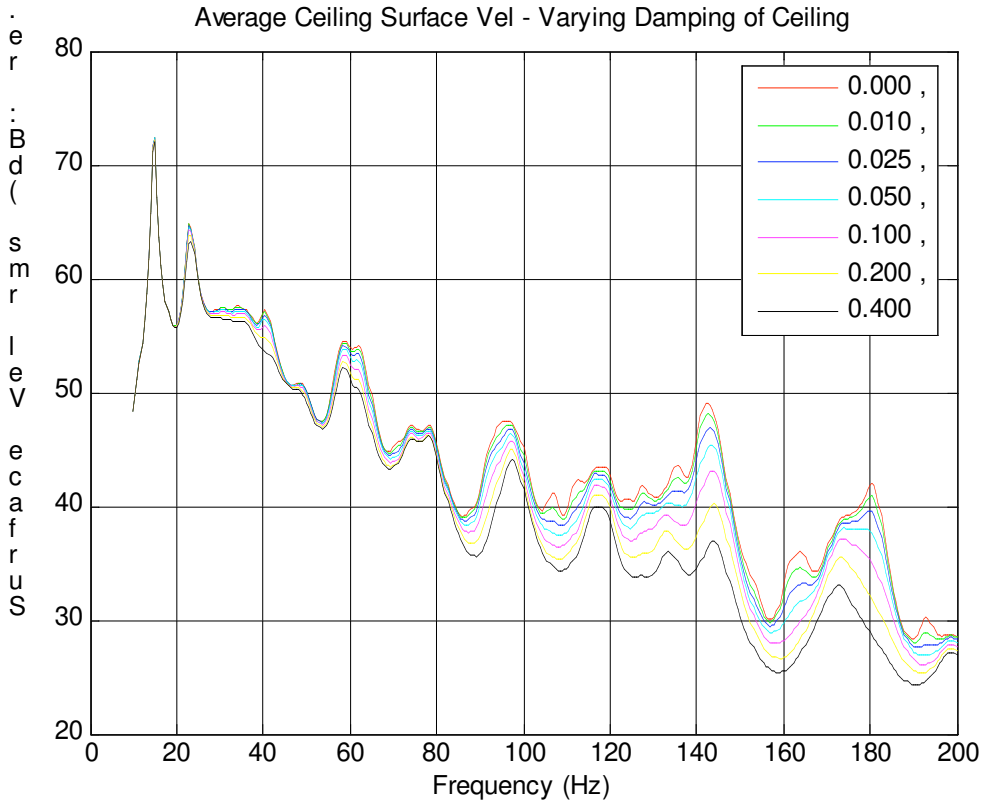

Figure 4-51. The predicted average ceiling surface velocity normalised against the force of the impact on the floor.

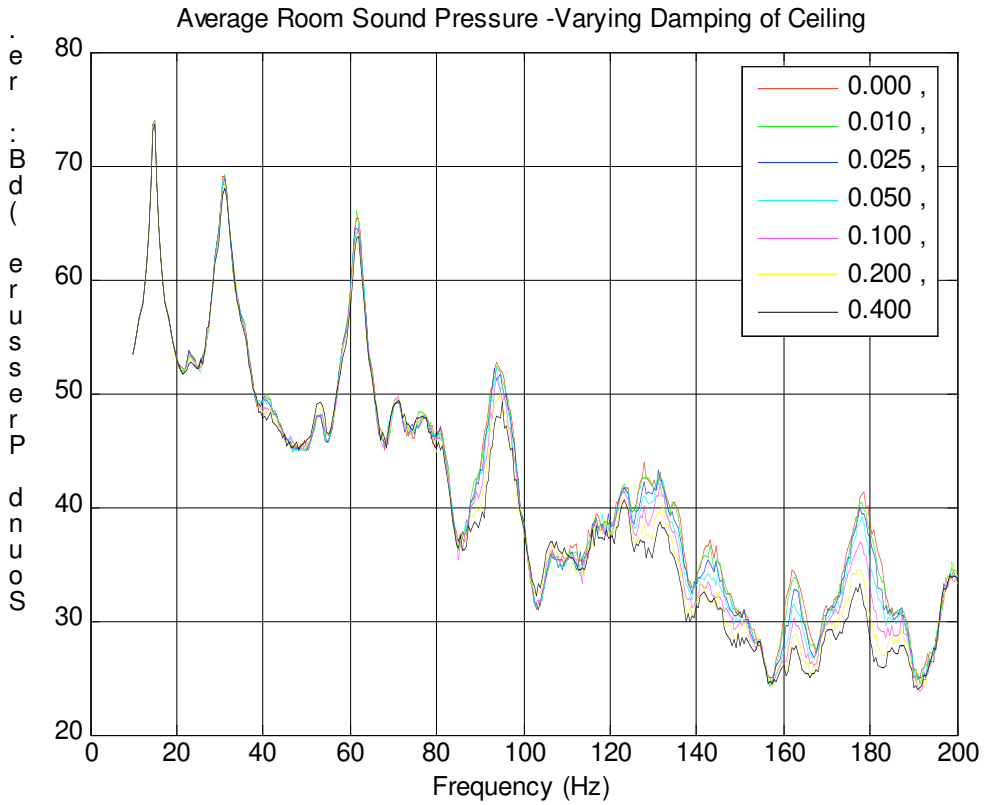

Figure 4-52. The predicted average room sound pressure generated in the receiving room normalised against the force of the impact on the floor.

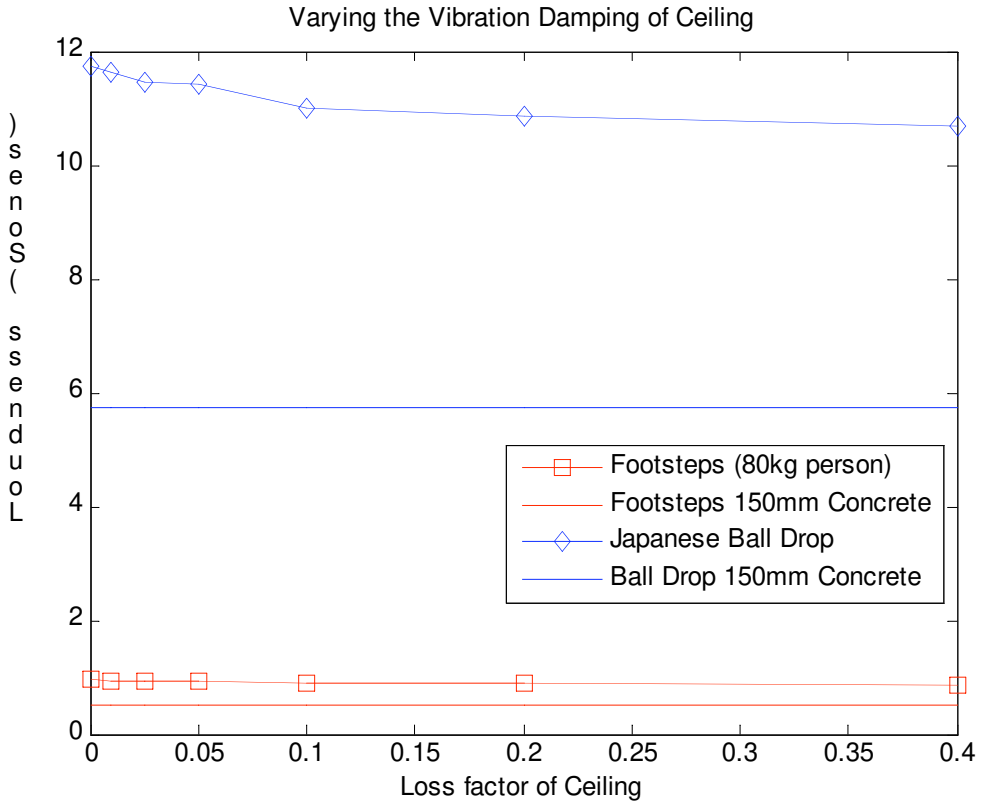

Figure 4-53. The average overall Loudness in Sones produced by a model footstep and a Japanese impact ball in the receiving room below the floor.

Changing the number of layers of plasterboard in the ceiling

In the previous sections, where we looked at the ceiling, we changed one parameter and somewhat artificially held other parameters constant. In this section we look at what happens when we increase the number of layers of plasterboard in the ceiling – in effect, we are changing both the surface density and bending stiffness of the ceiling. The noise control plasterboard has a Young's modulus of 3.7GPa, a thickness of 13mm and a surface density of 12.5 kg/m^2 per layer. It is assumed that the layers slip when the ceiling flexes.

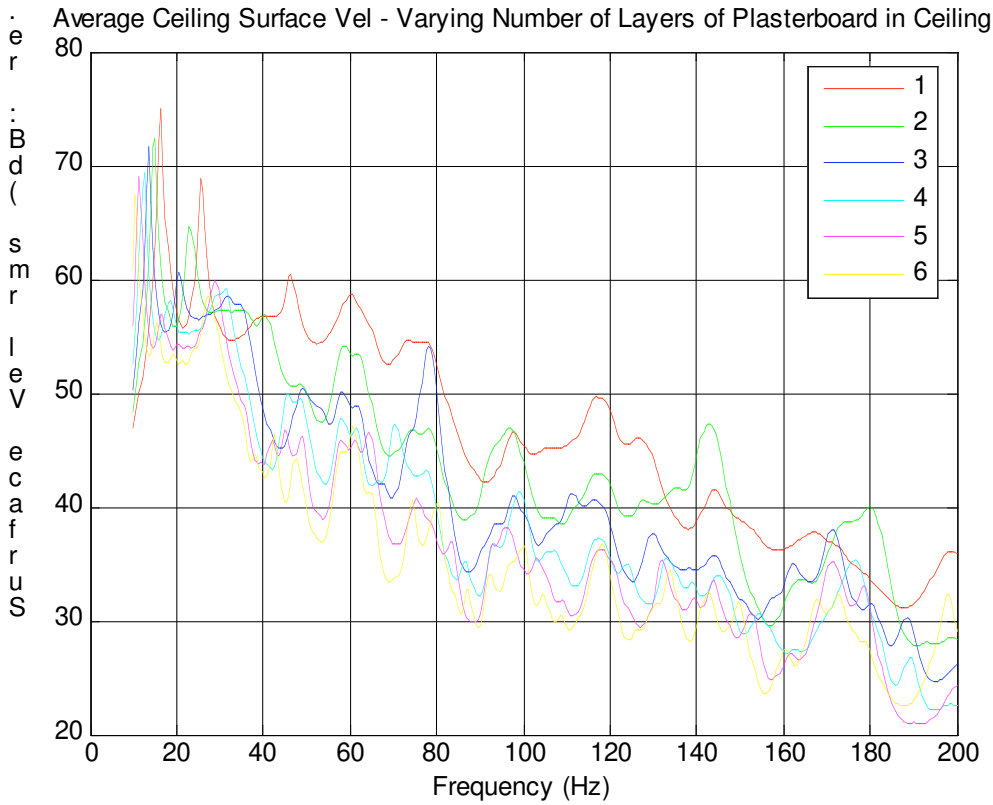

Figure 4-54. The predicted average ceiling surface velocity normalised against the force of the impact on the floor.

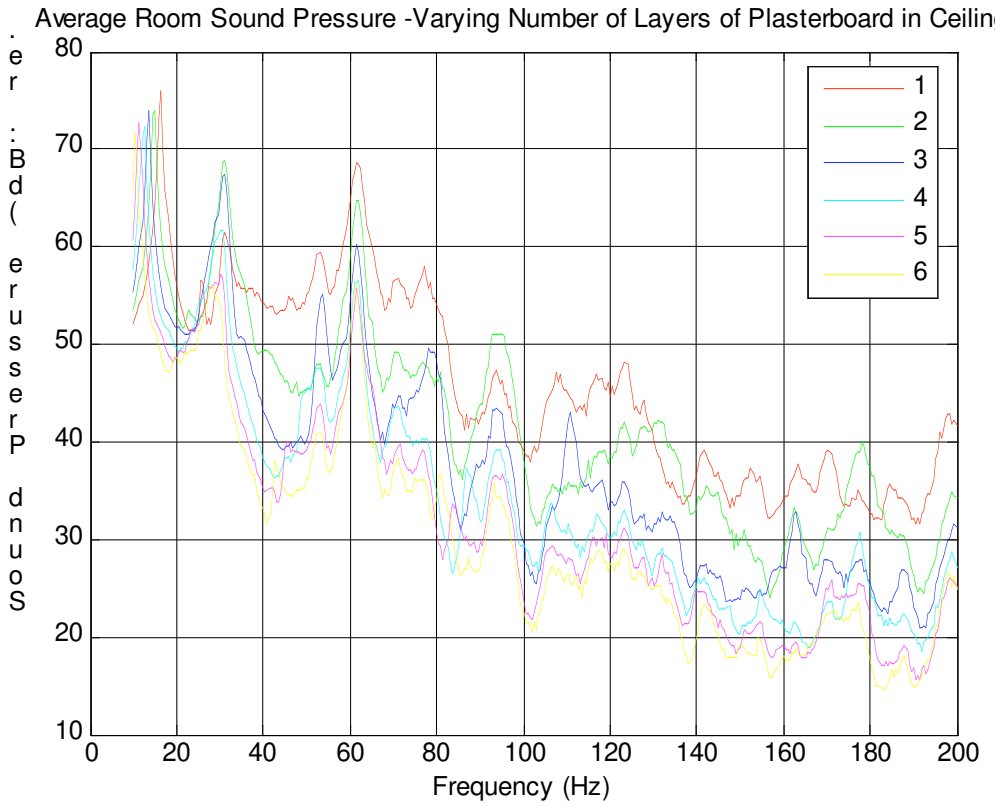

Figure 4-55. The predicted average room sound pressure generated in the receiving room normalised against the force of the impact on the floor.

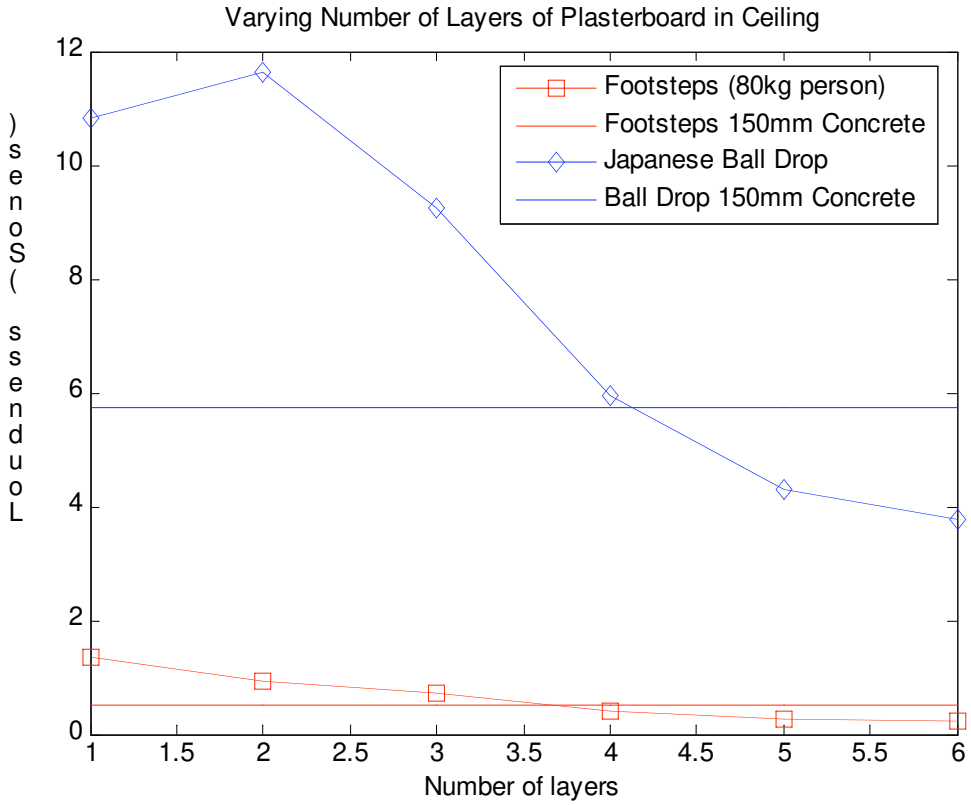

Figure 4-56. The average overall Loudness in Sones produced by a model footstep and a Japanese impact ball in the receiving room below the floor.

4.8 EFFECTS OF FLOOR SPAN AND ROOM SIZE

In this section we explore what happens when the dimension of the floor and hence the room change. We look at the floor span, floor width and height of the room. Since the floor dimensions are changing, the performance of the reference concrete floor is recalculated too.

Changing the length of the floor joists

In this section we look at changing the span of the joists, hence the length of the floor and the length of the room.

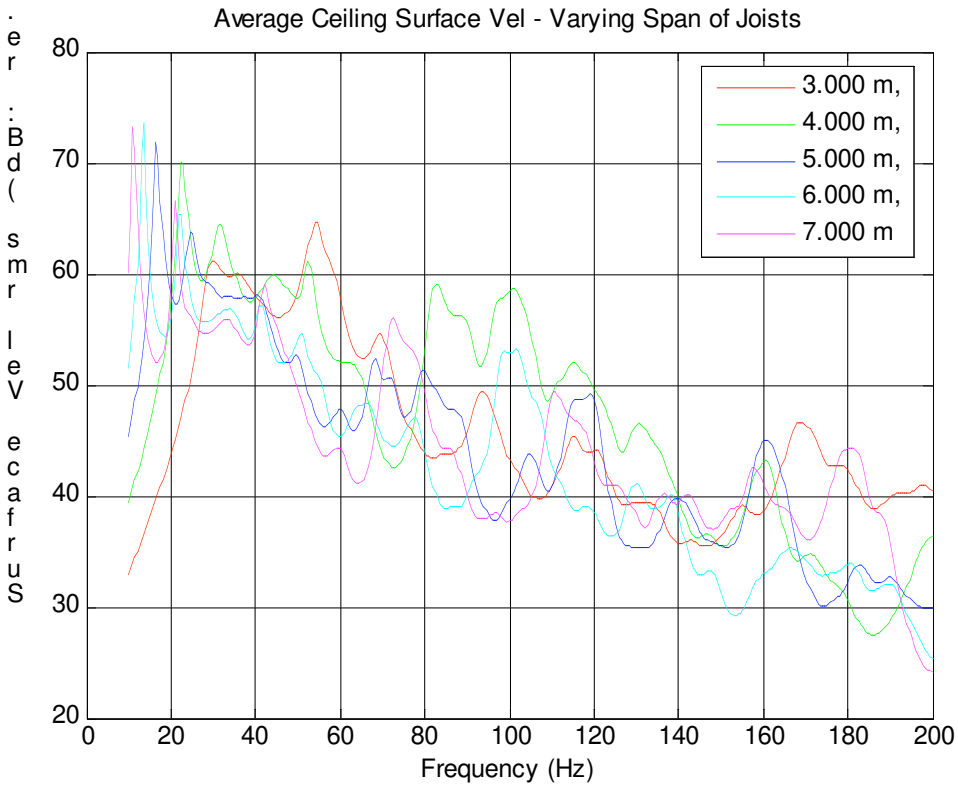

Figure 4-57. The predicted average ceiling surface velocity normalised against the force of the impact on the floor.

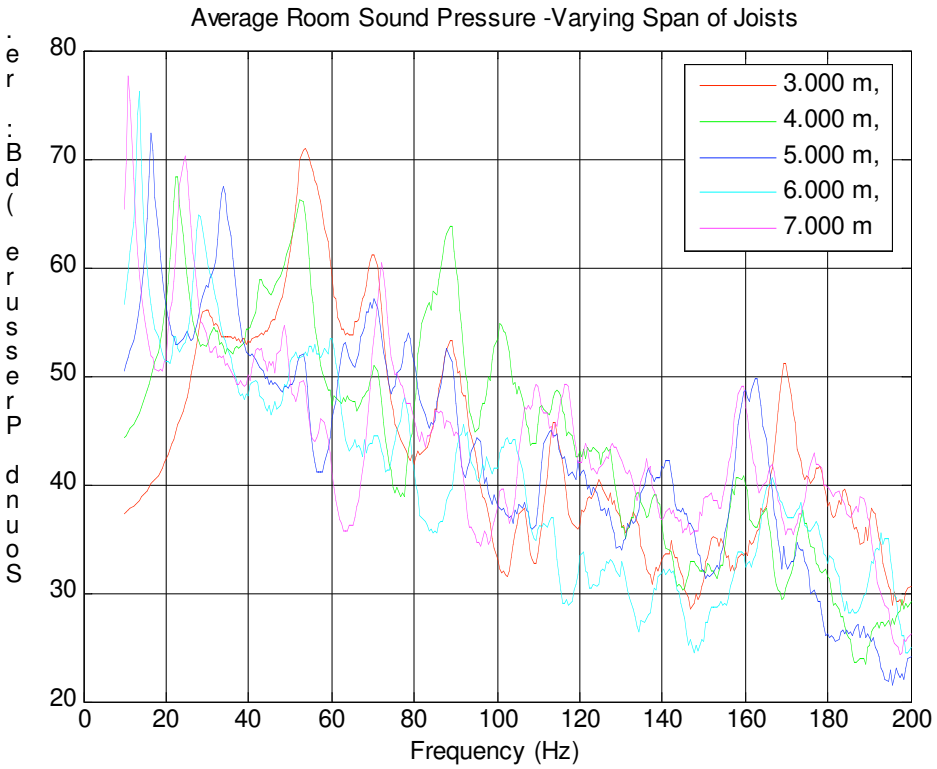

Figure 4-58. The predicted average room sound pressure generated in the receiving room normalised against the force of the impact on the floor.

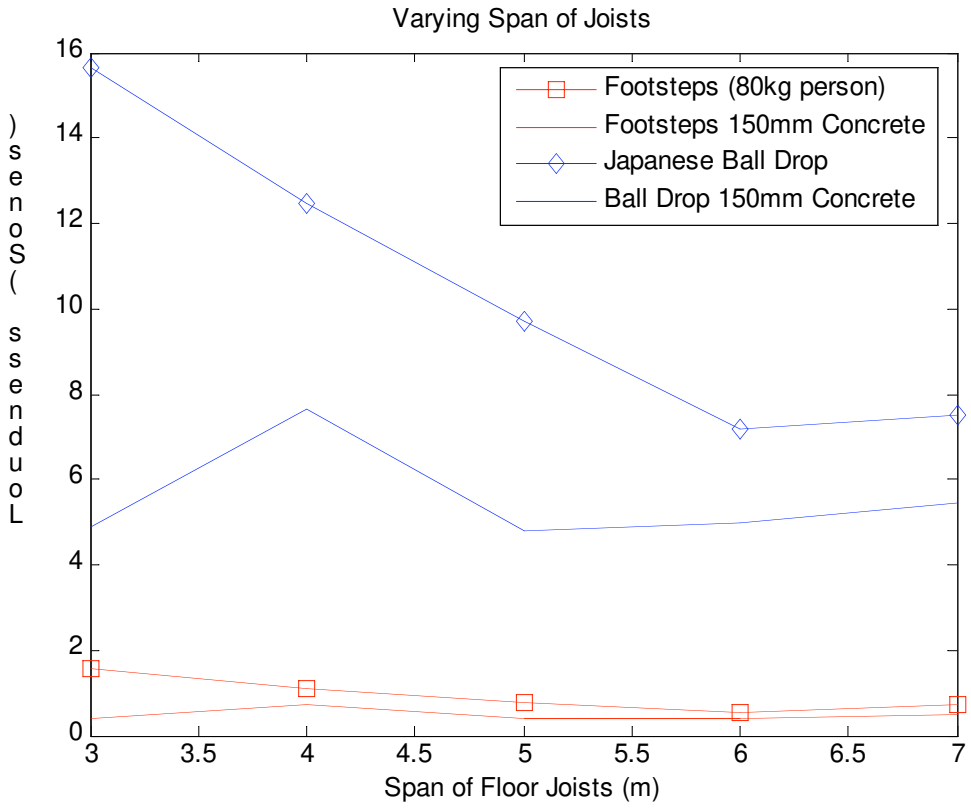

Figure 4-59. The average overall Loudness in Sones produced by a model footstep and a Japanese impact ball in the receiving room below the floor.

Changing the width of the floor

In this section we look at changing the width of the floor and hence the width of the room.

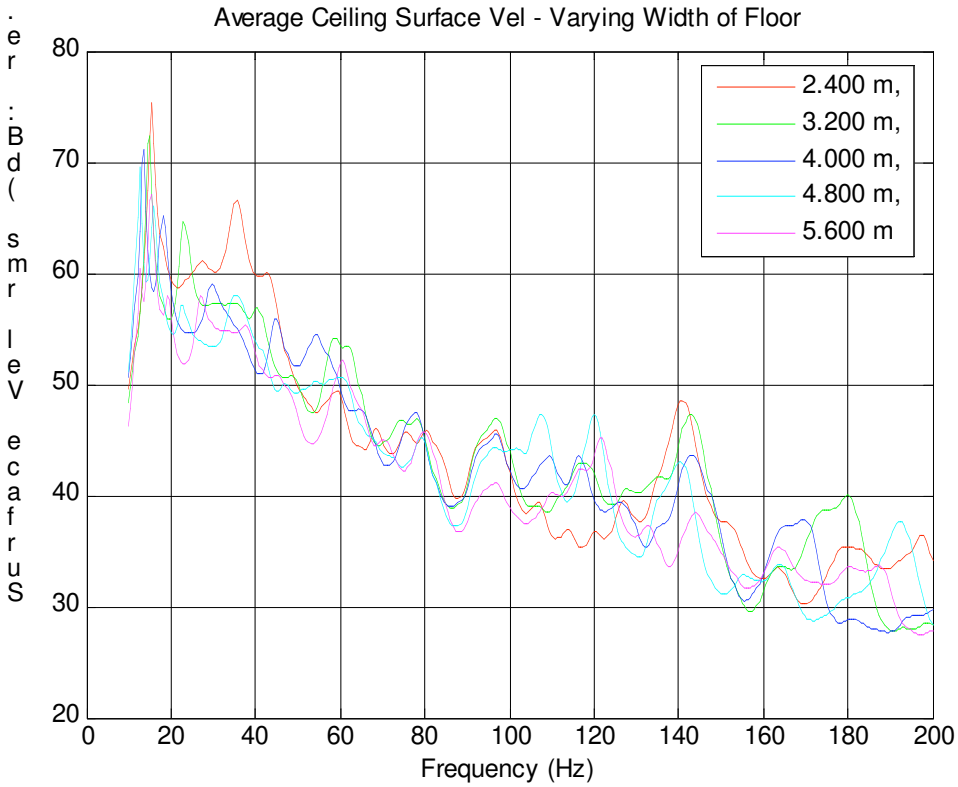

Figure 4-60. The predicted average ceiling surface velocity normalised against the force of the impact on the floor.

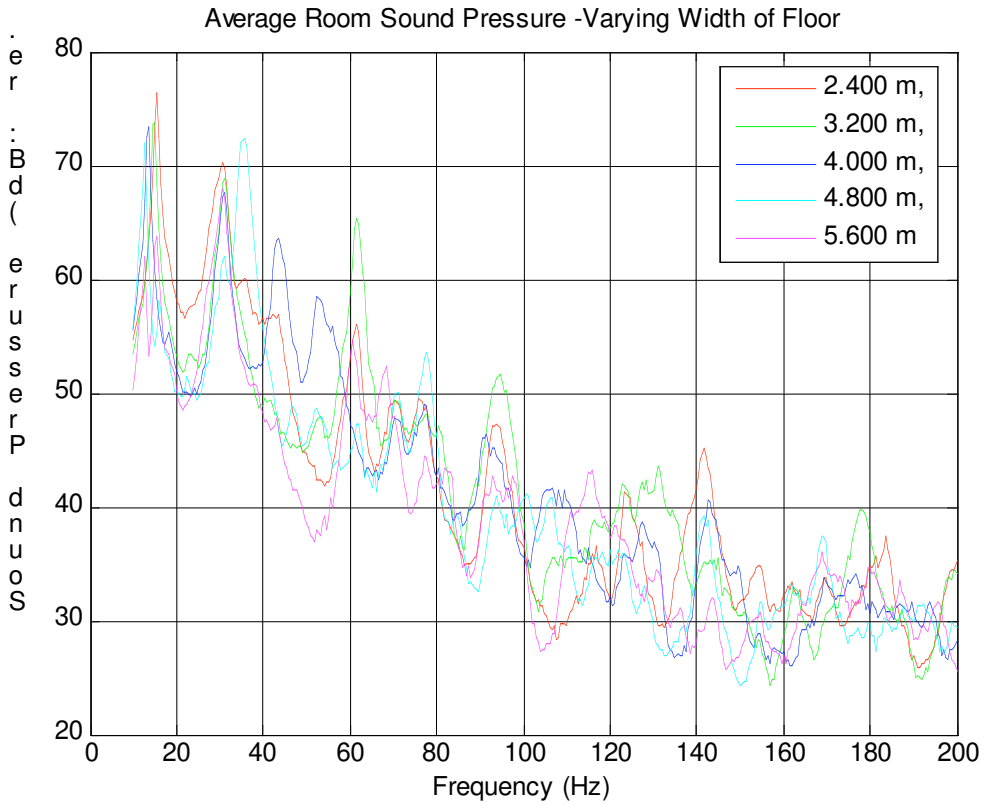

Figure 4-61. The predicted average room sound pressure generated in the receiving room normalised against the force of the impact on the floor.

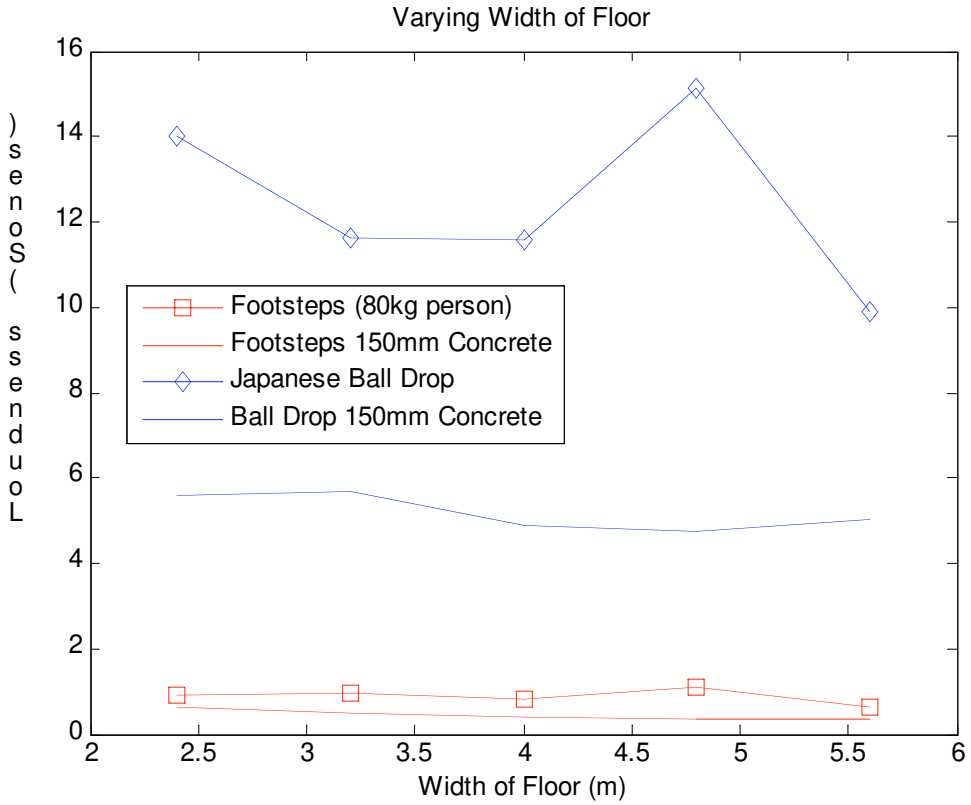

Figure 4-62. The average overall Loudness in Sones produced by a model footstep and a Japanese impact ball in the receiving room below the floor.

Varying the height of the receiving room

In this section we do not change the floor itself by rather look at changing the height of the receiving room to see how this might affect results.

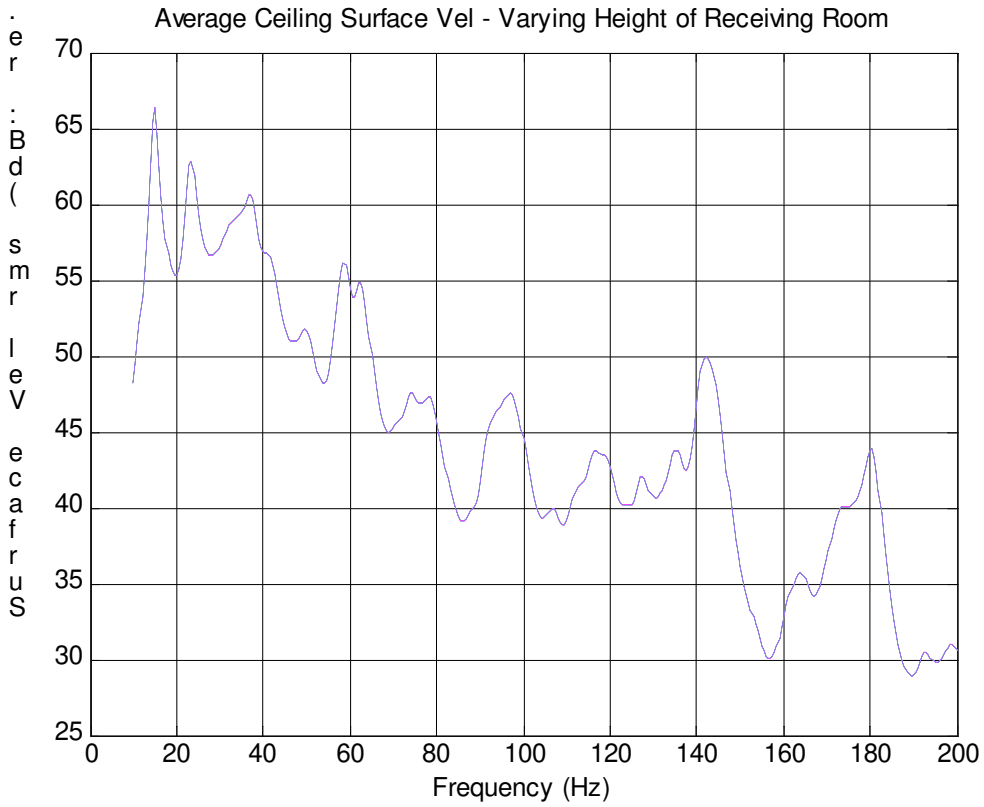

Figure 4-63. The predicted average ceiling surface velocity normalised against the force of the impact on the floor. Obviously this does not change with changing receiving room height (unless the room height becomes very small and significantly loads the ceiling vibration). The model, however, does not include such acoustic loading, which is very small for all reasonable floors and room heights.

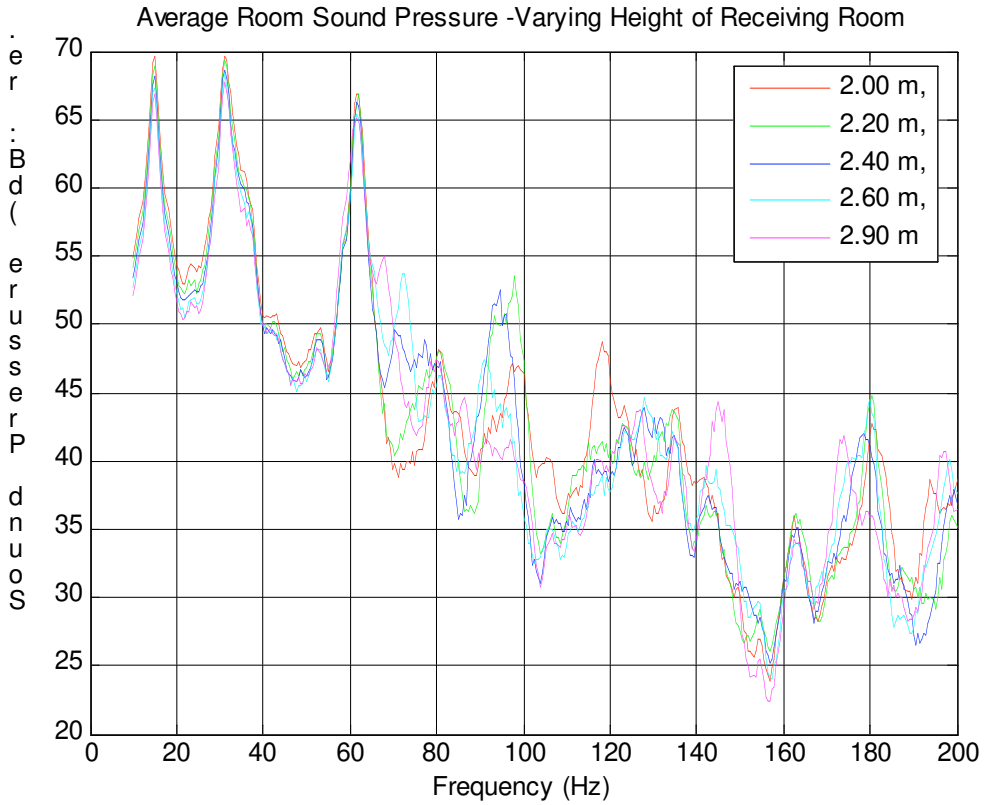

Figure 4-64. The predicted average room sound pressure generated in the receiving room normalised against the force of the impact on the floor.

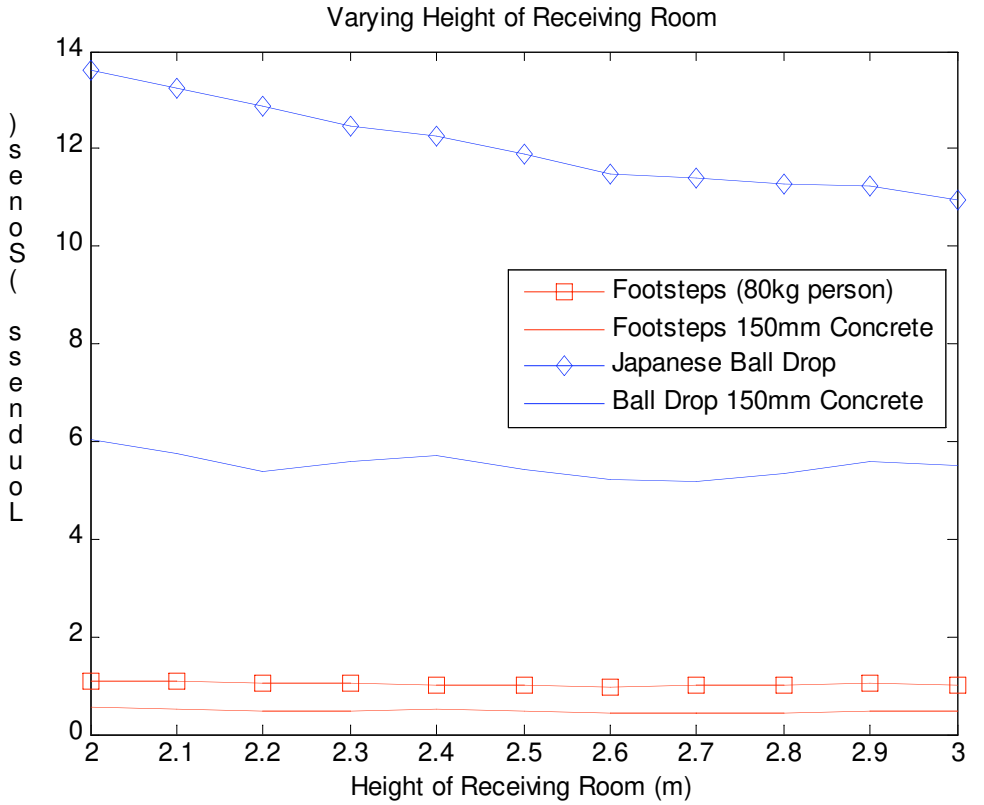

Figure 4-65. The average overall Loudness in Sones produced by a model footstep and a Japanese impact ball in the receiving room below the floor.

4.9 CONCLUSIONS OF THE TREND ANALYSIS

In this section we offer some conclusions from the prior trend analysis, divided into the floor sections.

Joists

- It would appear that increasing the stiffness of the joists substantially improves performance. However, a four-fold increase in bending stiffness is required on the existing joists for a significant gain.
- Increasing the damping of the joists does improve results by reducing the resonance peaks, especially the fundamental.
- The addition of transverse stiffeners can show some improvement by increasing the spacing between resonances. The improvement is not very great however, especially for wider floors where much greater transverse stiffness is required to achieve significant results. Such a feature may be best used for very narrow floors.

Floor upper

- It is no surprise that increasing the surface density does improve the performance, but after about 100kg/m^2 it would appear that minimal gains are to be had, unless unreasonable surface densities are used.
- Increasing the bending stiffness of the upper only offers slight gains.
- Increasing the damping of the upper offers some significant gains in the performance in terms of reducing the resonance peaks. However, the performance as indicated by the loudness of the low-frequency impacts is limited by the first horizontal resonance in the room (along the 5.5m side). In some cases, a resonance in the floor might coincide with that in the room, and in such cases damping would be obviously beneficial.

Floor cavity

- The major conclusion from the floor cavity results is that for cavity depths greater than about 200mm the resilient rubber ceiling clips are the dominant sound transmission path. It is clear that very significant gains could be had by reducing the stiffness of the ceiling clips, or by using independent ceiling joists. However, independent ceiling joists can be prone to flanking transmission issues in a similar way to staggered stud walls.
- It is interesting to observe the effect increasing the damping of the ceiling clips has on performance. This appears to be due to the fact that, since the ceiling clips are a dominant transmission path, increasing the ceiling clip damping reduces the mass-spring-mass resonance of the floor system at around 30-40Hz, which in the model tested couples very well into on of the room resonances. We also see an improvement in other low-frequency resonances.

Ceiling

- Increasing the surface density of the ceiling improves the performance significantly. In fact, doubling the surface density of the ceiling would appear to make the floor perform as well as the reference concrete floor. This result relates well to the fact that airborne sound in double-leafed constructions perform best for a given amount of mass when an equal amount of mass is to be found on each leaf.
- Greatly increasing the stiffness of the ceiling can have a detrimental effect whereas increasing the damping has a positive effect. Both of these results are probably related to the fact that the dominant sound path to the ceiling is through the ceiling clips.

Floor and room dimensions

- Increasing the span of the floor tends to improve performance up to a point. In part, this effect appears to be due to the movement of the fundamental resonance along the longest length of the room to a different frequency which might start to coincide with resonances in the floor.
- Changing the width of the floor does affect the results, but produces no trend as such, apart from increasing the size of the receiving room and hence the overall sound absorption.
- Changing the height of the receiving room only changes the results above the first vertical mode of the room (at around 60-80Hz, depending on the height). As a result, there is little influence on the loudness ratings, particularly for footstep sounds, since the energy is mostly concentrated below 80Hz.

4.10 REFERENCES

Blazier, W.E, DuPree, R. B. (1994). "Investigation of low-frequency footfall noise in wood-frame, multifamily building construction", *The Journal of the Acoustical Society of America*, 96(3), 521-1532

Shi W.; Johansson C.; Sundback U. (1997). An investigation of the characteristics of impact sound sources for impact sound insulation measurement,,Applied Acoustics, 51(1), 85-108.

Koizumi T. , Tsujiuchi N. , Tanaka H. , Okubo M. , Shinomiya, M. (2002). "Prediction of the vibration in buildings using statistical energy analysis", *http://www.femtools.com/download/docs/imacdu02.pdf*

5. ANALYSIS OF EXPERIMENTAL RESULTS

5.1 INTRODUCTION

In this chapter we analyse and compare the results obtained from the experimental measurements; primarily from the low-frequency vibration measurements, but also from the standard tapping machine measurements.
We first examine the results of the low-frequency vibration measurements, we then briefly look at the tapping machine standard results (the high-frequency results). As part of examining the low-frequency results, we look at illustrative mesh plots for various frequencies on various floors – this provides some interesting insights into what is happening when a floor vibrates under an impact.

5.2 EXAMINATION OF THE LOW-FREQUENCY RESULTS

In this section we look closely at the low-frequency results produced by the shaker and laser vibrometer measurements on the experimental floors. We compare the results of groupings of the floors based on similar themes. For each theme we illustrate the logic behind the inclusion each floor in the test and discuss the results.

The following section will then consider the high frequency tapping machine results.

Changing the floor upper of a 7m span floor

We consider floors with 300mm deep LVL joists at 400mm centres spanning 7m. These floors have a plasterboard ceiling consisting of 2 layers of 13mm dense plasterboard (25kg/m^2), attached to the joists via rubber ceiling clips (RSIC-1) and a cavity filled with sound control fibreglass batts.

We start with a basic floor where the floor upper consists only of 15mm plywood (Floor 2), we then test some additions to this basic floor upper:-

- The addition of 3 layers of 12.7mm (38mm) of gypsum fibreboard (GIB Sound Barrier - 1040kg/m^3) screwed to the plywood subfloor. (Floor 3). This addition tests the effect of the addition of mass (40kg/m^2) and stiffness to the floor, with a little extra damping provided by the interaction between the layers of gypsum fibreboard.
- The addition of 45mm deep battens at 450mm centres perpendicular to the joists with 15mm plywood on the battens; the cavity is infilled with 50mm fibreglass batts (Pink Batts). (Floor 4). This change tests the effect of providing extra stiffness across the floor upper, with a small increase in weight. The cavity is infilled with fibreglass to reduce resonances in the cavity (mostly a higher frequency effect, although this infill will provide some additional damping at lower frequencies too). Similar system to this have been tested by TRADA (Pitts, 2000).
- The removal of the fibreglass infill from the above system and the placement of 40mm of paving sand (1250 kg/m^3). (Floor 5). The use of sand tests for increasing floor upper mass (and extra mass – 54 kg/m^2) with potentially a lot more damping. As explained in the chapter on the overview of existing designs, sand is used in some floor systems in parts of Europe, and can provide significant vibration damping.

Results

The vibration results (Figure 5-1) show that addition of the upper layers have not changed the position of the fundamental frequency (1st peak), due to the extra stiffness provided by the upper layers compensating for the extra mass. There is a significant movement of the 2nd

resonance (2nd peak) due to the increase of the transverse stiffness provided by the additional upper layers.

We can see that the extra stiffness transverse to the joists in Floor 4 has help to reduce the size of the peaks in the 1st and 2nd harmonics, and has improved results to about 100Hz, but beyond that there is no real gain (the peak at 118Hz is appears to be caused by resonances of the upper layer of plywood).

The extra mass provided by the gypsum fibreboard has improved performance across the whole frequency range.

The extra mass and extra stiffness of the sand-filled cavity has improved performance across all frequencies, with significantly extra improvement due to the increased vibration damping showing in frequencies above 80Hz.

The predicted sound pressure results (Figure 5-2) show that the 2nd resonances is less important to sound generation, unless it is near a room resonance. Even order plate resonances usually radiate less sound than odd resonances due to more destructive interference of the radiated sound.

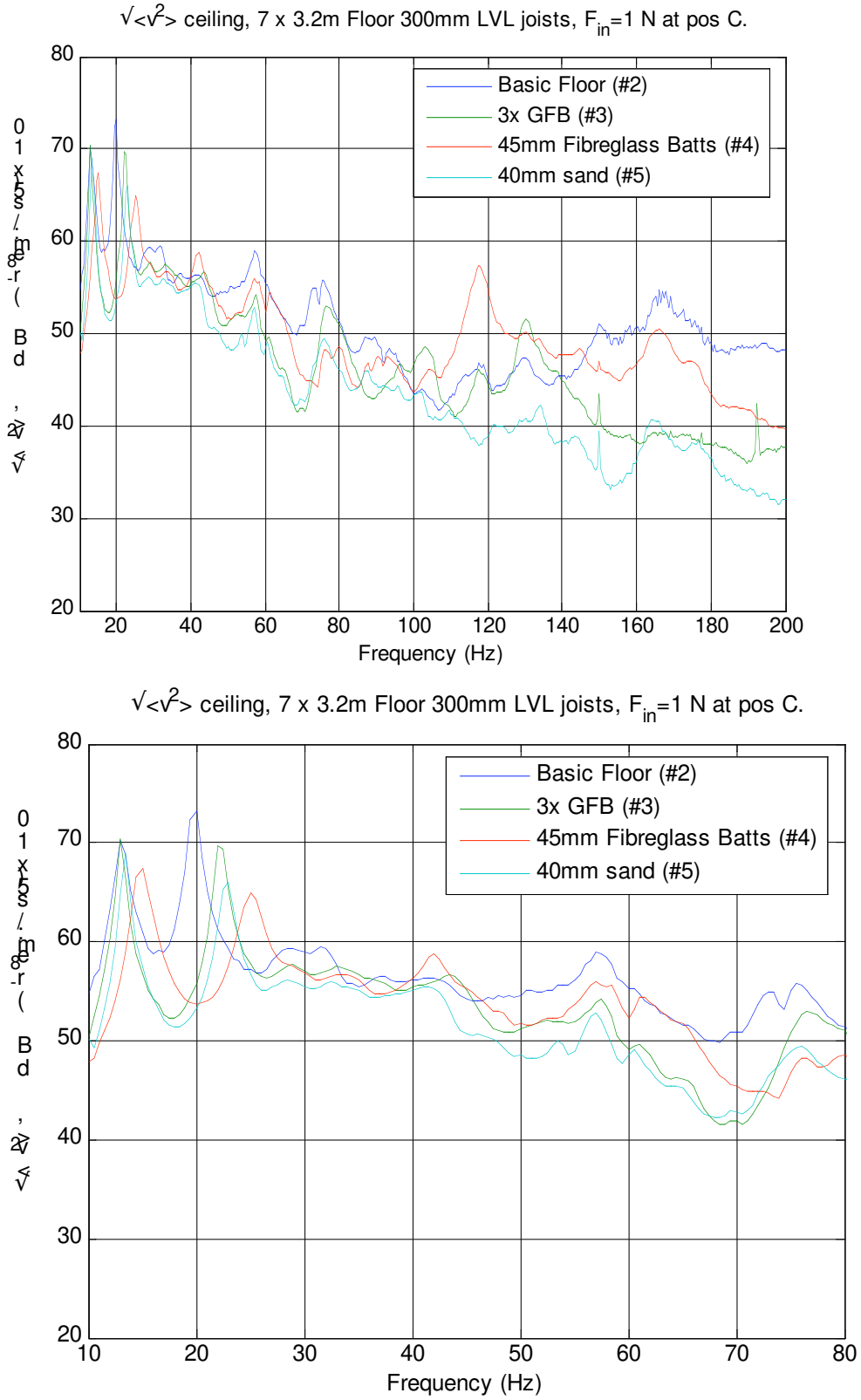

Figure 5-1. Averaged surface velocity plots in dB for Floors 2 to 5 as a function of frequency for the ceiling. The lower graph is a zoomed-in view of the upper graph, looking at very low frequencies. The surface velocity is measured by the scanning laser vibrometer, with force generated by the shaker at position C and normalised against the amplitude of the applied force (F_{in}) for each frequency.

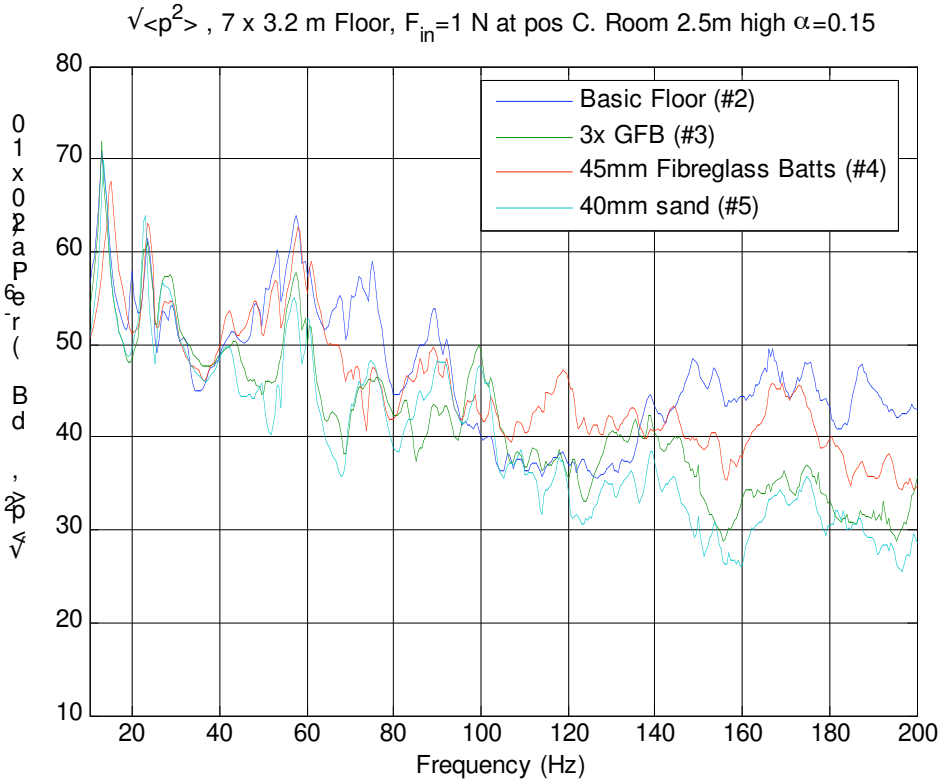

Figure 5-2. Averaged sound pressure in dB for Floors 2 to 5 calculated for a room 2.5m high and with a sound absorption coefficient of 0.15 over its surfaces. Generated by the force at position C and normalised against the amplitude of the applied force (F_{in}).

Improving the vibration damping of the sand

In this section we look at what happens when the damping of the sand-filled cavity is increased by mixing in an amount of sawdust. Mixing in sawdust with the sand increases the vibration damping by reducing the compaction of the sand under its own weight allowing more friction to occur, and by making the impedance of the sand more closely match that of timber.

To observe the effect of this we compare two floors where the only difference is the addition of sawdust with the sand. Floor 5 has 40mm of paving sand in the floor, whereas Floor 6 has a mix of 60% sand and 40% sawdust by loose volume (total density of the mix 1170 kg/m^3).

Results

The vibration and room pressure results (Figure 5-3 and Figure 5-4) show that the addition of sawdust with the sand has significantly increased the damping of the sand. This is apparent in the reduction of levels observed in the frequencies above 80Hz, where modelling has shown damping in the upper surface to play an important part, and where we expect the damping of the sand to be greater. The insignificant change in levels below 80Hz (particularly the 2nd resonance) does suggest that the vibration damping due to the sand is not very much.

Sun et al. (1986) observed from experiment that, when looking at sand laid on a vibrating metal plate, the vibration damping in the plate is a maximum at frequencies above when the thickness of the sand is about equal to $0.05\lambda_c$, where λ_c is the longitudinal wavelength of the vibrations in the sand ($\lambda_c = c/f$, where c is the propagation speed of the vibrations (100 to 200 m/s for sand) and f is the frequency). In our case, the depth of the sand is 40mm, and if

we assume a speed of sound of 150m/s in the sand then the maximum damping is found at 120Hz

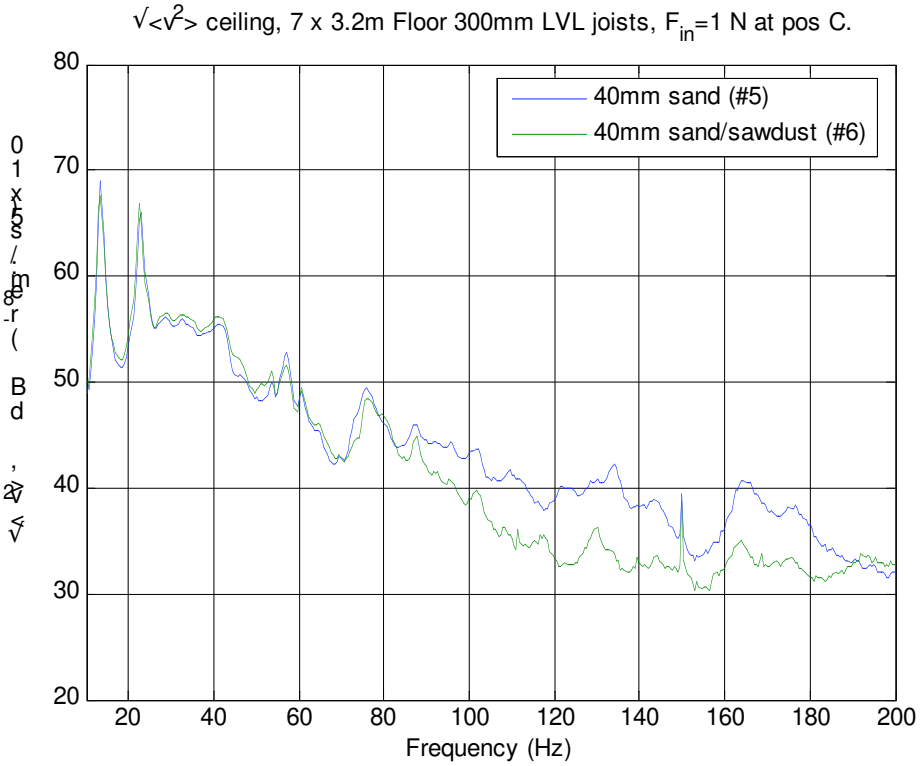

Figure 5-3. Averaged surface velocity plots in dB for Floors 5 and 6 as a function of frequency for the ceiling. The surface velocity is measured by the scanning laser vibrometer, with force generated by the shaker at position C and normalised against the amplitude of the applied force (F_{in}) for each frequency.

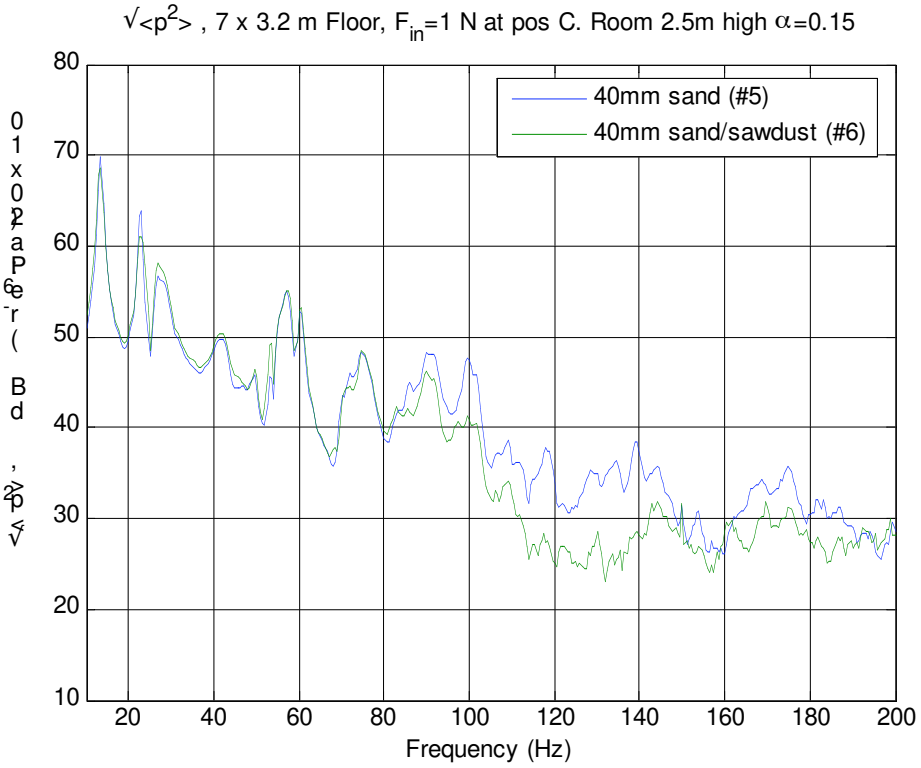

Figure 5-4. Averaged sound pressure in dB for Floors 5 and 6 calculated for a room 2.5m high and with a sound absorption coefficient of 0.15 over its surfaces. Generated by the force at position C and normalised against the amplitude of the applied force (F_{in}).

Clamping the ends of the joists

One of the assumptions of the model we used assumes that the joists are simply-supported. That is to say the ends of the joists are in effect resting on a pivot point so that there is little rotational stiffness experienced by the ends of the joists (the ends are not clamped). Work done previously by Scion has shown that in practise it is difficult to clamp the ends of joists (for example, joist hangers essentially simply support the joist ends). What we didn't know was whether joists in a platform type construction would be clamped by the weight of the remaining building on the joist ends. To find out whether or not there was an effect, we simulated an additional storey on the ends of the joists by clamping the ends of the joists with 2 beams (one on each end) through bottom plates. The beams were stressed so that the force they applied to the ends of the floor was equal to the weight of another storey on the floor. This floor with clamped ends was designated Floor 7.

Results

On comparing the results for clamped ends against non-clamped ends (Figure 5-5) we see that there is little difference between the two results. This means that we can continue testing isolated floors with simply-supported joists knowing that the results carry over to floors in buildings.

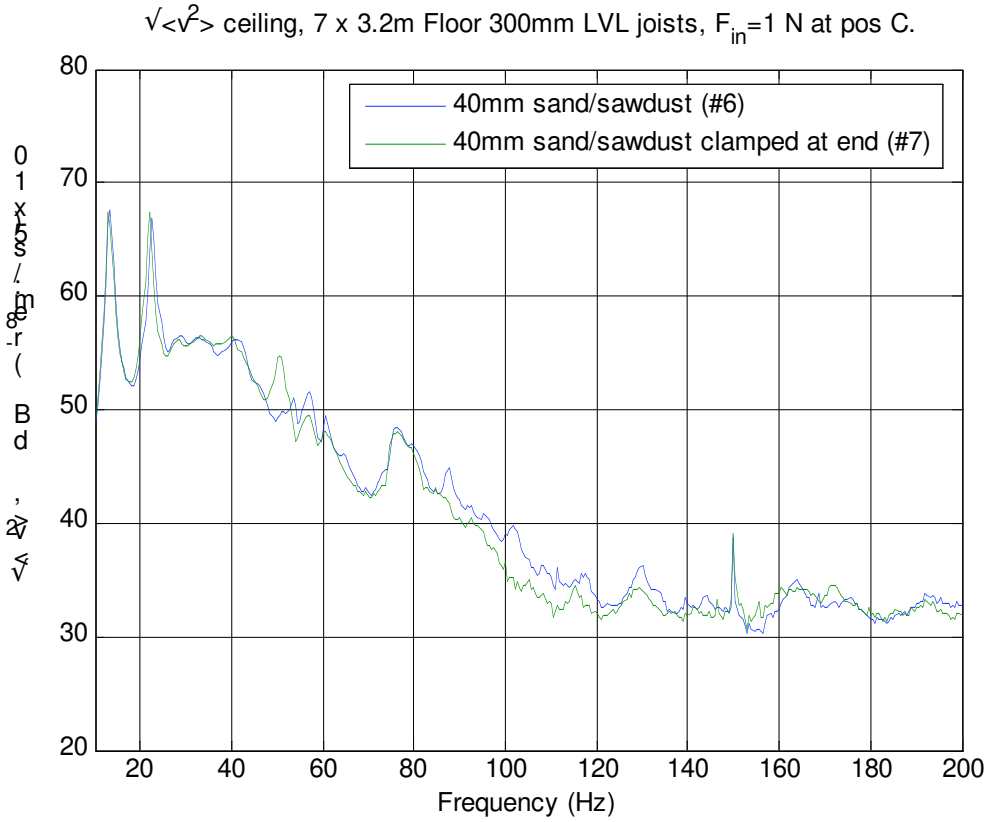

Figure 5-5. Averaged surface velocity plots in dB for Floors 6 and 7 as a function of frequency for the ceiling. The surface velocity is measured by the scanning laser vibrometer, with force generated by the shaker at position C and normalised against the amplitude of the applied force (F_{in}) for each frequency.

Changing the floor span from 7m to 5.5m

Initially we tested floors with an extreme span of 7m. For subsequent floors we tested a span of 5.5m – a span more likely to be used. In this section we compare two floors which only differ by their span (Floor 6 and Floor 8).

Results

While, since the forcing points are now on different parts of the floor, we can't make a meaningful amplitude comparison, we can compare the locations of resonaces. On comparing the low-frequency results for the two different spans (Figure 5-5) we see that the fundamental resonance has increased from 13Hz to 15Hz with a lesser increase for the 2nd resonance.

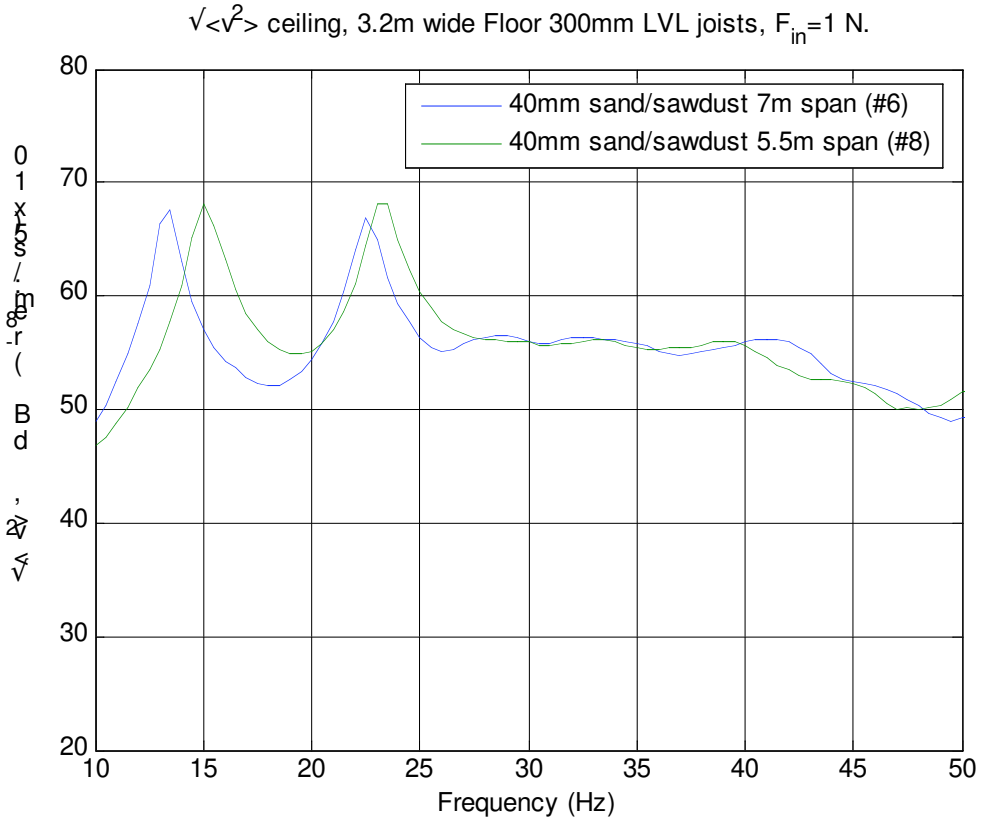

Figure 5-6. Averaged surface velocity plots in dB for Floors 6 and 8 as a function of frequency for the ceiling. The surface velocity is measured by the scanning laser vibrometer, with force generated by the shaker at position C for the 7m floor and position E for the 5.5m floor, and normalised against the amplitude of the applied force (F_{in}) for each frequency.

Different floor uppers and joists with same cavity depth and 5.5m span

We consider floors with 300mm deep joists at 400mm or 450mm centres spanning 5.5m. These floors have a plasterboard ceiling consisting of 2 layers of 13mm dense plasterboard (25kg/m^2), attached to the joists via rubber ceiling clips (RSIC-1) and a cavity filled with sound control fibreglass batts. Two floors have 300mm LVL joists at 400mm centres and two have 300mm I-beams at 450mm centres.

We start with Floor 8 which the same as the sand/sawdust cavity-filled Floor 6 but with a shorter span, as a sort off reference floor. We then consider three more floors:-

- We considered that Floor 8 had some promise but was not good enough to compare well to a 150mm concrete floor. Theoretical results showed that acoustically a floor upper with a surface mass of just over 110kg/m^2 can perform significantly better, and that a stiffer floor upper is also useful. Structural analysis also shows that keeping the floor system mass to less than 150kg/m^2 requires only normal bracing techniques (particularly for seismic forces). Studies by others have also shown that a deeper layer of sand results in much greater damping at lower frequencies and that floor upper damping is beneficial to performance. With these things in mind we started with Floor

8 and increased the sand layer to 85mm by replacing the 45mm battens with 90mm deep battens (90 by 45mm timber on edge) in the cavity, we also reduced the amount of sawdust to an 80/20 by loose volume mix (density of sand/sawdust mix is 1210kg/m^3). This floor is designated Floor 9.

- CSR of Australia have a floor design consisting of aerated, autoclaved concrete (Hebel slabs) glued and screwed to 300mm deep I-beam joists at 450mm centres. This floor was tested and is designated Floor 21.
- In the US and Canada it is common to use a gypsum concrete screed as a topping on a timber subfloor. Current practise and tests by other countries suggest that floating the screed on a resilient layer produces the best results (particularly for higher frequencies). This floating floor screed design was tested with 30mm of USG Levelrock 3500 on 10mm polyurethane foam on a plywood 300mm I-beam subfloor - Floor 22. However, the screed wasn't laid well and there was significant variation in its thickness.

Results

Looking at the results of the measurements (Figures 5-7 and 5-8) we can see that Floor 9 outperforms all the other floors in this test. The surface density of the floor upper for Floor 9 is 108 kg/m^2 and so performs best at lower frequencies. The high damping of the sand/sawdust mix in Floor 9 provides the best performance at higher frequencies too. By comparing the performance of Floor 9 with that of Floor 22 (which has a floor upper surface density of 67 kg/m^2), it would seem that the vibration damping of Floor 9 starts becoming quite large at above 60Hz.

Comparing the 40mm sand/sawdust Floor 8 (with a floor upper surface density of 48 kg/m^2) to the 75mm Hebel slab Floor 21 (52 kg/m^2), it would seem that although the floor upper surface is of similar mass the performance of Floor 8 is superior – the extra damping offered by the sand/sawdust mix is beneficial, especially at higher frequencies. It must be remembered, however, that the LVL joists used in Floor 8 give an extra 12kg/m^2 of mass to the floor over the I-beams used in Floor 21.

It is interesting to note that although the floating screed is designed to provide improved impact insulation at higher frequencies due to it floating on a very resilient foam layer, the sand/sawdust floors are able to provide a similar or much better higher frequency performance. This is even though the top layer of plywood of the sand/sawdust is directly connected to the subfloor without any floating arrangements. This shows the effectiveness of the sand in damping the vibrational energy.

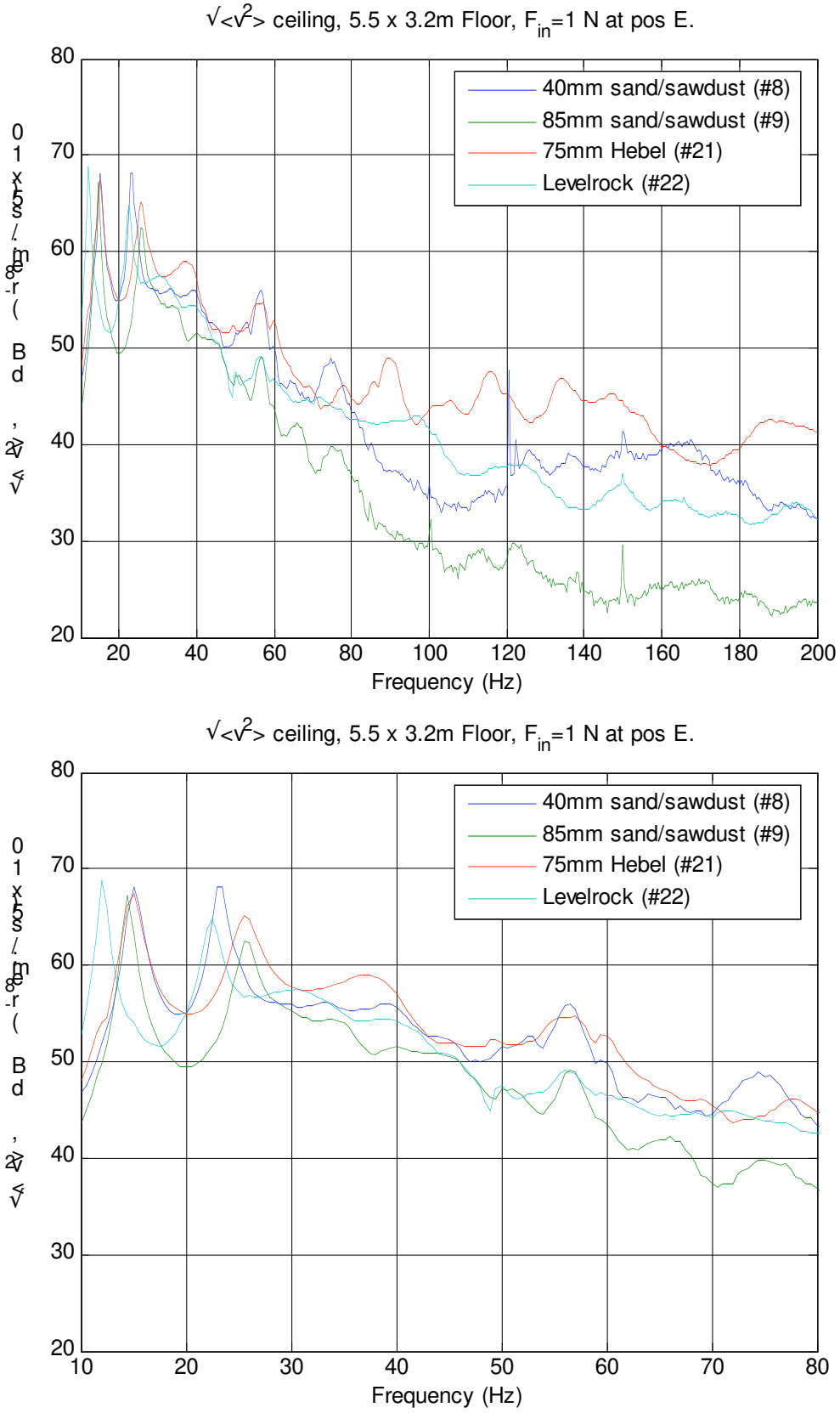

Figure 5-7. Averaged surface velocity plots in dB for Floors 8,9,21 and 22 as a function of frequency for the ceiling. The lower graph is a zoomed-in view of the upper graph, looking at very low frequencies. The surface velocity is measured by the scanning laser vibrometer, with force generated by the shaker at position E and normalised against the amplitude of the applied force (F_{in}) for each frequency.

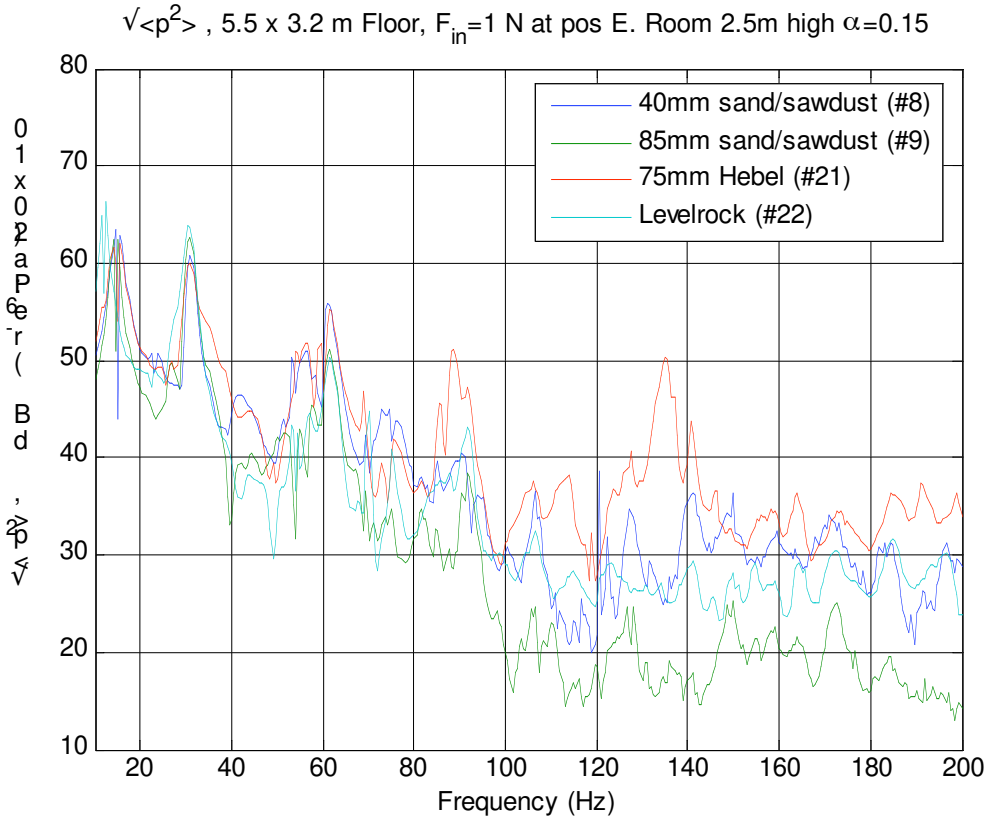

Figure 5-8. Averaged sound pressure in dB for Floors 8,9,21 and 22 calculated for a room 2.5m high and with a sound absorption coefficient of 0.15 over its surfaces. Generated by the force at position E and normalised against the amplitude of the applied force (F_{in}).

Transverse stiffening

It was thought that one way to improve the low-frequency performance was to reduce the number of resonances occurring in the very low frequency region. Now since a lot of the resonances occurring in the very low frequency region are due to the floor bending in the direction perpendicular to the joists (as can be seen in section 0), one way to achieve that aim would be to greatly stiffen the floor in the direction perpendicular to the joists. Such stiffening has been dubbed 'transverse stiffening', and can be achieved by introducing blocking or sections of joists which fit between the floor joists. Each block needs to be connected to the neighbouring block to enable rotational moments to be transmitted, one way to do this is to clamp the blocks or joist sections together using tie rods.

One problem to avoid with the addition of transverse stiffeners is making the fundamental frequency of the floor becoming higher in frequency making the human hearing more sensitive to the sound. If the width of the floor is relatively narrow, the addition of transverse stiffeners may make the fundamental resonance more audible (unless its amplitude is correspondingly reduced). To reduce this issue and to make the installation of transverse stiffeners easier, it was thought that the blocking which constituted the transverse stiffeners would not be installed between the floor edge and the next joist (See diagrams and photographs of Floor 12 and Floor 15 to illustrate this. One problem with this is that we now have introduced a rotational mode in the floor, whose frequency depends on the bending stiffness of the floor upper. However, since it is an even type mode the sound radiation efficiency would be quite low.

Results

In Figure 5-9 we see the results of introducing transverse stiffeners into a floor which consists of plywood on joists without a ceiling (Floor 10). We can see that inclusion of the transverse stiffeners has not changed the fundamental resonance (at 23Hz), and the transverse resonances which occurred up to about 60Hz have been eliminated or reduced. We also see, however, that another mode (at 27.5Hz, and illustrated in section 0) has been added; this is a rotational mode. We see that for this width and length of floor (3.2 m and 5.5m respectively) the use of 2 transverse stiffeners (in Floor 13) is about a good as 4 (in Floor 12).

One of the hoped for advantages of including transverse stiffeners in a floor is to produce a floor which is light in weight. Floor 14 is the same as Floor 13 expect a ceiling has been added. In Figure 5-10 we compare the low-frequency performance of Floor 14 against a floor with some extra mass and stiffness in the floor upper – 75mm Hebel slab (Floor 21). We observe a similar performance at frequencies below 100Hz, but an apparently poorer performance for frequencies above 100Hz.

Transverse stiffeners made from I-beam sections were added to the Hebel floor (Floor 20) to observe whether they would improve performance for such a floor. While there is some increase in the fundamental and 2^{nd} order resonance, the overall result is much the same, showing that there is no point in adding transverse stiffeners to a floor with an already significantly built up upper. And, while there appears to be some benefit to using transverse stiffening to improve very low frequency performance for floors with thin uppers, it is probably not enough for what we need.

Another issue with transverse stiffeners, which is illustrated in the theoretical analysis chapter, is that the wider the floor becomes the more transverse stiffening you need to provide effective shifting of the resonances.

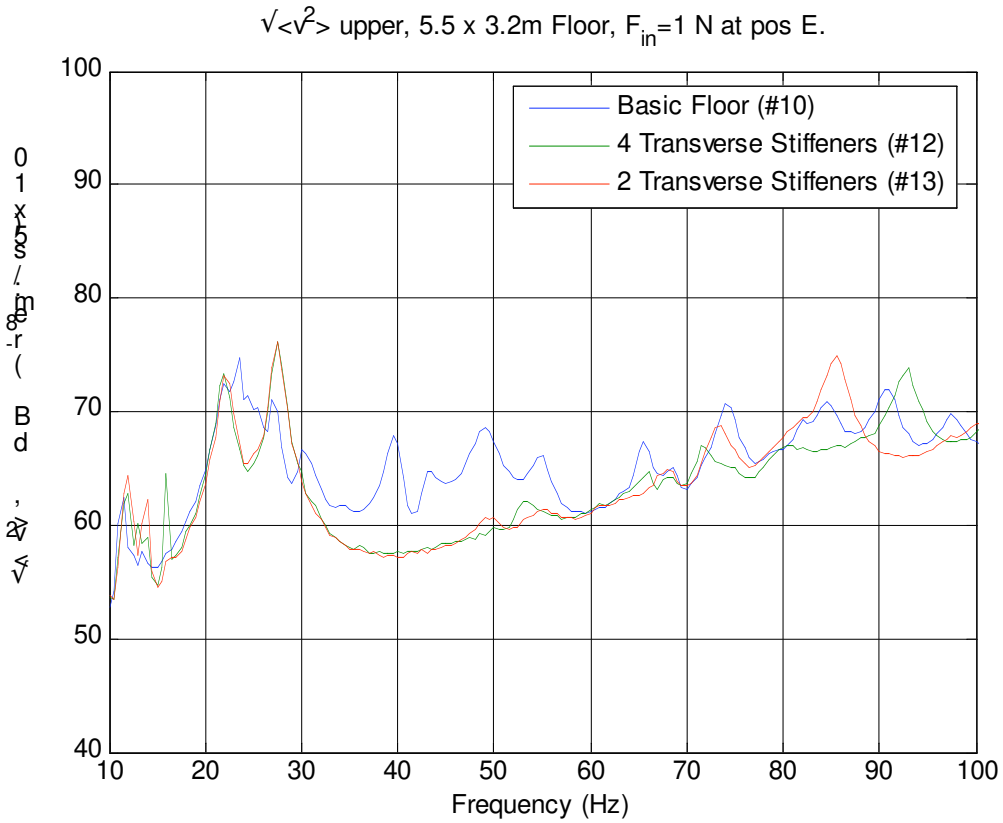

Figure 5-9. Averaged surface velocity plots in dB for Floors 10, 12 and 13 as a function of frequency for the floor upper surface. The surface velocity is measured by the scanning laser vibrometer, with force generated by the shaker at position E and normalised against the amplitude of the applied force (F_{in}) for each frequency.

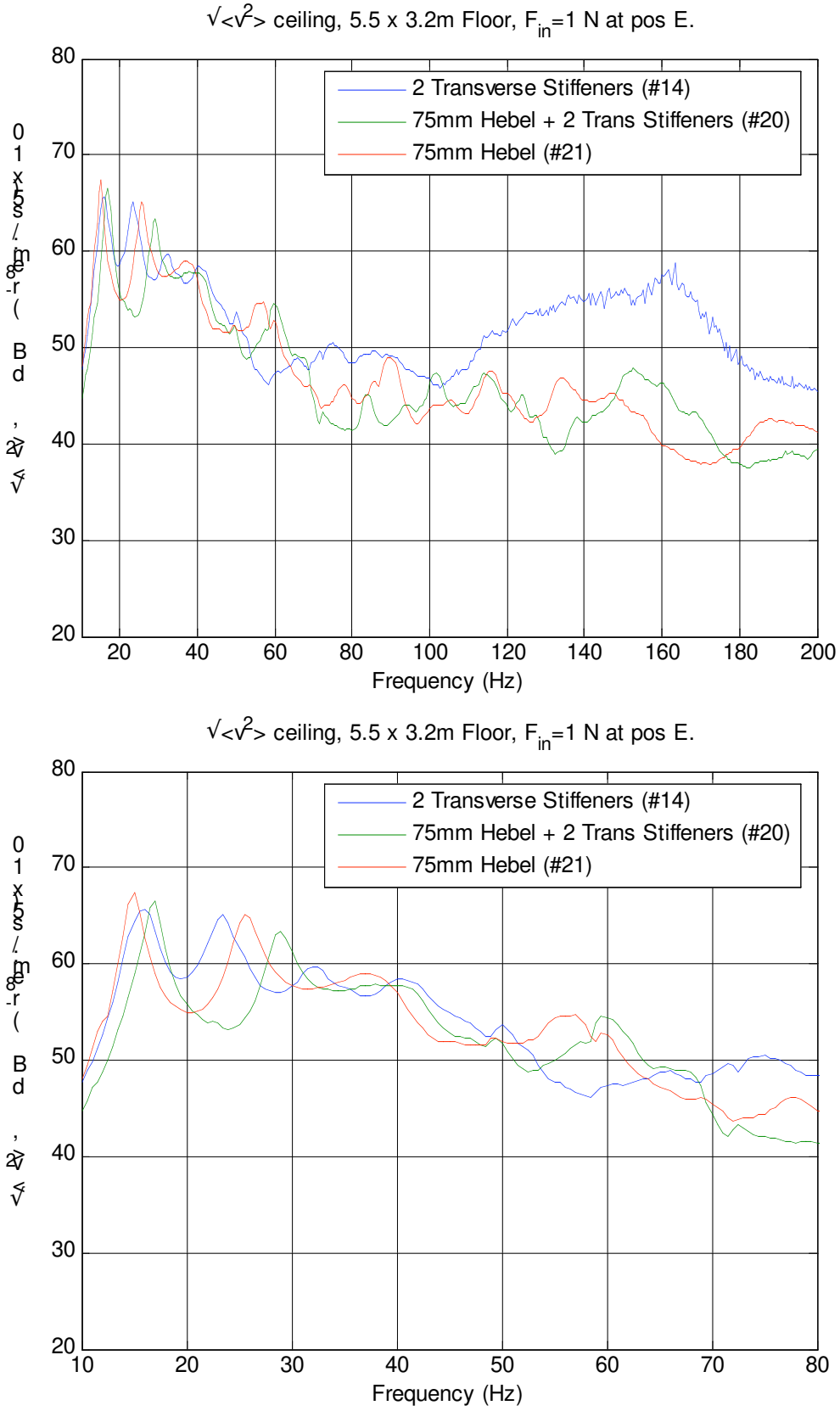

Figure 5-10. Averaged surface velocity plots in dB for Floors 14, 20 and 21 as a function of frequency for the ceiling. The lower graph is a zoomed-in view of the upper graph, looking at very low frequencies. The surface velocity is measured by the scanning laser vibrometer, with force generated by the shaker at position E and normalised against the amplitude of the applied force (F_{in}) for each frequency.

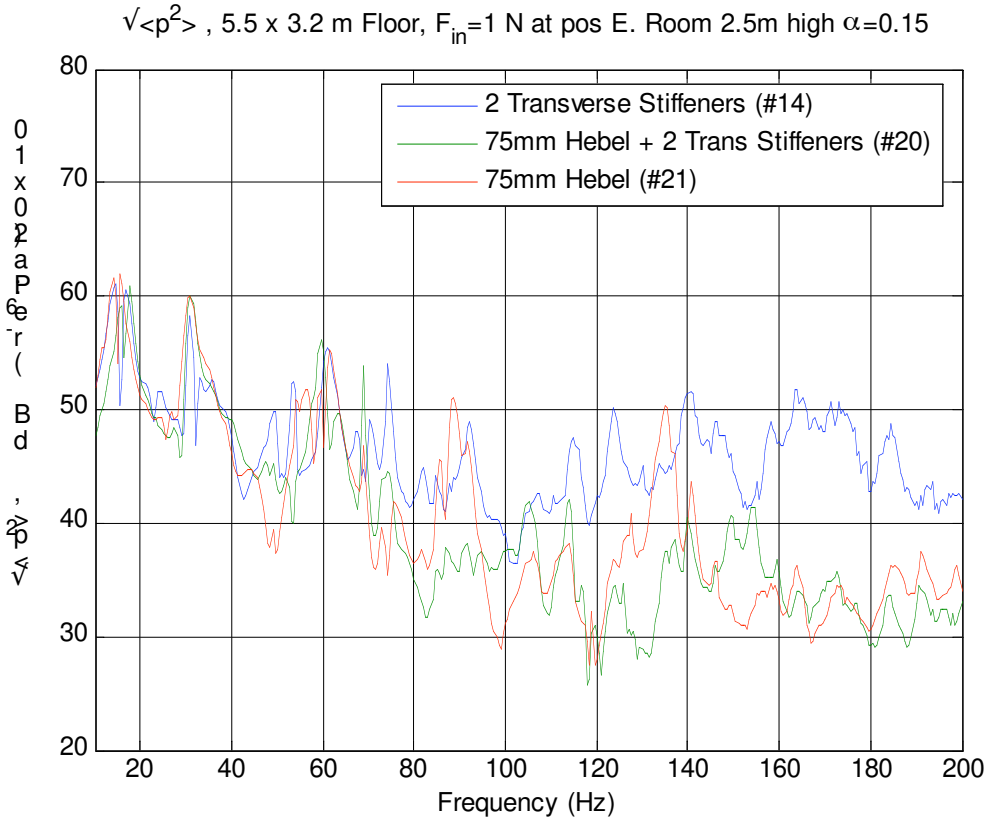

Figure 5-11. Averaged sound pressure in dB for Floors 14, 20 and 21 calculated for a room 2.5m high and with a sound absorption coefficient of 0.15 over its surfaces. Generated by the force at position E and normalised against the amplitude of the applied force (F_{in}).

Comparing a deeper cavity against more mass in the floor upper

Measurements were made on a floor consisting of 400mm deep I-beams at 600mm centres spanning 5.5m with 20mm particleboard as the floor upper (Floor 18), and a floor consisting of 300mm deep I-beams at 450mm centres spanning 5.5m with 75mm Hebel aerated concrete as the floor upper (Floor 18). The ceiling and ceiling fixing details were the same for both floors. By comparing the results of these floors we can observe differences in performance a deeper cavity makes against a floor with greater mass in the floor upper.

Results

Looking at Figure 5-12 we can see that the fundamental frequency of Floor 18 is greater than that of Floor 21 indicating a stiffer and lighter floor. Overall, however, we can see that Floor 21 tends to perform better.

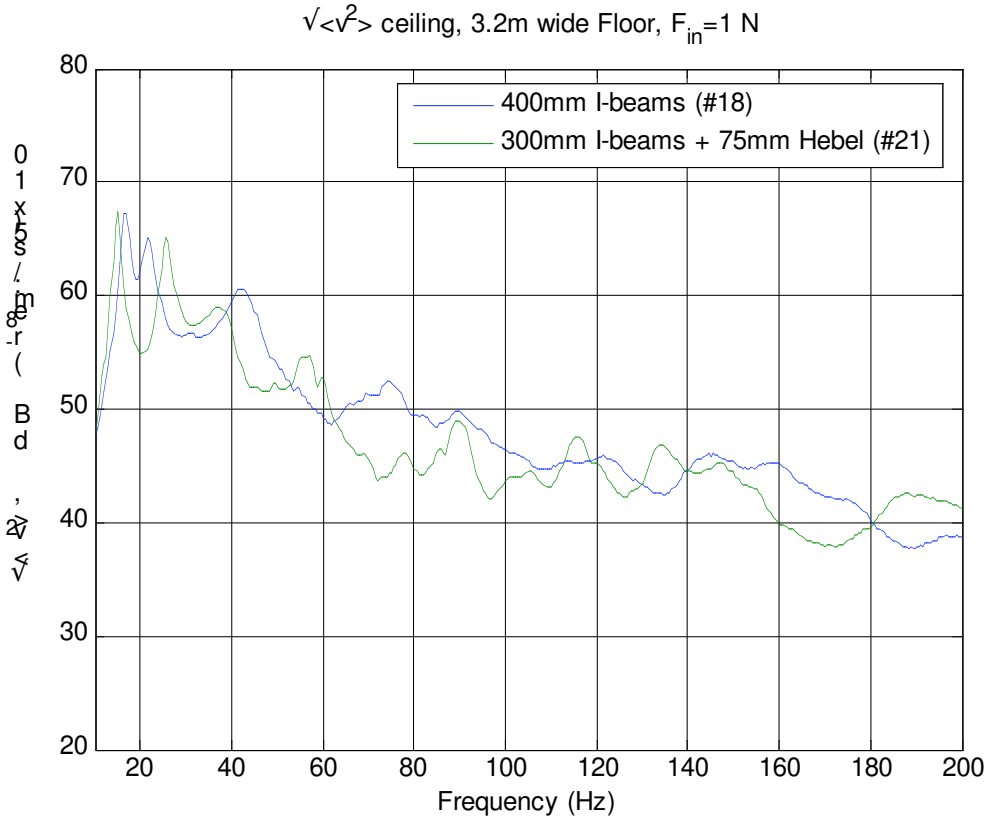

Figure 5-12. Averaged surface velocity plots in dB for Floors 2 and 18 as a function of frequency for the ceiling. The surface velocity is measured by the scanning laser vibrometer, with force generated by the shaker at position C (for Floor 2) and E (for Floor 18) and normalised against the amplitude of the applied force (F_{in}) for each frequency.

Adding mass to the ceiling

Instead of adding mass to the floor upper it is possible (but possibly less convenient) to add mass to the ceiling. This was tested out on Floor 18 by adding another two layers of 13mm noise control plasterboard giving the ceiling 50kg/m^2 of mass, letting everything else remain the same, to produce Floor 19.

Results

Figure 5-13 and 5-14 show the results of the measurements of Floors 18 and 19. We see that the doubling of the ceiling mass does reduce the vibration levels of the ceiling by up to 5dB, but this doesn't always correspond to the same changes in the predicted sound pressure levels, as is often the case since changing the properties of the radiating surface changes the bending wavespeed and hence its radiation efficiency.

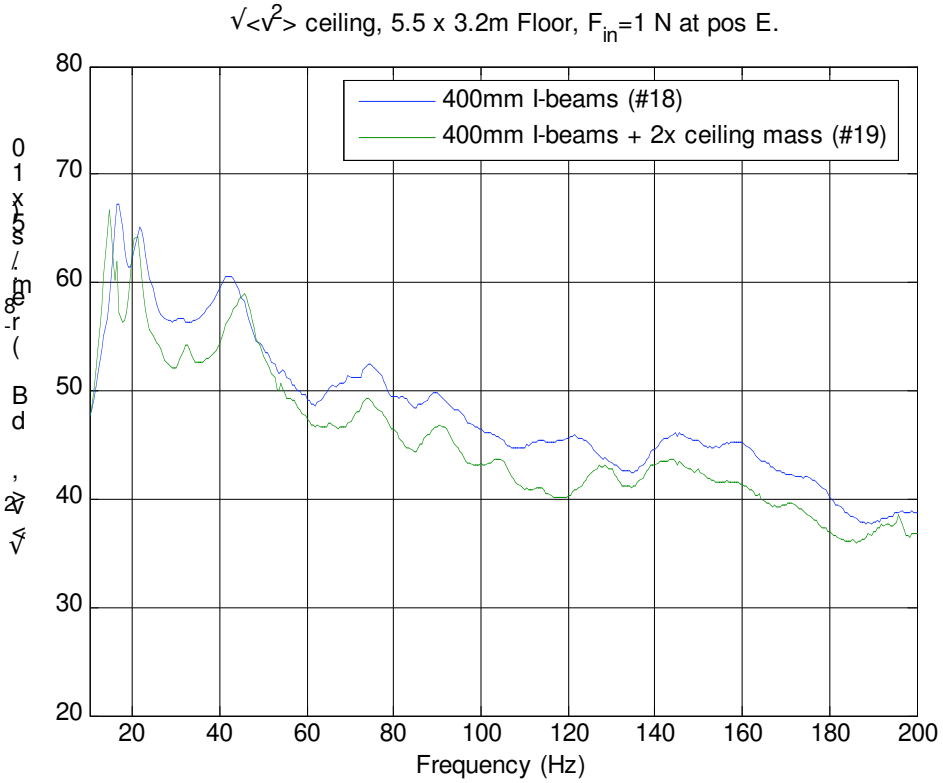

Figure 5-13. Averaged surface velocity plots in dB for Floors 18 and 19 as a function of frequency for the ceiling. The surface velocity is measured by the scanning laser vibrometer, with force generated by the shaker at position E and normalised against the amplitude of the applied force (F_{in}) for each frequency.

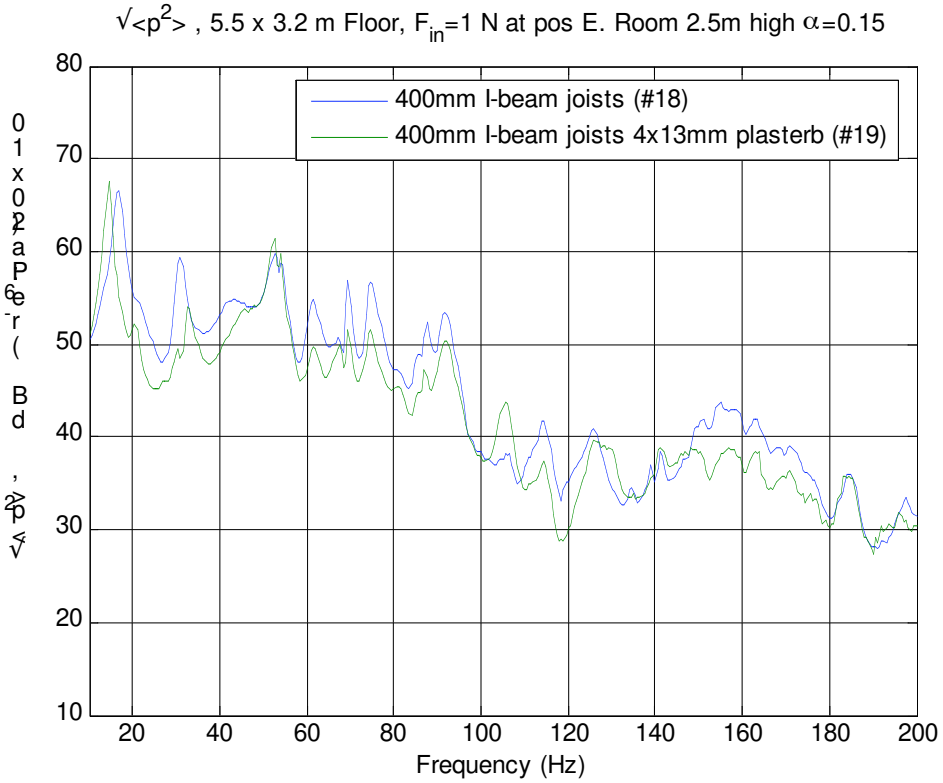

Figure 5-14. Averaged sound pressure in dB for Floors 18 and 19 calculated for a room 2.5m high and with a sound absorption coefficient of 0.15 over its surfaces. Generated by the force at position E and normalised against the amplitude of the applied force (F_{in}).

Independent ceiling joists

The theoretical modelling of the floor systems showed that the ceiling clips (RSIC-1) used to resiliently attach the ceiling to the joists were the major sound transmission path for a cavity depth of about 200mm or greater. One way to overcome this problem is to remove the ceiling clips by using independent ceiling joists. To test the effectiveness of using independent ceiling joists the resiliently attached ceiling of the gypsum concrete floor system (Floor 22) was removed and replaced with a ceiling supported by way of a independent ceiling joist system (Floor 23). It was know that one of the problems that can occur with such a independent ceiling joist system is that flanking transmission of vibration around the edge of the floor can be a compromising factor. To reduce such flanking the ends of the ceiling joists were mounted on rubber pads and the ceiling perimeter, including the battens, was cut with a 10mm gap so that it didn't touch the wall.

Results

Figures 5-15 and 5-16 show the results of the measurements comparing the resiliently attached ceiling to the ceiling attached to independent ceiling joists. It is cleat that there is little difference between the resilient attached ceiling and the ceiling with independent ceiling joists with no special anti-flanking treatment (Floor 22 cf. Floor 23). However, once we include special treatment to reduce flanking issues, we observe a significant decrease in the ceiling vibration levels, which is in line with theoretical observations.

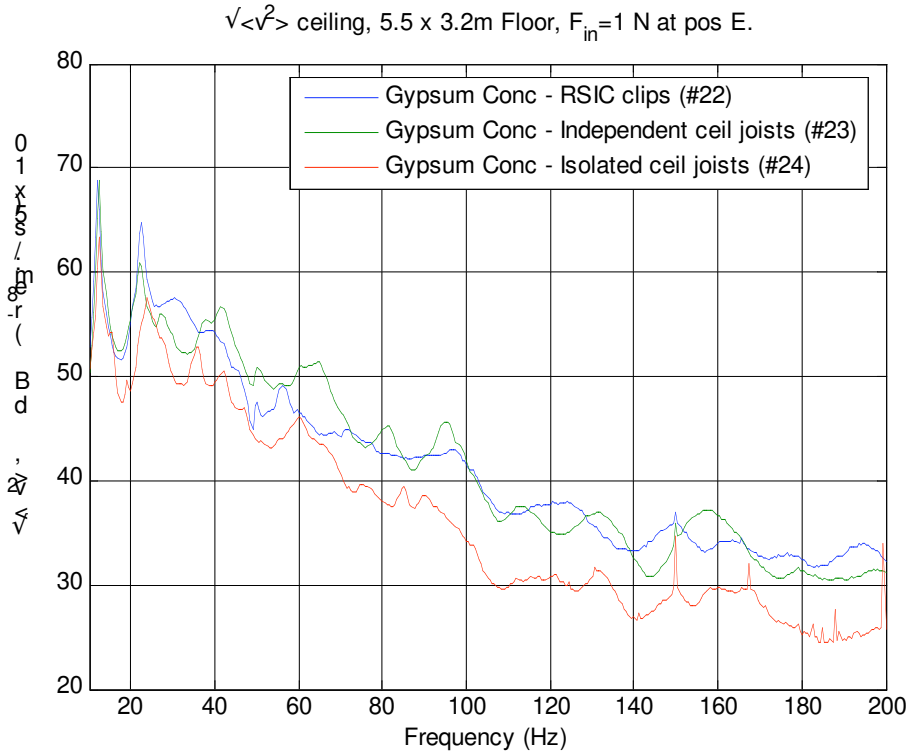

Figure 5-15. Averaged surface velocity plots in dB for Floors 22 to 24 as a function of frequency for the ceiling. The surface velocity is measured by the scanning laser vibrometer, with force generated by the shaker at position E and normalised against the amplitude of the applied force (F_{in}) for each frequency.

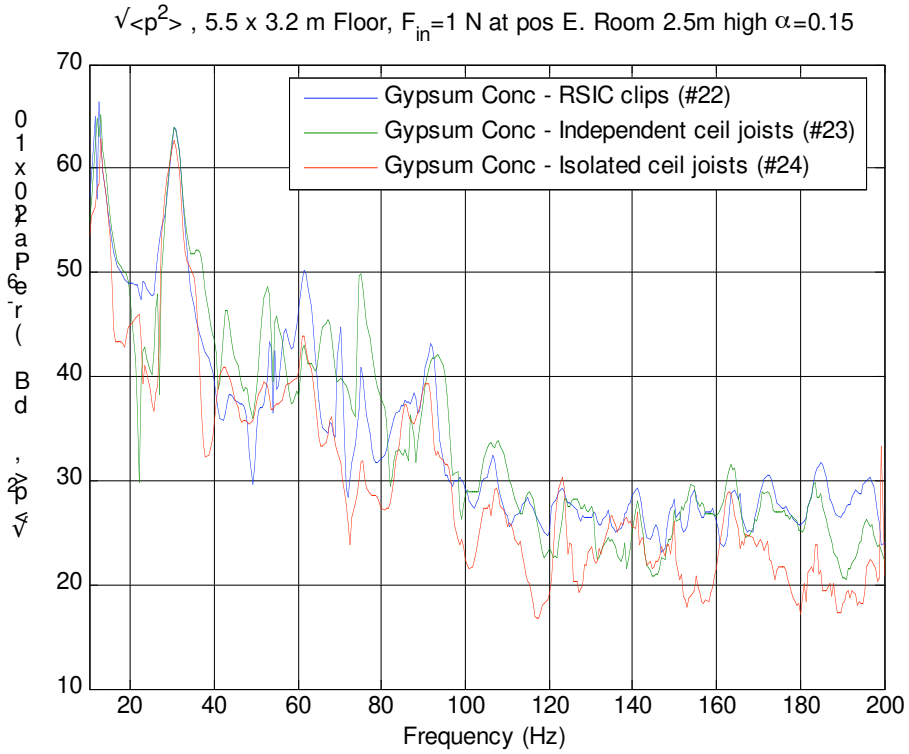

Figure 5-16. Averaged sound pressure in dB for Floors 22 to 24 calculated for a room 2.5m high and with a sound absorption coefficient of 0.15 over its surfaces. Generated by the force at position E and normalised against the amplitude of the applied force (F_{in}).

Final Floor Designs

Subjective analysis of sounds recorded from Floor 9 showed that the overall performance of this floor was similar to that of a 150mm concrete slab floor with a suspended ceiling (the concrete floor being designated Floor 0). We can therefore regard this floor design (Floor 9) as being an effective floor design. If we regard the performance of this timber floor as being a suitable standard for timber floors, we can compare the performance of other potential final floor designs.

Using the learning gained from the theoretical and experimental analysis, another final floor design built and tested was Floor 25. This floor combines the ideas of using mass and damping in the form of a sand/sawdust mix in the floor upper, but with a reduced amount to decrease overall weight, and to make the floor less deep. The proposed amount of sand/sawdust mix to use was 65mm (in a cavity 70mm deep). However, after the measurements it was discovered that the builders did not fill the cavity to 65mm, but rather filled the cavities to about 50mm on average. Although not ideal, this may be regarded as a test of buildability. The reduction of sand and sawdust in the floor upper was offset by using independent ceiling joists mounted on rubber pads. The edges of the ceiling were not firmly mechanically connected to the wall, but were sealed with a bead of acoustic sealant, which provides a resilient connection between the edge of the ceiling and the wall. In one measurement coving was used to cover this resilient connection, to test the effect of such a detail on this flanking sensitive design.

Results

Figure 5-17 shows the ceiling surface vibration results for the Floor 9 and Floor 25; in the same figure we also compare Floor 2 – the ‘basic’ floor. Figure 5-18 shows the predicted

sound pressure levels for Floors 9 and 25 – we don't compare with Floor 2, since that floor and hence room is a different size. We see that Floor 25 performs about as well as Floor 9 up to 100Hz, beyond that, however, Floor 25's performance is slightly worse than Floor 9 (about 4dB, on average). However, when considering soft-shoe footsteps of an 80kg person walking, and after factoring in the threshold of hearing from 100Hz to 200Hz, we find that the frequencies from 100Hz to 200Hz would still be inaudible for footsteps on Floor 25. Therefore, it can be concluded that Floor 25 performs similarly to Floor 9 in the low-frequency range.

Figure 5-19 shows the effect the coving has on the performance. It does seem that the coving has indeed affected the performance of the system, particularly above 60Hz.

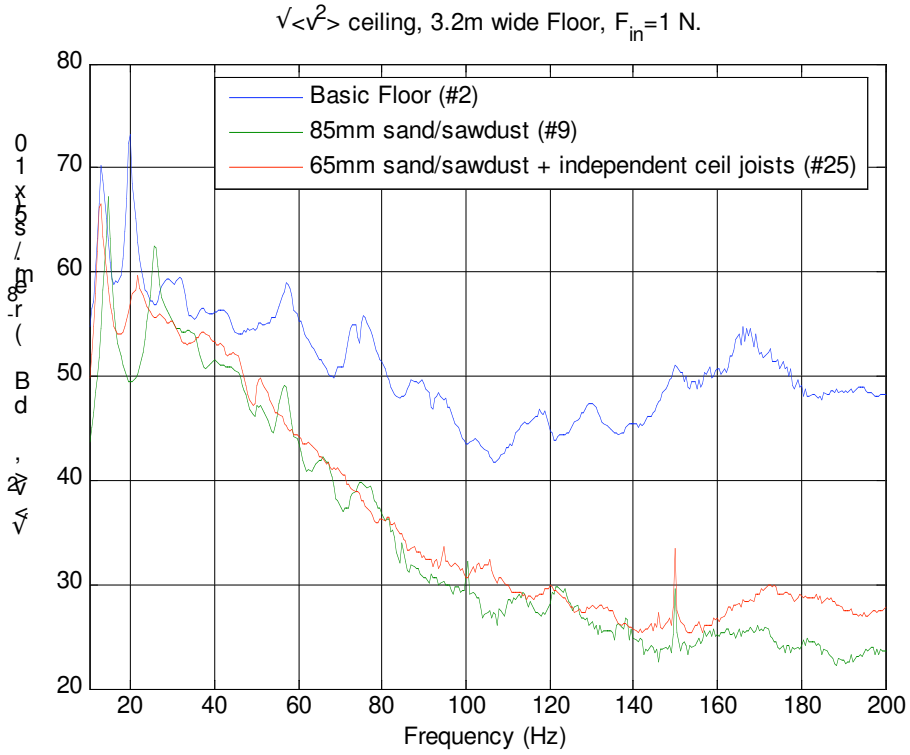

Figure 5-17. Averaged surface velocity plots in dB for Floors 2, 9 and 25 as a function of frequency for the ceiling. The surface velocity is measured by the scanning laser vibrometer, with force generated by the shaker at position C (for the Floor 2) and E (for Floors 9 and 25) and normalised against the amplitude of the applied force (F_{in}) for each frequency. The spike at 150Hz is due to electrical interference of the measurement process.

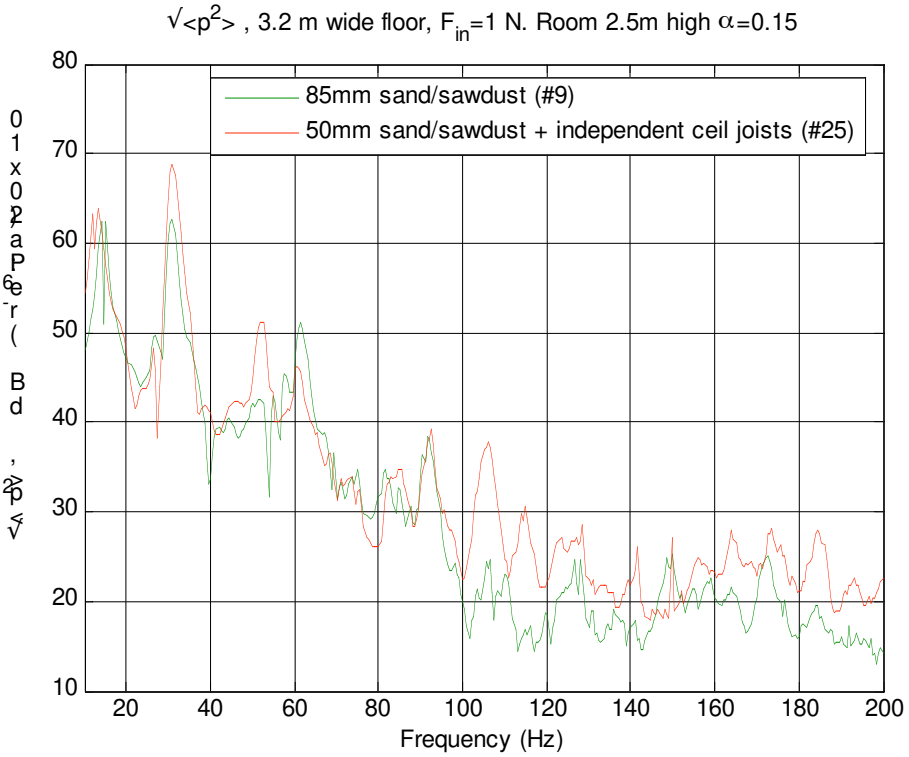

Figure 5-18. Averaged sound pressure in dB for Floors 2, 9 and 25 calculated for a room 2.5m high and with a sound absorption coefficient of 0.15 over its surfaces. Generated by the force at position E and normalised against the amplitude of the applied force (F_{in}).

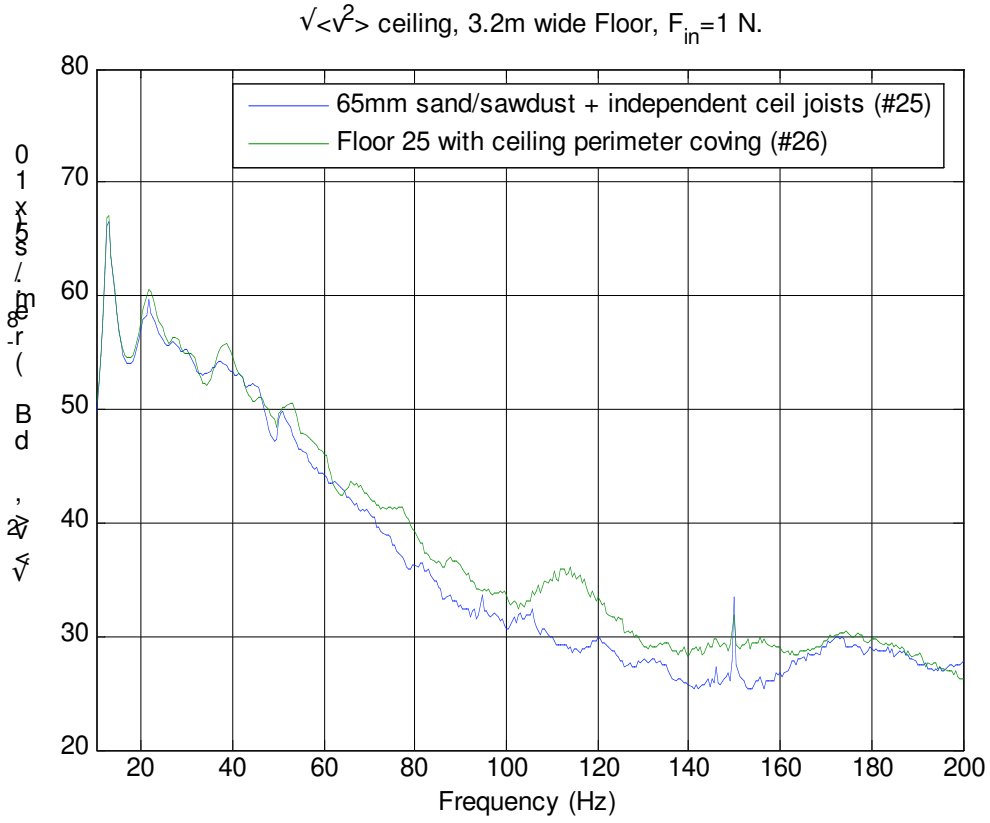

Figure 5-19. Averaged surface velocity plots in dB for Floors 25 and 26 as a function of frequency for the ceiling. The surface velocity is measured by the scanning laser vibrometer, with force generated by the shaker at position E and normalised against the amplitude of the applied force (F_{in}) for each frequency. The spike at 150Hz is due to electrical interference of the measurement process.

5.3 EXAMINATION OF THE HIGH-FREQUENCY RESULTS

In this section we consider the impact insulation results produced by the standard tapping machine on the bare floors (that is without any additional covering). We do this by looking at the overall $L_{n,w}$ rating each floor achieved as a result. We used the relevant part of ISO 140 for the test and the single figure ratings are produce in accordance with ISO 717-2. We also include IIC ratings (in accordance with ASTM E989) and spectrum adaptation terms to give $L_{n,w} + C_I$, although $L_{n,w} + C_I$ tends to have mid-frequency emphasis. We only have these results for floors that had ceilings or complete ceilings.

The worst performing floors for high-frequency impact insulation as indicated by a high $L_{n,w}$ rating are Floor 0 (the 150mm concrete slab), Floor 21 and 22 (the floors with 75mm aerated concrete slabs on top). Although these floors would meet the Australian building code requirements ($L_{n,w} + C_I \leq 62$), they would not nearly meet the New Zealand building code requirements (IIC $\geq$ 55), and would require an additional soft surface covering to perform. This is due to their hard upper surfaces with very little damping in the floor upper.

Floor 23 (the gypsum concrete floor) also has a hard surface, but to compensate for this, the floor is floating on a resilient foam layer, this results in good high-frequency performance.

We also note that when we compare the resiliently attached ceiling (Floor 22) with the ceiling using independent ceiling joists without any special anti-flanking treatment (Floor 23), we get the same result. This suggests that we can use independent ceiling joists to replace the use of RSIC ceiling clips.

The other floors of plywood, particleboard and gypsum fibreboard tended to have a softer upper surface, resulting in less generation of impact vibration in the floor structure. Their high frequency performance tends, as a result to be better. The basic floor (Floor 2) as a result has a much better rating for $L_{n,w}$, although because of its lesser mass the mid-frequencies range performance is not so good and $L_{n,w} + C_I$ rating is not that good. The extra layer of plywood on battens (in Floor 4) has improved the high frequency performance over Floor 2. However the biggest gains are to be had by the floors with a more massive upper with extra damping in the upper (Floors 3, 5, 6, 7, 8, 9 and 25).

Comparing Floor 18 with 19 we see that the extra ceiling layers did nothing to improve the high-frequency performance.

Comparing Floor 6 with 8 we see that changing the span of the floor makes no real difference to the results.

Comparing Floor 18 with 2 we see that a deeper floor, the use of I-beams with a greater spacing improves the high frequency impact insulation performance.

Comparing Floor 25 with 26 we see that the addition of coving around the perimeter of the ceiling has caused problems resulting in a drop in performance.

We do, however, find that the addition of transverse stiffeners (Floor 14 cf. Floor 2) does seem to improve the high frequency performance quite significantly. However, the transverse stiffeners in Floor 20 seemed to offer no change.

The best performing floors for the high-frequency ratings are Floor 3, Floor 9 and Floor 25. We expect Floor 9 and Floor 25 to perform well because of their high mass and damping and, in the case of Floor 25, the isolated ceiling (However the addition of coving . Floor 3

performs well possibly because it upper surface consists of gypsum fibreboard, which seems to be softer than plywood and particleboard. Floor 3 also has some significant damping due to the interaction of the layers gypsum fibreboard as well as due to the extra mass of the gypsum fibreboard.

Floor	IIC	$L_{n,w}$	C_I	$L_{n,w}+C_I$
Floor 0	37	69	-12	57
Floor 2	49	61	-1	60
Floor 3	61	45	1	46
Floor 4	53	58	-1	57
Floor 5	57	52	0	52
Floor 6	58	52	-1	51
Floor 7	58	52	-1	51
Floor 8	59	51	-1	50
Floor 9	62	48	-2	46
Floor 14	55	56	0	56
Floor 18	52	58	0	58
Floor 19	51	59	0	59
Floor 20	35	71	-9	62
Floor 21	35	72	-10	62
Floor 22	58	52	-2	50
Floor 23	58	53	-2	51
Floor 25	62	48	-2	46
Floor 26	60	50	-1	49

Table 5-1. The standard single figure ratings of the tapping machine results for the tested floors without any floor covering (bare floor).

5.4 BRIEF EXAMINATION OF THE VIBRATION WAVEFORMS OBSERVED

One of the important results of doing vibration measurements on the test floors, as was done for this project, is that we can see the shapes of vibrations which are being produced this enables us to identify the modes which are producing resonances and to have a deeper understanding of what is happening in a floor. This is particularly useful for developing a theoretical model of such floors.

In this section we examine a few mesh plots of the results of the measurements of some floors to illustrate a few features found in the vibration of floors. Obviously the data produced by such was enormous and we can only hope to pick a few points in the hope that they will be illuminating.

Simple floor – panel on solid joists

We start with examining floor 10 as it is simply 15mm plywood screwed to 300mm deep LVL joists spanning 5.5m and which are spaced at 400mm centres. It has no ceiling.

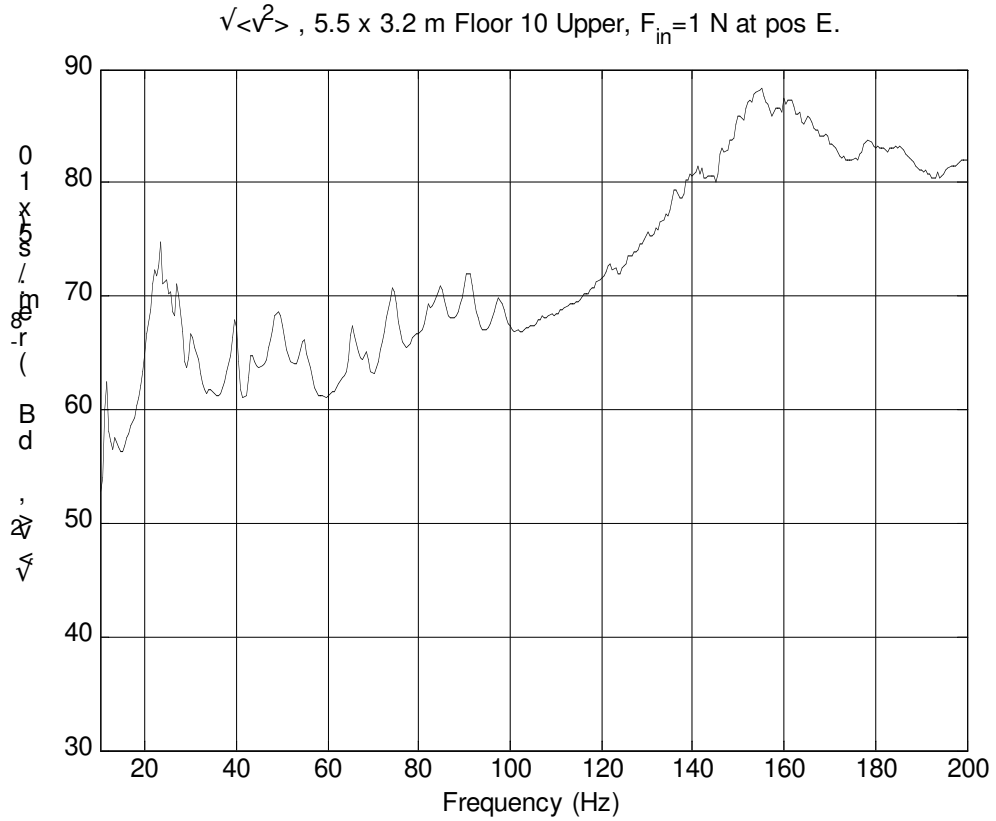

Figure 5-20. Averaged surface velocity plot in dB for Floor 2 as a function of frequency for the upper part of the floor (there is no ceiling). As measured by the scanning laser vibrometer, generated by the force at position E and normalised against the amplitude of the applied force (F_{in}) for each frequency.

Referring to Figure 5-20,we see that there are clear peaks at 21 to 23Hz, these correspond to the fundamental (1,1) and second modes (1,2) of the floor and are shown in Figure 5-21 and Figure 5-22, but since they are close together, their shapes are not very distinct. The next peak is at 40Hz, this corresponds to the fourth mode (1,4) and is shown in Figure 5-23. The third mode is not clearly observed for this floor under the applied force. The next clear mode (1,5) is at 50Hz as shown in Figure 5-24. Similarly, modes (1,6) and (1,7) are at 55Hz and 65Hz, respectively. The first mode where we see more bending along the joists is at 74Hz; this is mode (2,2), and is shown in Figure 5-25. We would also expect to see mode (2,1), but this is not apparent, and may be very close to mode (2,2). From 74Hz we see a number of peaks in the response which correspond to higher floor modes, e.g. mode (2,5) is at 90Hz and is shown in Figure 5-26. Above 100Hz we find that the modes don't form clear peaks anymore. They tend to become close together and the average surface velocity tends to be dominated by vibration near the excitation point, as illustrated by the response at 155Hz, Figure 5-27.

The above observations suggest that this simple floor behaves, at very low-frequencies below about 100Hz, like a plate with orthotropic stiffness – the joists are firmly connected to the plywood. At frequencies above 100Hz the wavelengths of the vibrations on the plywood become shorter than you might expect if the plywood was attached firmly to the joists. This suggests that the plywood is starting to separate from the joists at regions between screws.

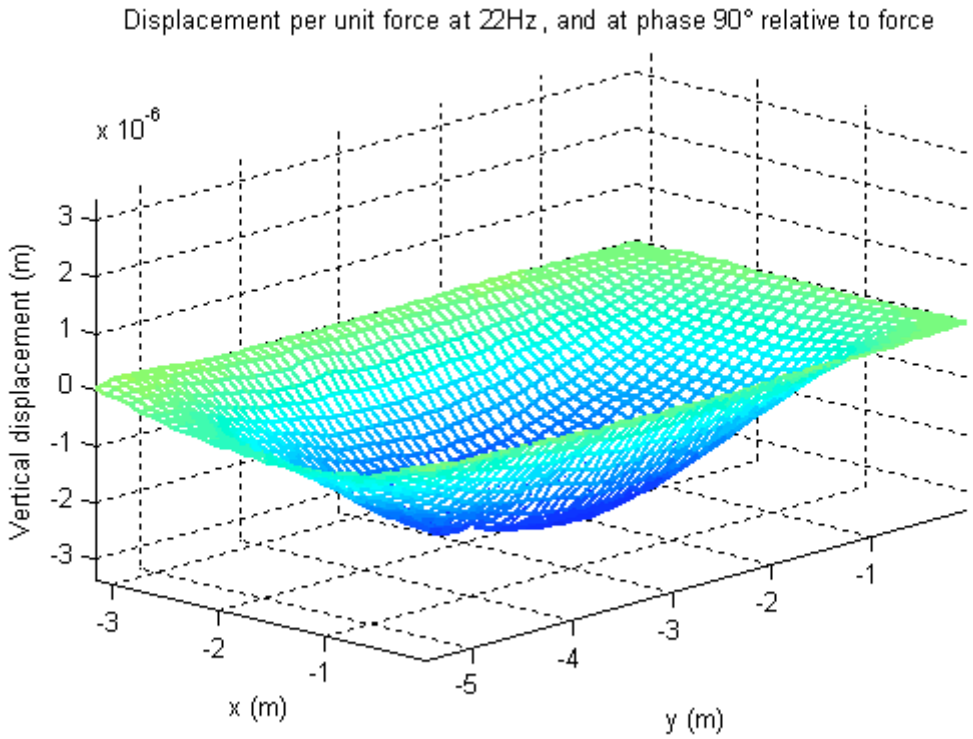

Figure 5-21. Illustration of mode (1,1) on floor 10.

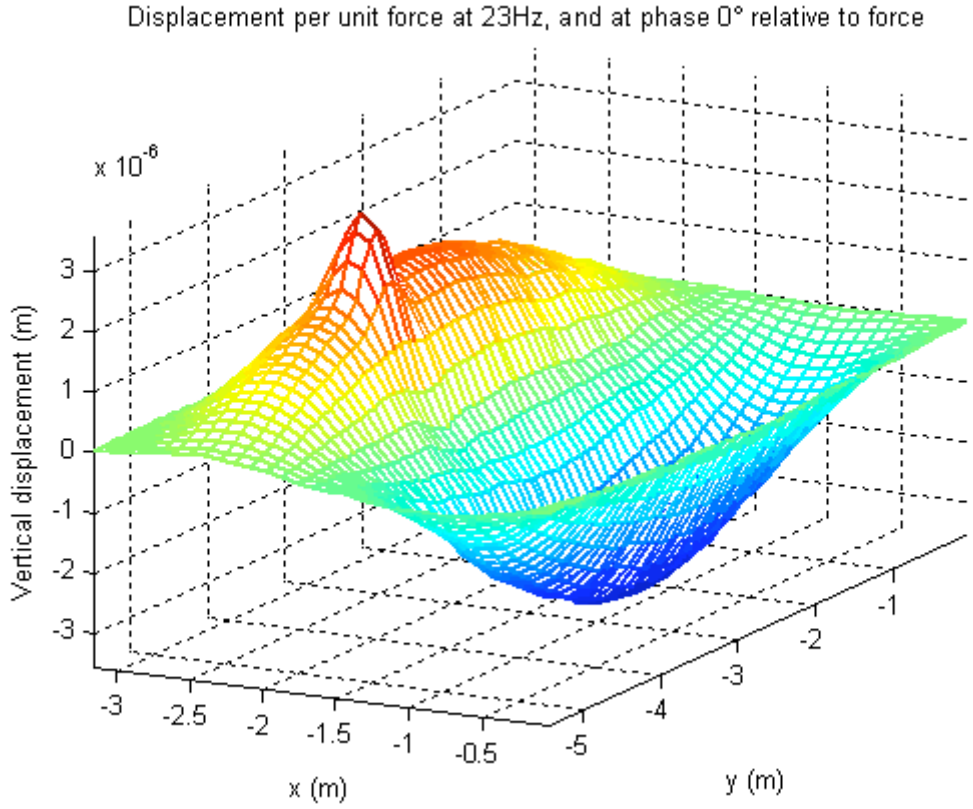

Figure 5-22. Illustration of mode (1,2) on floor 10. Note that the phase with respect to the force is 0 in this illustration. This illustrates the reactionary vibration near the forcing point. It is not apparent for a phase of 90 degreees.

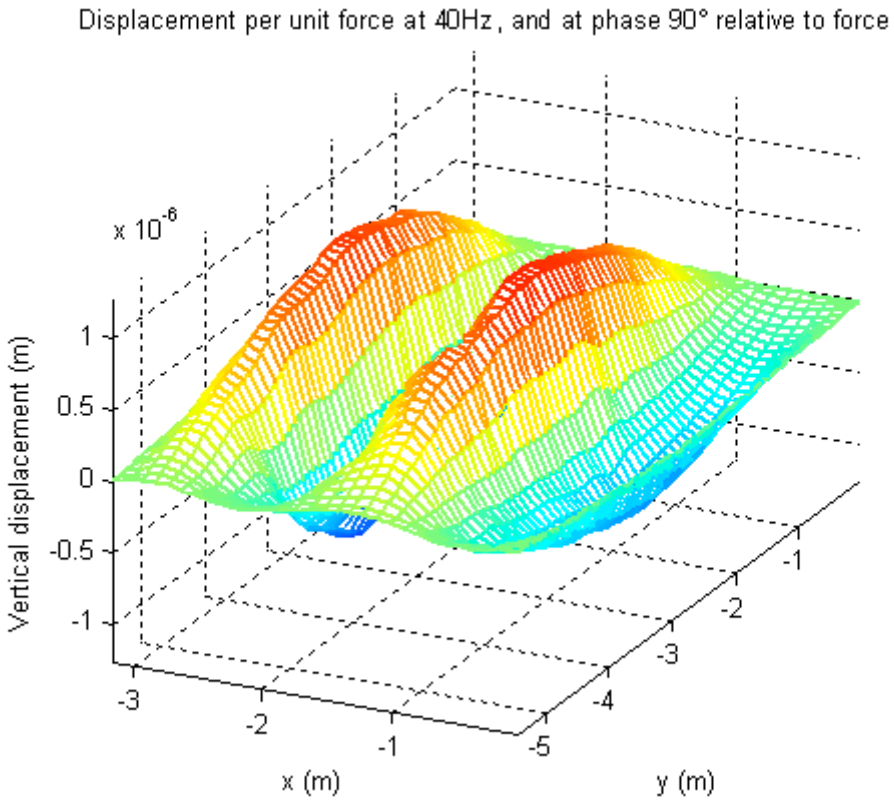

Figure 5-23. Illustration of mode (1,4) on floor 10.

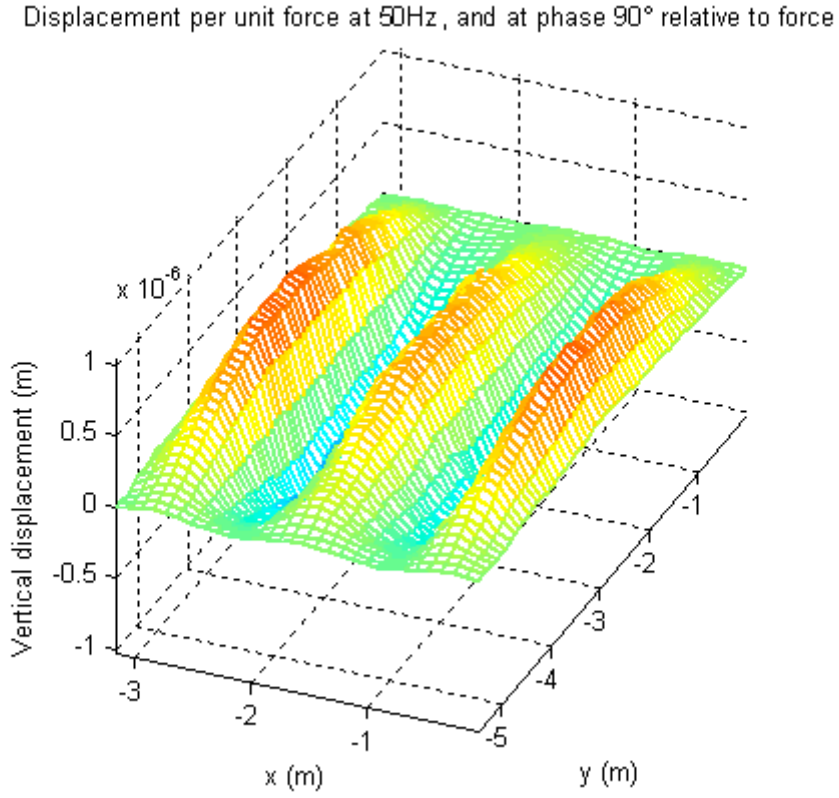

Figure 5-24. Illustration of mode (1,5) on floor 10.

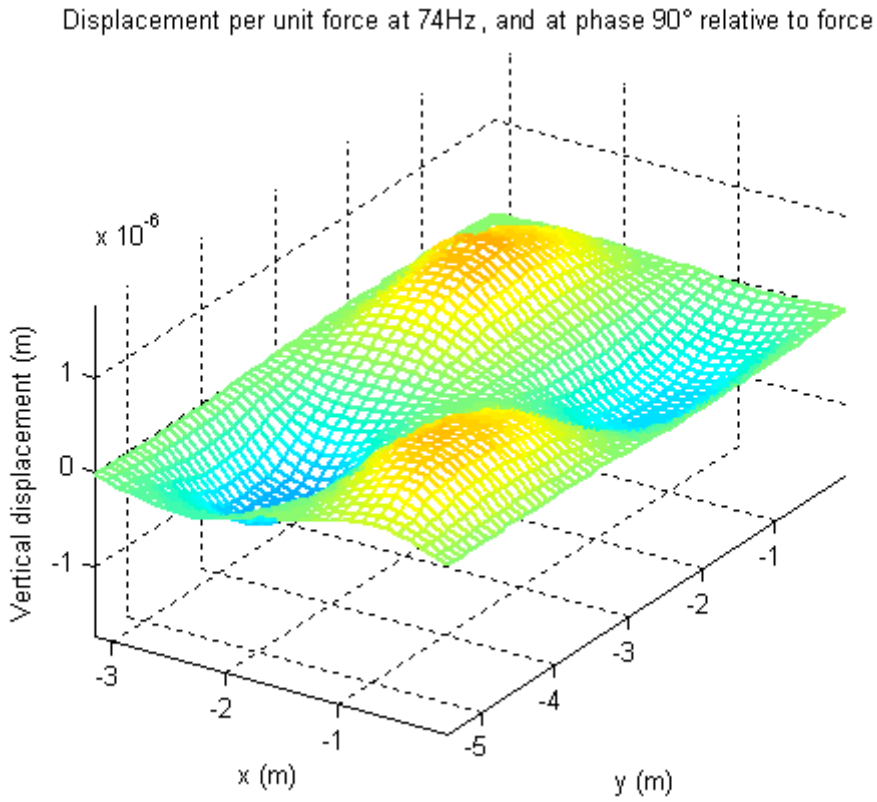

Figure 5-25. Illustration of mode (2,2) on floor 10.

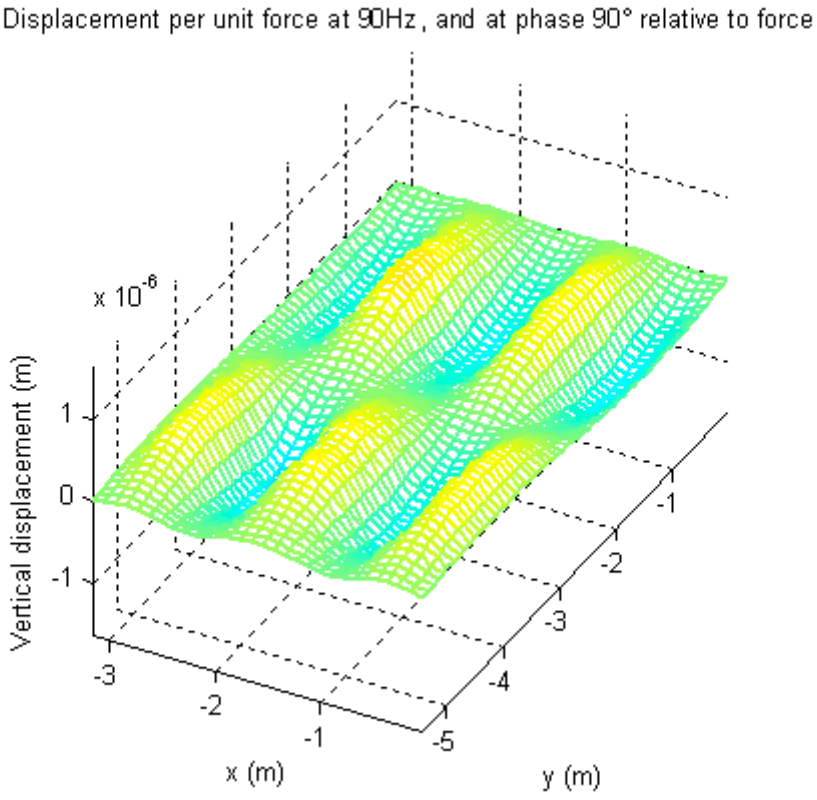

Figure 5-26. Illustration of mode (2,5) on floor 10.

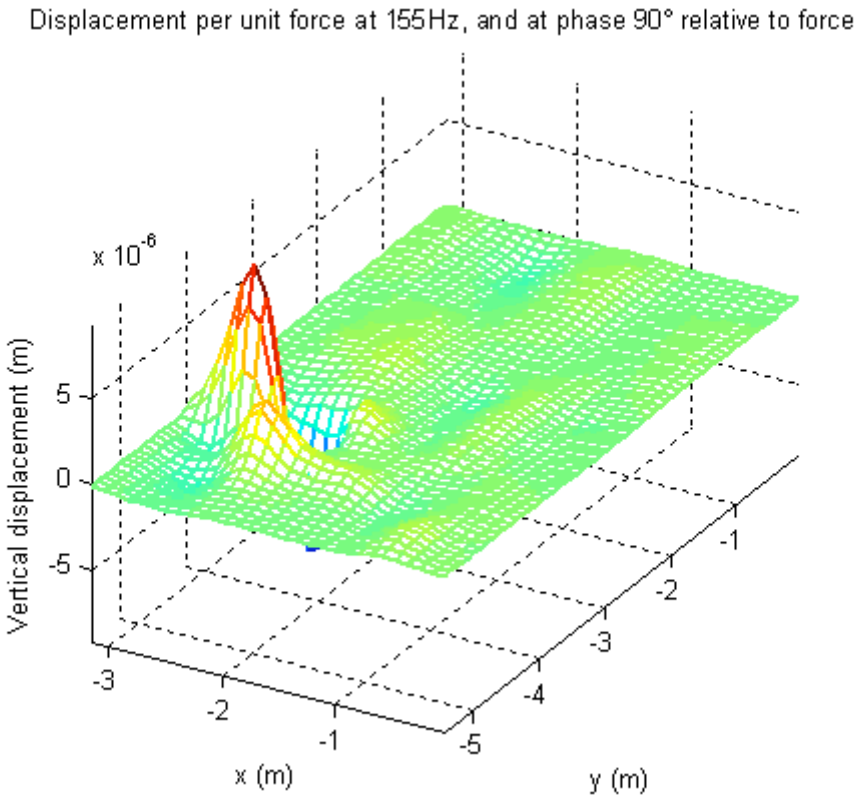

Figure 5-27. Illustration of response at 155Hz on floor 10. The region near the forcing point is showing a lot of reactionary movement (vibration which doesn't send energy into the structure, but oscillates the energy back and forth between the forcing device and the floor).

Basic floor with ceiling

The next floor to consider is floor 2. This is a basic floor with a ceiling, consisting of two layers of plasterboard screwed to ceiling battens connected to the underside of the joists through resilient rubber clips (RSICs). The cavity is infilled between the joists with a 300mm depth of fibreglass batts (flow resistivity = 7200 Rayls/m). The overall cavity depth is 340mm. This floor spans 7m.

We will examine some 3D mesh plots of the vibrations on the surfaces of this floor to illustrate some points to do with coupling of the vibrations of the upper part of the floor to the ceiling vibrations. We observe that for modes (1,1) and (1,2) at 13Hz and 20Hz respectively, the ceiling is closely coupled to the upper part of the floor. This is illustrated in Figure 5-29, for mode (1,2). We also see that at 32Hz the ceiling is starting to decouple from the floor upper (see Figure 5-30). The coupling of the ceiling to the floor upper is through the air and the ceiling clips under the joists. The frequency above which this decoupling occurs is related to the mass and coupling stiffnesses of the floor/ceiling system. This is called the mass-stiffness-mass resonance frequency, and assuming the floor upper and ceiling has no bending stiffness (totally limp) and the cavity has no infill, is given by

$$f = 2\pi\left[k\left(\frac{m_1 + m_2}{m_1 m_2}\right)\right]^{1/2}, \qquad (0\text{-}26)$$

where m_1 is the surface density of the floor upper, m_2 is the surface density of the ceiling, and k is the stiffness coupling the two together. k is given by

$$k = \frac{\rho_0 c^2}{d} + k_{clips}, \qquad (0\text{-}27)$$

where $_0$ is the density of air, c is the speed of sound in the air, d is the cavity depth, k_{clips} is the average stiffness of the ceiling clips per unit area. For the case of Floor 2 using the above assumptions we find that the mass-stiffness-mass resonance frequency is 39Hz. A rough approximation since our floor and ceiling clearly are not limp.

In the vibration response of the ceiling we see that there frequencies where we get peaks. This is most probably due to the situation where we have floor resonances coupling well into ceiling resonances. This is illustrated for a range of peaks in Figure 5-31, Figure 5-32 and Figure 5-33. Since it would appear that resonance are occurring in the ceiling, this would suggest that a lot of the vibration in the ceiling is being transmitted by point source coupling, presumably through the ceiling clips.

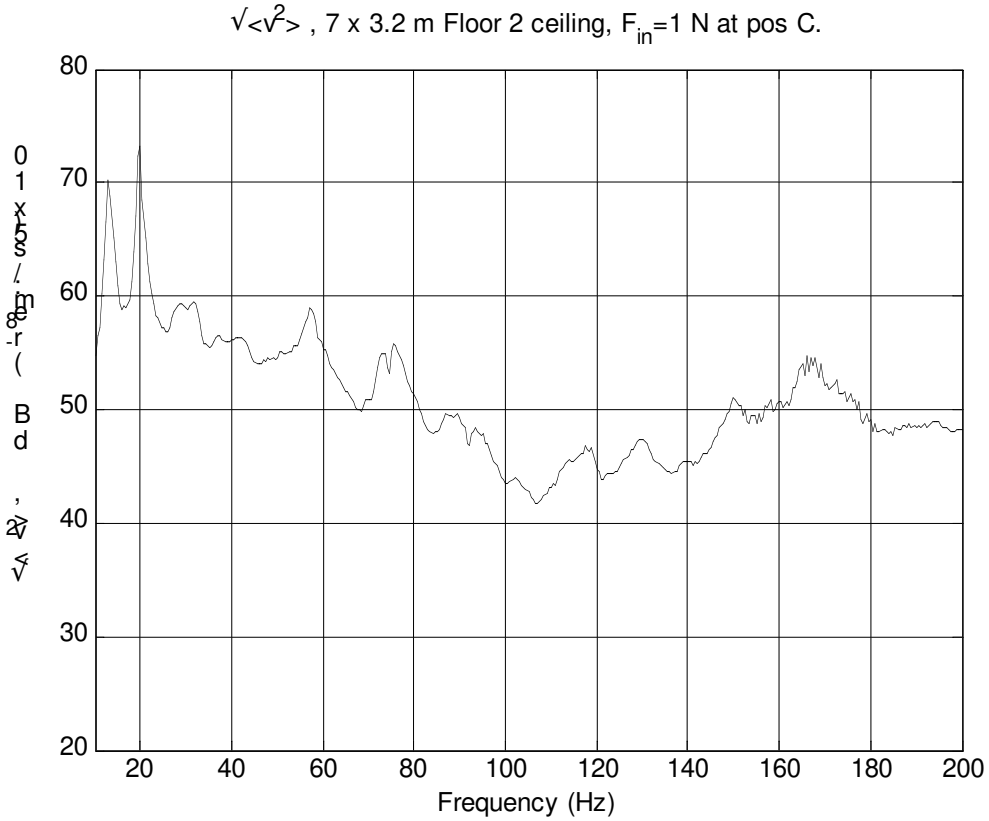

Figure 5-28. Averaged surface velocity plots in dB for Floor 2 as a function of frequency for the ceiling. As measured by the scanning laser vibrometer, generated by the force at position C and normalised against the amplitude of the applied force (F_{in}) for each frequency.

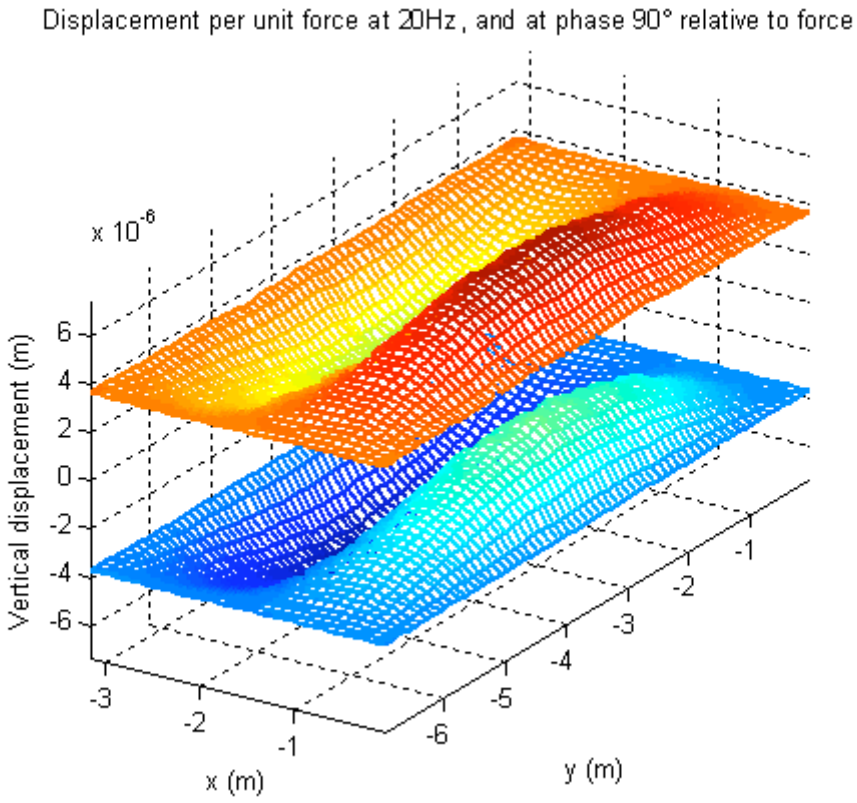

Figure 5-29. Illustration of vibration response of upper surface and ceiling at 20Hz on floor 2. This is mode (1,2). At this frequency the ceiling is clearly closely coupled to the floor upper surface.

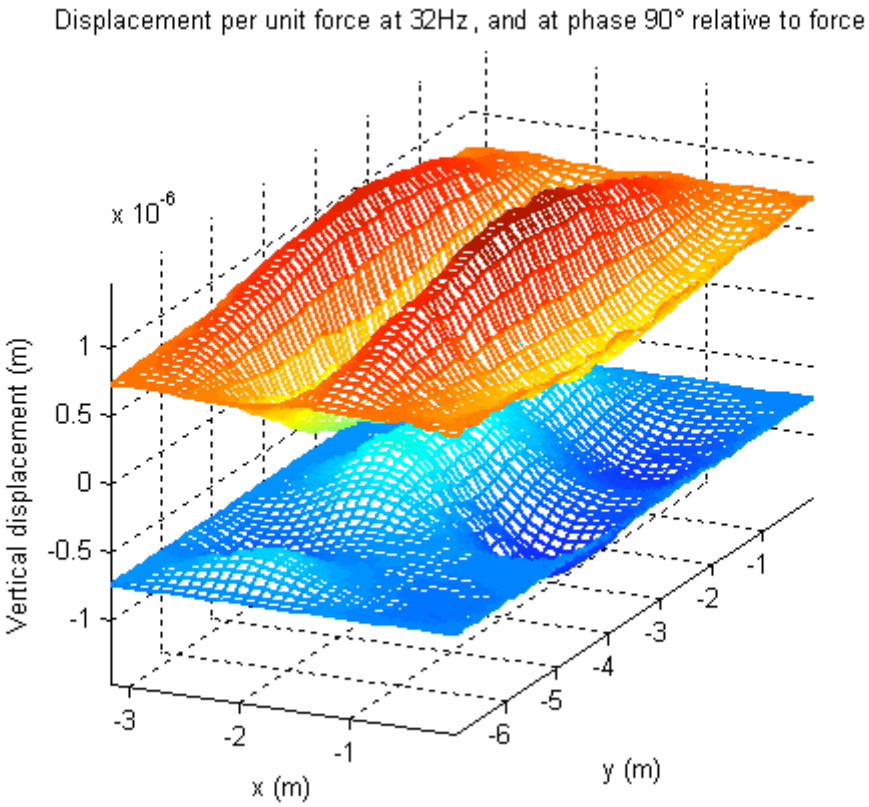

Figure 5-30. Illustration of vibration response of upper surface and ceiling at 32Hz on floor 2. This is mode (1,4). At this frequency the ceiling is starting to decouple from the floor upper surface, and produce modes of its own.

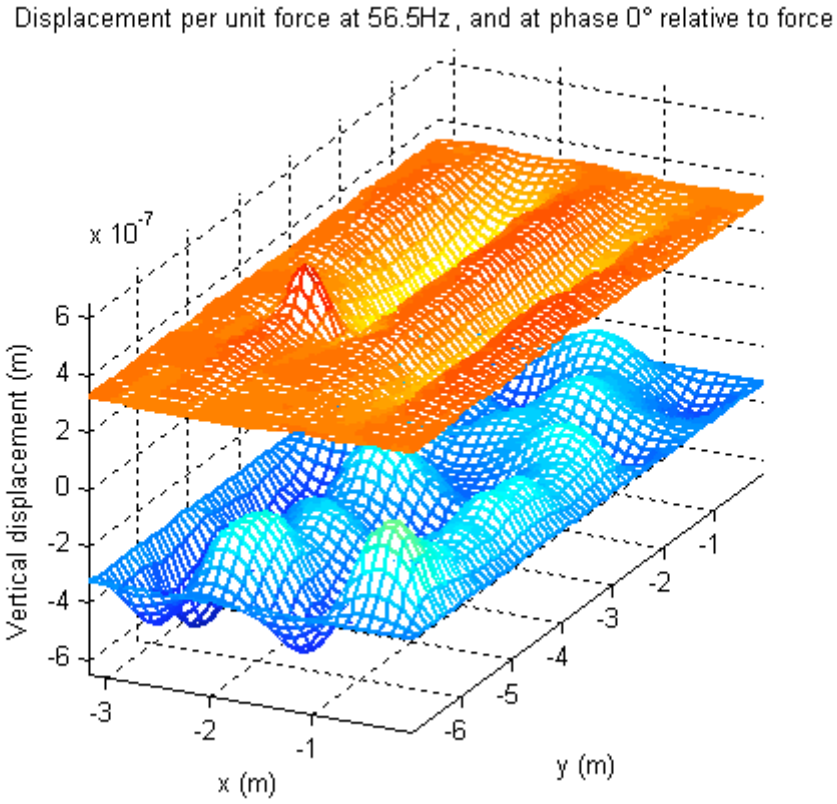

Figure 5-31. Illustration of vibration response of upper surface and ceiling at 56.5Hz on floor 2. At this frequency the ceiling is quite decoupled from the floor upper surface, and appears to be resonating. This is a peak in the response of the system, probably due to a resonance in the upper floor coupling to a resonance in the ceiling.

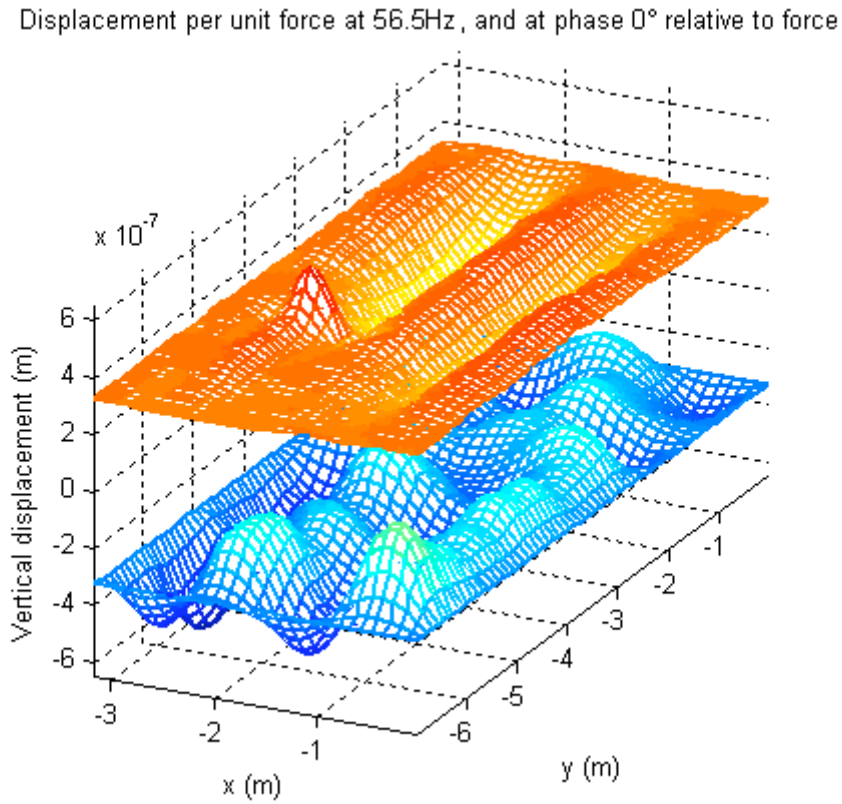

Figure 5-32. Illustration of vibration response of upper surface and ceiling at 75Hz on floor 2. This is another peak in the response of the system, and is also probably due to a resonance in the upper floor coupling to a resonance in the ceiling.

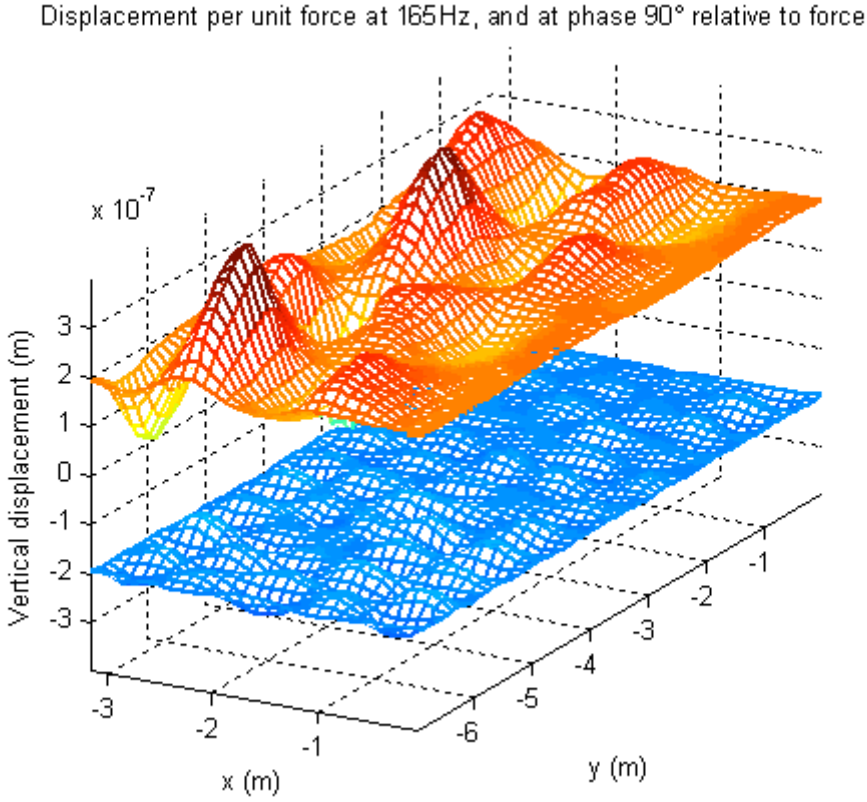

Figure 5-33. Illustration of vibration response of upper surface and ceiling at 165Hz on floor 2. This is at another peak in the response of the system, and is also probably due to a resonance –mode (4,5) – in the upper floor coupling to a resonance in the ceiling. The vibrations in the upper floor die away quite quickly due to the coupling of energy into the ceiling.

A floor with a thick, stiff upper surface

In this section we examine a few plots from Floor 21, which consists of 75mm of Hebel aerated concrete screwed to I-beam joists. In Figure 5-34 we see the measurements results of the floor at 190Hz. What is clear from the relatively long wavelengths at this frequency is the floor upper is quite stiff in all directions. We also see that the waves in the floor upper do not die away at all, indicating very low damping in the floor upper.

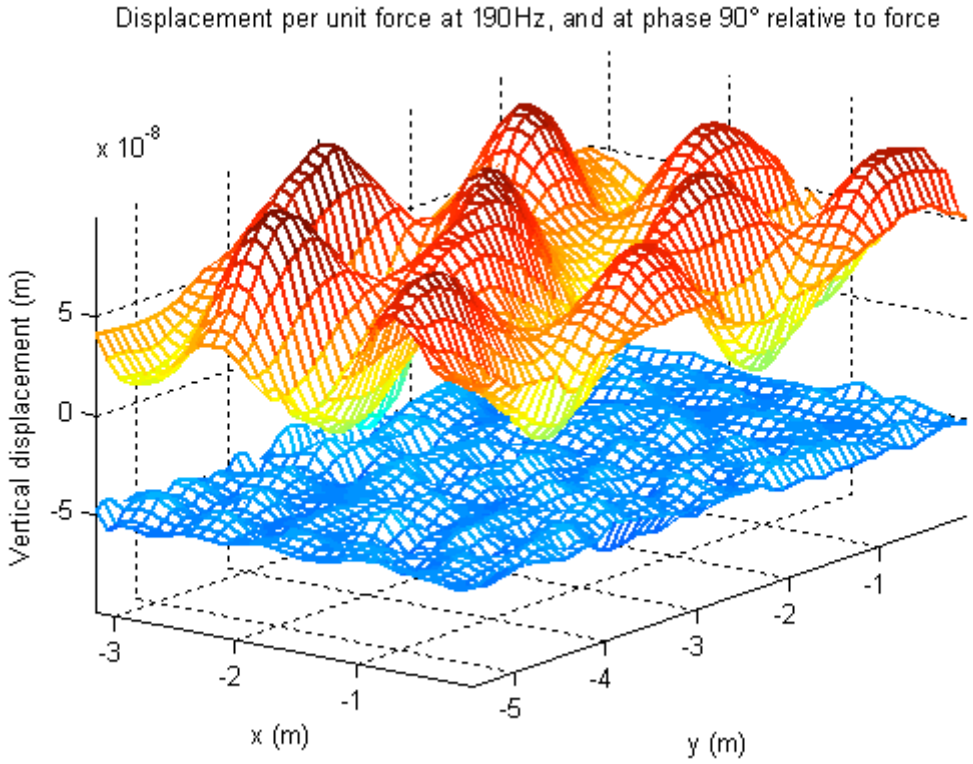

Figure 5-34. Illustration of vibration response of upper surface and ceiling at 190Hz on Floor 21. This is at another peak in the response of the system, and is also probably due to a resonance –mode (6,5) – in the upper floor coupling to a resonance in the ceiling.

A floor with more mass and high damping

In Figure 5-35 we see the effect on the vibrations in the floor upper when we have a floor which is highly damped (Floor 9). We observe that the vibrations are quickly damped by the floor upper, resulting in a relatively quick reduction in their amplitude as they travel along the floor. This means that less vibration is transmitted to the ceiling as a whole; it also means that in such a floor flanking is less of an issue, since less vibrational energy gets to the rest of the structure.

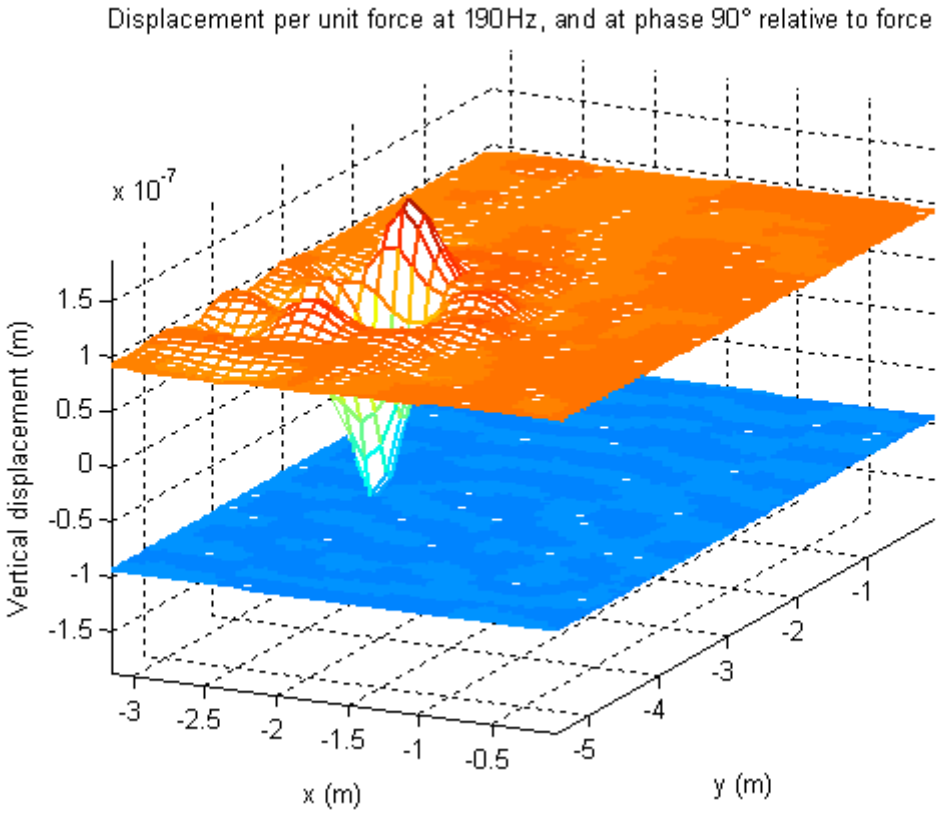

Figure 5-35. Illustration of vibration response of upper surface and ceiling at 190Hz on floor 9. The vibrations in the upper floor die away quite quickly due to the energy lost by the internal damping of the floor upper.

A floor with transverse stiffeners

In Floor 14 we considered the case of having transverse stiffeners in a relatively simple floor. It was said before that one concern was not to increase the frequency of the fundamental resonance, as it is believed that this would make it more audible to listeners. One way around that problem was to provide a gap between the end of the transverse stiffener and the edge of the floor. This, however, resulted in an additional rotational mode. This mode (at 25Hz) is shown in Figure 5-36.

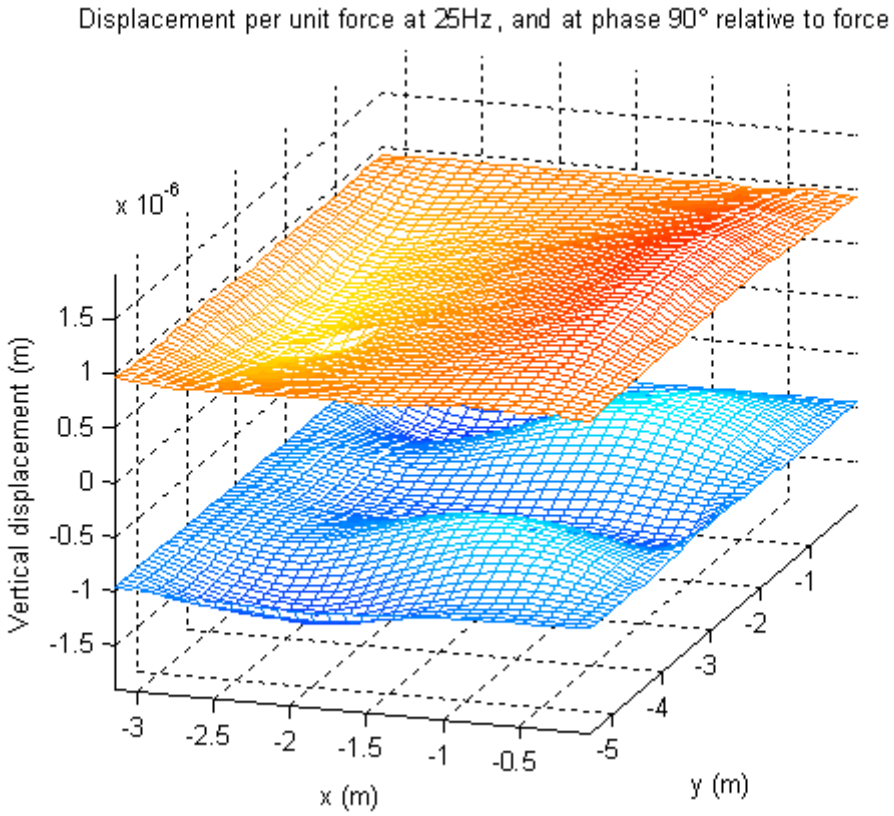

Figure 5-36. Illustration of vibration response of upper surface and ceiling at 25Hz on floor 14. This is an illustration of the rotational mode found in the floor, due to the transverse stiffeners not going completely to the wall.

A floor with a floating topping

In this example we consider Floor 22, which has a gypsum concrete screed floating on a foam layer on the floor. The gypsum concrete is relatively stiff and heavy and the function of the foam is to isolate the vibrations of the screed from the rest of the floor. This is more effective at higher frequencies. In Figure 5-37 we can see that this is happening – the gypsum concrete is vibrating with little damping occurring, with the edges obviously being free to move.

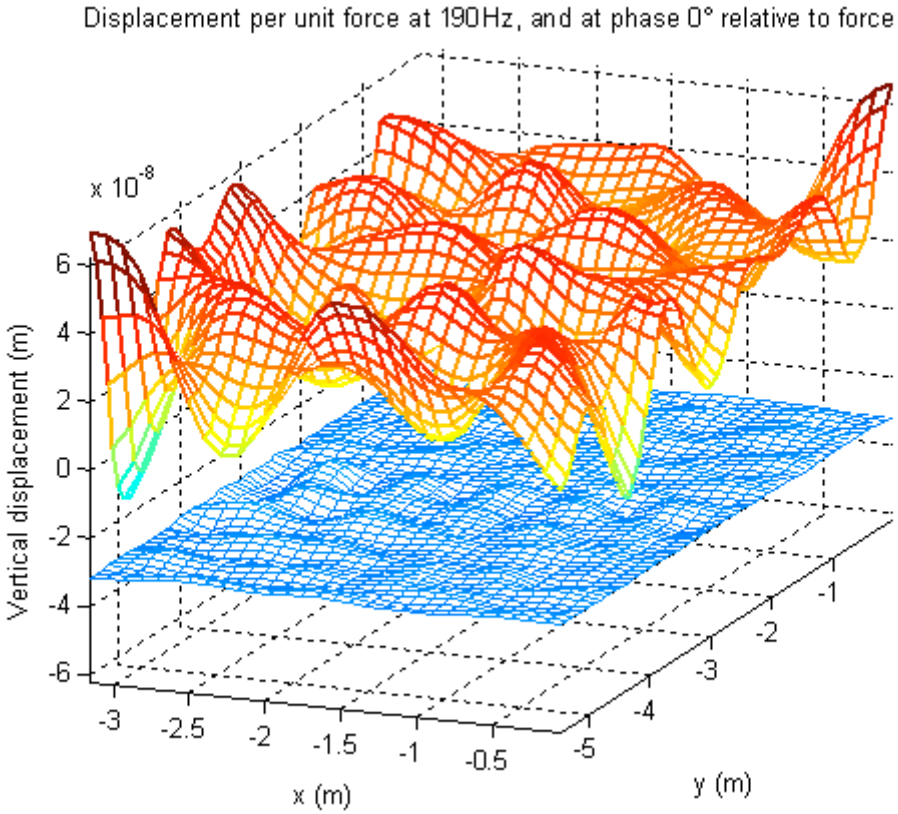

Figure 5-37. Illustration of vibration response of upper surface and ceiling at 190Hz on floor 22. This is an illustration of what happens when we have a floating topping.

5.5 REFERENCES

Pitts, G. (2000). *Acoustic Performance of party floors and walls in timber framed buildings*, TRADA Technology report 1/2000.

Sun, J.C., Sun, H.B., Chow, L.C., Richards, E.J. (1986). "Predictions of total loss factors of structures, part II: Loss factors of sand-filled structure", *Journal of Sound and Vibration*, 104(2), 243-257.